



SCHOOL of
GRADUATE STUDIES
EAST TENNESSEE STATE UNIVERSITY

East Tennessee State University
Digital Commons @ East
Tennessee State University

Electronic Theses and Dissertations

Student Works

5-2016

Computational Studies of Spin Trapping of Biologically Relevant Radicals by New Heteroaryl Nitrones

Eyram Asempa
East Tennessee State University

Follow this and additional works at: <https://dc.etsu.edu/etd>

 Part of the [Physical Chemistry Commons](#)

Recommended Citation

Asempa, Eyram, "Computational Studies of Spin Trapping of Biologically Relevant Radicals by New Heteroaryl Nitrones" (2016).
Electronic Theses and Dissertations. Paper 3029. <https://dc.etsu.edu/etd/3029>

This Thesis - Open Access is brought to you for free and open access by the Student Works at Digital Commons @ East Tennessee State University. It has been accepted for inclusion in Electronic Theses and Dissertations by an authorized administrator of Digital Commons @ East Tennessee State University. For more information, please contact digilib@etsu.edu.

Computational Studies of Spin Trapping of Biologically Relevant Radicals by New
Heteroaryl Nitrones

A thesis

presented to

the faculty of the Department of Chemistry

East Tennessee State University

In partial fulfillment

of the requirements for the degree

Master of Science in Chemistry

by

Eyram A. Asempa

May 2016

Dr. Scott J. Kirkby, Chair

Dr. Marina Roginskaya

Dr. David Close

Keywords: heteroaryl nitrones, FxBN, PBN, DMPO, biologically relevant radicals, Hartree-Fock
Self-Consistent Field, Density Functional Theory

ABSTRACT

Computational Studies of the Spin Trapping of Biologically Relevant Radicals by New Heteroaryl Nitrones

by

Eyram A. Asempa

Heteroaryl nitrone spin traps have been suggested to act as free radical scavengers. The geometry optimizations and the single-point energies of the spin trapping reactions of the heteroaryl nitrones, 5,5-dimethylpyrroline-N-oxide (DMPO) and α -phenyl-N-*t*-butylnitron (PBN) have been computationally studied using *ab initio* (Hartree-Fock (HF) and second-order Møller-Plesset (MP2)) methods and Density Functional Theory (DFT) methods. The effects of new heteroaryl substituents on a parent nitrone spin trap have been examined at the HF and MP2 levels with the 6-31G*, and cc-pVnZ (n=D, T, Q) basis sets. The thermodynamics of the spin trapping at the C-site and O-site with \bullet H, \bullet CH₃ and \bullet OH radicals were studied at the HF/6-31G* and DFT/m06/6-31G* levels. The addition reactions favor at the C-sites and the double adducts are thermodynamically more stable than the mono adducts. The spin trapping of DMPO, PBN and α (Z)-(3-methylfuroxan-4-yl)-N-*tert*-butylnitron (FxBN) with \bullet OH have also been studied.

DEDICATION

I dedicate this work to My Almighty God for His deepest Love He has towards me.

ACKNOWLEDGEMENTS

“The Lord is mine helper and my defender; and mine heart hoped in him, and I am helped.

And my flesh flowered again; and (out) of my will I shall acknowledge to Him.

(The Lord is my helper and my defender; and my heart trusted Him, and I was helped.

And my heart full out joyed, or rejoiced; and I shall praise him with my song)”

~~ Psalm 28:7 (WYC).

My sincere appreciation goes to my Almighty God for His abundant Love He has towards me, His protection, guidance and grace through my graduate studies and research. I am grateful to the Lord for providing me with wonderful parents and siblings who love, support and sacrifice to see me soar higher in life.

I would like to express my gratitude to my advisor, Dr. Scott Kirkby for his immense guidance, support and useful critiques of this research work. I would also like to thank Drs. Roginskaya and Close (my thesis committee), Dr. Eagle (Chair of the Department of Chemistry), and all faculty members of department. Thank you to the Department of Chemistry, ETSU, for the graduate assistantship during my graduate studies and the ETSU School of Graduate Studies Student Research Grant for funds for my research work.

My appreciation also goes to Ms. Libby Tipton, Disability Services, and Vital Signs for the accommodations.

Not forgetting Bread of Life Ministries, Duke Debrah, Martha Essandoh, Constance Warden, Faisal Ibrahim, Isaac Addo, Angelica Bridges and her family, and all loved ones in the Department of Chemistry who have been supportive and kind during my studies.

Benedicite omnes, God bless you all!

TABLE OF CONTENTS

	Page
ABSTRACT.....	2
DEDICATION	3
ACKNOWLEDGMENTS	4
LIST OF TABLES	7
LIST OF FIGURES	8
LIST OF ABBREVIATIONS.....	11
Chapter	
1. INTRODUCTION	13
Free Radicals	13
Nitron Spin Traps	14
2. QUANTUM MECHANICS.....	19
General Introduction to Computational Chemistry.....	19
The Schrödinger Equation	22
The Hamiltonian Operator	23
Atomic Units.....	24
The Born-Oppenheimer Approximation.....	25
The Hartree-Fock Self Consistent Field Method	27
Hartree's Procedure	29
The Wave Function as a Slater Determinant	33

The Variational Principle	33
The Roothaan-Hall Equations.....	35
Restricted and Unrestricted Hartree-Fock Methods	37
Møller-Plesset Perturbation Theory.....	38
Density Functional Theory	39
Basis Sets	44
3. RESULTS AND DISCUSSION	48
Computational Details	48
Discussion of the Results	48
4. CONCLUSIONS	80
REFERENCES	81
APPENDIX: Tables of Additional Data from the Calculations	95
VITA	144

LIST OF TABLES

Table	Page
1. Calculated bond lengths for formaldonitrone and the new heteroaryl nitrones at HF/6-31G* 50	50
2. Energies of selected biologically relevant radicals and their dipole moments52	52
3. Energies of formaldonitrone and the new heteroaryl nitrones at the HF/6-31G*, MP2/cc-pVDT, MP2/cc-pVTZ, MP2/cc-pVQZ, the MP2 CBS limit, and DFT/m06/6-31G* levels of theory. The dipole moments were calculated at the HF/6-31* level55	55
4. Energies of the spin trapping reactions of selected radicals with formaldonitrone and the new heteroaryl nitrones at the C-site for (a) HF/6-31G* and (b) DFT/m06/6-31G*57	57
5. Energies of the spin trapping reactions of biologically relevant radicals with the new heteroaryl nitrones the O-site for (a) HF/6-31G* and (b) DFT/m06/6-31G*58	58
6. Energies of the spin trapping reactions of •H with formaldonitrone and the new heteroaryl nitrones at both C- and O-sites at (a) HF/6-31G* and (b) DFT/6-31G*67	67
7. Energies of the spin trapping reactions of •CH ₃ with formaldonitrone and the new heteroaryl nitrones at both C- and O-sites at (a) HF/6-31G* and (b) DFT/m06/6-31G*68	68
8. Energies of the spin trapping reactions of •OH with formaldonitrone and the new heteroaryl nitrones at both C- and O-sites at (a) HF/6-31G* and (b) DFT/m06/6-31G*69	69
9. Energies of the addition of •OH to DMPO, PBN and FxBN at the DFT/m06/6-31G* and HF/6-31* levels of theory.....75	75

LIST OF FIGURES

Figure	Page
1. The addition of a nitron spin trap to a free radical to produce a nitroxide.....	14
2. The resonance stabilization of nitroxide	15
3. Chemical structures of linear PBN, cyclic DMPO, and several derivatives commonly used as spin traps	16
4. The reaction of a prototype nitron with a radical to form a spin adduct	17
5. The chemical structures of the proposed novel heteroaryl nitron spin traps.....	18
6. Algorithm for self-consistent field theory.....	32
7. A flowchart summary of the procedure for solving the Roothaan-Hall equations	36
8. A graphical representation of the orbital treatment for the RHF, UHF and ROHF methods	38
9. The optimized geometry of formaldonitron and the new heteroaryl nitrons. All bond lengths are measured in Å	51
10. NWChem optimized geometries of biologically relevant radicals	53
11. ChemDraw® representations of the new heteroaryl spin adducts with •H added at the C-site carbon	59
12. ChemDraw® representations of the new heteroaryl spin adducts with •CH ₃ added at the C-site carbon	60
13. ChemDraw® representations of the new heteroaryl spin adducts with •OH added at the C-site carbon	61
14. ChemDraw® representations of the new heteroaryl spin adducts with •H at added at the O-site oxygen	62

15. ChemDraw® representations of the new heteroaryl spin adducts with •CH ₃ added at the O-site oxygen	63
16. ChemDraw® representations of the new heteroaryl spin adducts with •OH added at the O-site oxygen	64
17. NWChem Optimized Geometries of new heteroaryl spin adducts at C- and O- sites. The colors follow standard colors: red - oxygen, hydrogen - white, grey - carbon, blue - nitrogen, and yellow - sulfur.....	65
18. ChemDraw® representations of the new heteroaryl diadducts with •H added at both the C-site carbon and the O-site oxygen	70
19. ChemDraw® representations of the new heteroaryl diadducts with •CH ₃ added at both the C-site carbon and the O-site oxygen	71
20. ChemDraw® representations of the new heteroaryl diadducts with •OH added at both the C-site carbon and the O-site oxygen	72
21. NWChem optimized geometry of the most stable diadduct thermodynamically of 1,2,3-thiadiazol-5-yl nitron with di •OH at both the C- and O-sites. The colors follow standard colors: red - oxygen, hydrogen - white, grey - carbon, blue - nitrogen, and yellow - sulfur ...	73
22. ChemDraw® representations of 5,5-dimethylpyrroline-N-oxide, phenyl-N-t-butylnitron and (Z)-(3-methylfuroxan-4-yl)-N-tert-butylnitron	76
23. NWChem optimized geometry of the spin adduct of PBN with •OH radical at C- site. The colors follow standard colors: red - oxygen, hydrogen - white, grey - carbon, and blue - nitrogen	77
24. NWChem optimized geometry of diadduct of DMPO with di •OH at both the C- and O-sites. The colors follow standard colors: red - oxygen, hydrogen - white, grey - carbon, and blue - nitrogen	78
25. NWChem optimized geometries of a) the spin adduct of FxBN with •OH at C-site and b) the diadduct of FxBN with di •OH at both C- and O- sites. The intramolecular	

hydrogen bonds are present in both a) and b). The colors follow standard colors: red - oxygen, hydrogen - white, grey - carbon, and blue - nitrogen.....79

LIST OF ABBREVIATIONS

ROS:	Reactive Oxygen Species
I-R:	Ischemia-Reperfusion
EPR:	Electron Spin Resonance
DFT:	Density Functional Theory
a.u.:	Atomic Units
E_h :	hartree
PBN:	α -phenyl-N- <i>t</i> -butylnitrone
DMPO:	5,5-dimethylpyrroline-N-oxide
DEMPO:	5-Diethoxyphosphoryl-5-methyl-1-pyrroline N-oxide
EMPO:	2-ethoxycarbonyl-2-methyl-3,4-dihydro-2H-pyrrole-1-oxide
BocMPO:	5- <i>tert</i> -butoxycarbonyl-5-methyl-1-pyrroline N-oxide
AMPO:	5-carbamoyl-5-methyl-1-pyrroline N-oxide
FxBN:	α (Z)-(3-methylfuroxan-4-yl)-N- <i>tert</i> -butylnitrone
HSCF:	Hartree Self-Consistent Field
HF:	Hartree-Fock
HF-SCF:	Hartree-Fock Self-Consistent Field
RHF:	Restricted Hartree-Fock
ROHF:	Restricted Open-shell Hartree-Fock
UHF:	Unrestricted Hartree-Fock
BO:	Born-Oppenheimer

MPPT: Møller-Plesset Perturbation Theory
RSPT: Rayleigh-Schrödinger Perturbation Theory
STO: Slater-Type Orbital
CBS: Complete Basis Set

CHAPTER 1

INTRODUCTION

Free Radicals

A free radical is any species that contains one or more unpaired electrons in the outermost (valence) shell of an atom or molecule.¹ The unpaired electrons change the chemical reactivity of the molecule,² which makes it more reactive and unstable than the corresponding diamagnetic specie. Free radicals are classified by different criteria and these include reactive oxygen species (ROS, *e.g.* superoxide radical anion ($O_2^{\bullet-}$) and hydroxyl radical ($OH\bullet$)), reactive nitrogen species (nitric oxide ($NO\bullet$), peroxynitrite ($ONOO^-$)), sulfur-centered radicals (thiyl radicals ($RS\bullet$)), and carbon-centered radicals (trichloromethyl ($CCl_3\bullet$)). They are produced in a wide variety of chemical and biological systems including the formation of plastics, the ageing of paints, the combustion of fuels, and in the human body.³ Human bodies generate free radicals through the action of internal and external factors.⁴ Internal factors include metabolic processes that generate free radicals in the biological systems such as mitochondria and phagocytes.⁵ External factors generating free radicals include exposure to X-rays, ozone, cigarette smoking, air pollutants, and industrial chemicals.⁶ Psychological factors, like stress and emotion, can also generate free radicals through physiological responses.⁷

Most of the radicals of interest in biological systems are short-lived molecules with half-lives ranging from 10^{-3} to 10^{-9} s.⁸ They are required for normal cell function in controlled amounts, but when in excess, can cause damage to cell membranes and other tissue leading to cancer, cardiovascular disease, neurological disorders, ischemia-reperfusion (I-R), and other diseases.⁹⁻¹²

Nitron Spin Traps

Spin traps are diamagnetic compounds that have the ability to trap and stabilize free radicals in chemical and biological systems. Spin trapping was named by E.G. Janzen and is a chemical reaction in which free radicals add to diamagnetic compounds (spin traps) to produce more stable radical products (spin adducts).^{13,14} Franchi *et al.*¹⁵ and Spulber *et al.*¹⁶ have stated that the use of spin trapping for the detection of radicals has contributed significantly to the understanding of some of the fundamental free-radical-mediated processes in chemical and biological systems.

Nitrones are organic compounds that are used as spin traps in both chemical and biological systems. The simplest chemical formula for a nitron is given as X-CH=NO-Y where X and Y are alkyl or aryl substituents.¹⁷ They are used as a key synthetic precursor,¹⁸ therapeutic agent,^{19,20} and a spin trapping agent for the detection and characterization of free radicals.²¹⁻²⁴ The design of the nitron spin traps plays an important role in determining how informative and sensitive the spin trapping technique may be for a particular free radical.²⁵ The addition of a nitron spin trap to a free radical leads to the formation of a stable nitroxide.

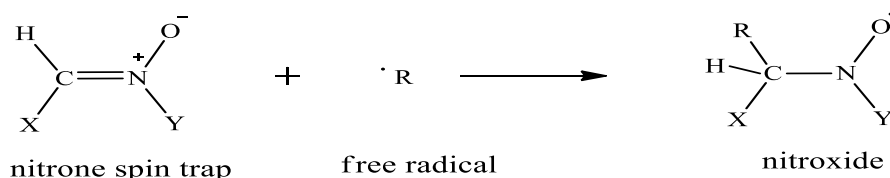


Figure 1: The addition of a nitron spin trap to a free radical to produce a nitroxide

A nitroxide is a stable free radical because of resonance stabilization of the unpaired electron between the nitrogen and the oxygen of the nitroxyl functional group.²⁶

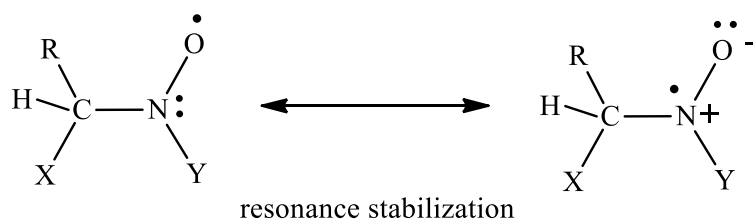


Figure 2: The resonance stabilization of nitroxide

Novelli *et al.*²⁷⁻²⁹ proposed the use of nitrones as potential pharmacological agents. They are mostly non-toxic and are used as nitrone-based therapeutics in the treatment of oxidation stress-mediated diseases such as neurodegeneration, cardiovascular disease, and cancer. They are able to survive long enough in biological systems to allow detection of the radicals. Nitrone spin traps can also be used as reagents for the detection of radicals in fuel cell research,³⁰⁻³² nanotechnology,^{33,34} catalysis,³⁵ environmental remediation,³⁶ and photodynamic therapy.³⁷⁻³⁹ Basically, there are two classes of nitrone spin traps. There are the linear nitrones: α -phenyl-N-t-butyl nitrone (PBN, see Figure 3) and its derivatives and the pyrroline-based cyclic nitrones: 5,5-dimethyl pyrroline-N-oxide (DMPO) and its derivatives.⁴⁰⁻⁴³ The linear nitrones are mostly used as spin traps in *in-vitro*, *in-vivo* and *ex-vivo* systems^{44,45} and have shown neuroprotective and antioxidant activities as well as free radical scavenger properties.⁴⁶⁻⁵⁰ The pyrroline based cyclic nitrones, DMPO and its derivatives have shown to have better ability to trap oxygen-centered radicals and reactive nitrogen species. These are 5-diethoxyphosphoryl-5-methyl-1-pyrroline N-oxide (DEPMPO),⁵¹ and 2-ethoxycarbonyl-2-methyl-3,4-dihydro-2H-pyrrole-1-oxide (EMPO),⁵² 5-tert-butoxycarbonyl-5-methyl-1-pyrroline N-oxide (BocMPO).⁵³ However, these spin traps are not effective for all free radical species. A new family of spin traps of EMPO derivatives has been synthesized and their spin adducts have shown to give reasonable stability.^{54,55} Also, research has shown that an amido derivative, 5-carbamoyl-5-methyl-1-pyrroline N-oxide (AMPO) has the highest rate constant of superoxide trapping, followed by

EMPO, with both DEPMPO and DMPO having the slowest reactivity.^{56,57} The advantages of using nitron spin traps are: they are less sensitive to light, oxygen, and water vapor; they are soluble in a large number of solvents at fairly high concentrations (~0.1M); and the spin adducts are considerably more stable because a carbon atom separates the nitron functional group from the trapped radical species.^{24,58} However, the available nitron spin traps present many disadvantages such as low water solubility, sensitivity to nucleophilic attack by water, and low stability of the spin adduct formed. Also, the information regarding the nature and structure of the trapped species is difficult to obtain from the Electron Paramagnetic Resonance (EPR) spectrum of the spin adduct.⁵⁸⁻⁶¹

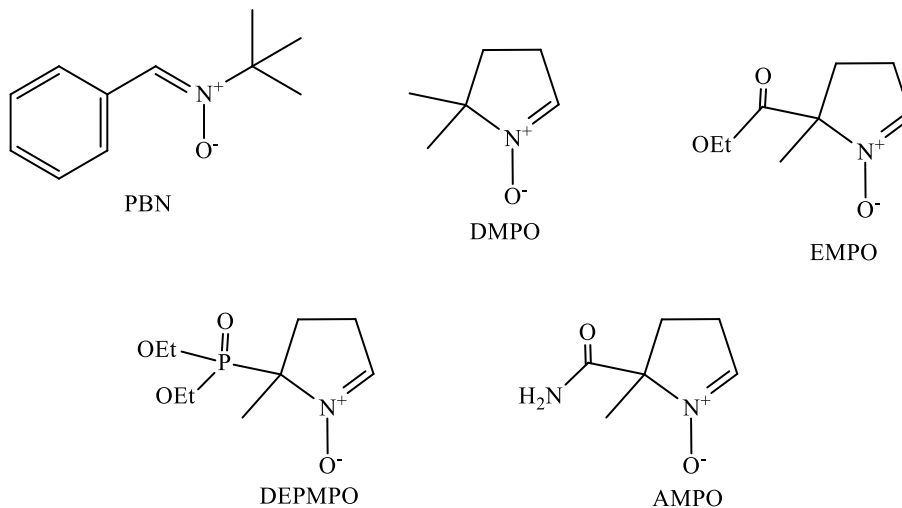


Figure 3: The chemical structures of linear PBN, cyclic DMPO, and several derivatives commonly used as spin traps

Heteroaryl nitrones consist of a heteroaromatic substituent on the carbon atom of the nitron function.⁶² New heteroaryl nitrones were synthesized through the condensation reaction between heteroaromatic aldehyde and N-monosubstituted hydroxylamines.⁶³ Porcal *et al.*⁶³ synthesized thiadiazolyl and furanoxyl nitron derivatives and found that these new heteroaryl

nitrones have an excellent ability to add free radicals to produce stable products. The EPR spectroscopy demonstrated their ability to scavenge different free radicals. They also stated that these heteroaryl nitrones showed a therapeutic potential as neuroprotective agents in preventing the death of cells from oxidative stress and damage in biological systems. Barriga *et al.*⁶⁴ experimentally studied new heteroaryl nitrones with spin trap properties. They stated that the physicochemical characterization of new heteroaryl nitrones by EPR demonstrated their capability to trap and stabilize oxygen-, carbon-, sulfur-, and nitrogen- centered free radicals.

Although, the parent nitron spin trap ($\text{H}_2\text{C}=\text{NHO}$) with radicals ($\bullet\text{H}$, $\bullet\text{CH}_3$, $\bullet\text{OH}$, and $\bullet\text{OOH}$) were computationally examined by Boyd and Boyd⁶⁵ to determine the most probable site of radical addition, the minimum-energy geometries of the spin adducts, and the energy changes involved in the addition reaction; the effects of heteroaryl (furoxanyl and thiadiazolyl) substituents on this parent nitron spin trap (see Figure 5) have not been computationally studied to understand the chemical and physical basis that can influence the spin trapping efficiency of these nitrones and the corresponding stability of their spin adducts. Hence this work aims to computationally study the spin trapping of selected biologically relevant radicals ($\bullet\text{H}$, $\bullet\text{CH}_3$, and $\bullet\text{OH}$) using these novel heteroaryl (furoxanyl and thiadiazolyl) nitrones (suggested by the work of Porcal *et al.*⁶³) using *ab initio* and Density Functional Theory (DFT) methods.

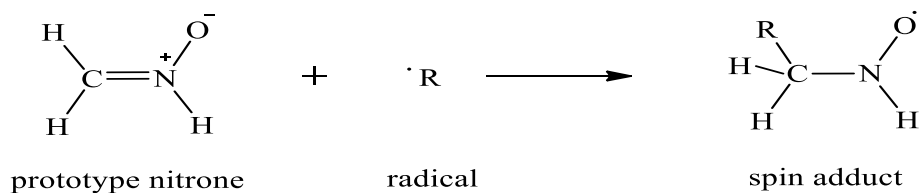
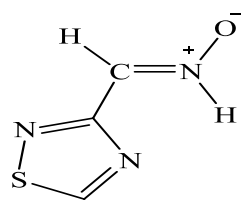
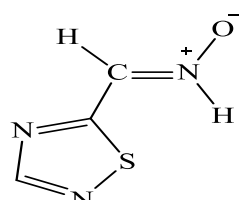


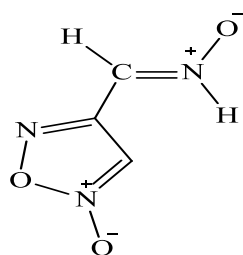
Figure 4: The reaction of a prototype nitron with a radical to form a spin adduct



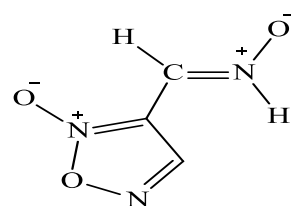
1,2,4 - thiadiazol - 3 - yl nitronium



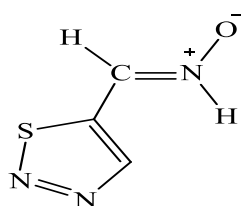
1,2,4 - thiadiazol - 5 - yl nitronium



furoxan - 4 - yl nitronium



furoxan - 3 - yl nitronium



1,2,3 - thiadiazol - 5 - yl nitronium

Figure 5: The chemical structures of the proposed novel heteroaryl nitronium spin traps

CHAPTER 2

QUANTUM MECHANICS

General Introduction to Computational Chemistry

Theoretical chemistry is the mathematical description of chemistry. Currently, there are two ways to approach theoretical chemistry problems, namely computational theoretical chemistry and non-computational theoretical chemistry. Computational theoretical chemistry deals with the numerical computation of molecular electronic structures and interactions while non-computational theoretical chemistry deals with the formulation of analytical expressions for the properties of molecules and their reactions.⁶⁶ Theoretical chemistry is further divided into two categories based on the methodology. These are static methods (based on the solution of the time independent Schrödinger Equation) and dynamic methods (based on the time dependent Schrödinger Equation).⁶⁷

Computational chemistry is a natural outgrowth of theoretical chemistry, the traditional role of which involves the creation and dissemination of a penetrating conceptual infrastructure for the chemical sciences, particularly at the atomic and molecular levels. Serious attempts have been made to obtain highly accurate quantitative information about the chemical behavior of molecules through numerical approximations to the solution of the Schrödinger equation since the appearance of digital computers.⁶⁸

There have been revolutionary expansions in the breadth and capability of computational chemistry, with an equal rise in optimism regarding the ability of computational chemistry to resolve challenging problems both of a fundamental scientific character and of clearly practical interest.⁶⁸ Computational chemistry is central to rational drug design; it contributes to the

selection and synthesis of new compounds, and guides the design of catalysts.⁶⁸ New quantum mechanical techniques have provided an understanding of the electronic properties of materials and have advanced the level of precision at which molecules, of at least moderate size, can be modeled.⁶⁹ Such techniques are used for electronic structure determination, geometry optimization and the calculation of potential energy surfaces, frequency calculations, definition of transition-state structures and reaction pathways, protein folding, electron charge distribution calculations, calculations of rate constants for chemical reactions, thermodynamics calculations such as heat of reaction and energy of activation, and calculations of many molecular bulk physical and chemical properties.⁷⁰ Computational chemistry studies may be carried out to find a starting point for a laboratory synthesis or to assist in understanding experimental data such as the position and source of spectroscopic peaks. Hence, computational chemistry is an important field of chemistry that may be applied in many areas such as material science, pharmaceuticals, nanoscience, polymer science and in the petroleum industry.

The most important tools of computational chemistry are:⁷¹

Molecular mechanics (MM): This is a purely empirical scheme based on a model of a molecule as a collection of balls (atoms) held together by springs (bonds). It is used to calculate the energy of a given molecule and the geometry for the molecule (geometry optimization). It is fast and can be used to study small molecules as well as large biological systems such as proteins and DNA.⁷² Examples of molecular mechanics methods are the Molecular Mechanics, MM2 and MM3⁷³ and the Universal Force Field (UFF) of Rappè.⁷⁴

Ab initio calculations: These are based on solutions of the Schrödinger equation from first principles without introducing empirical parameters. *Ab initio* calculations describe how

electrons in a molecule behave. The *ab initio* methods solve the Schrödinger equation to give a molecule's energy and wave functions (a mathematical function used to calculate the electron distribution of a molecule). Examples of *ab initio* methods are the Hartree–Fock (HF) method, Møller-Plesset Perturbation Theory (MPPT) methods and Configuration Interaction (CI) methods.⁷⁵

Semi-empirical calculations: These are based on the Schrödinger equation, but parameterized with empirical data to reproduce experimental observables. Examples of semi-empirical methods are AM1 of Dewar, PM3 of Stewart and PM3 of Hehre.⁷⁶

Density Functional Theory (DFT) calculations: Like *ab initio* and other semi-empirical calculations, DFT is also based on the Schrödinger equation. However, it calculates the electron density of a molecule instead of the wave function. Examples of DFT functionals are Becke, three-parameter, Lee-Yang-Parr (B3LYP), and Perdew-Burke-Ernzerhof (PBE).⁷⁷

Molecular dynamics calculations: Molecular dynamics is the computer simulation of the physical movement of atoms and molecules. It applies Newton's laws of motion to molecules by numerically solving the equations for a system of interacting particles where the forces between the particles and the potential energy are defined by molecular mechanics force fields. Thus, the motion of an enzyme can be simulated as it changes shape on binding to a substrate, or the motion of a swarm of water molecules around a molecule of solute can be modeled.⁷⁸

The Schrödinger Equation

The time dependent Schrödinger equation for one spatial dimension is of the form: ^{79,80}

$$\frac{-\hbar^2}{2m} \frac{\partial^2 \Psi(x,t)}{\partial x^2} + V(x)\Psi(x,t) = i\hbar \frac{\partial \Psi(x,t)}{\partial t} \quad (2-1)$$

The equation describes the time dependence of any quantum chemical system, where \hbar is Planck's constant, h , divided by 2π , m is the mass of the system, V is the potential energy operator, i is the imaginary operator ($\sqrt{-1}$) and $\Psi(x, t)$ is the wave function of the system, which is a function of position (including possibly spin), x , and time, t . The wave function originated from classical mechanics. The time-dependent Schrödinger equation may be used to derive the time-independent equation. The potential energy operator in the time-dependent Schrödinger equation serves to set conditions on the spatial part of the wave function and it is helpful to separate the equation into the time-independent Schrödinger equation for one dimension and the relationship for time evolution of the wave function.

$$\hat{H}\Psi = i\hbar \frac{\partial \Psi}{\partial t} \qquad \frac{-\hbar^2}{2m} \frac{\partial^2 \Psi(x)}{\partial x^2} + V(x)\Psi(x) = E\Psi(x) \quad (2-2)$$

Time evolution

Time independent equation

Solving the time evolution of the system yields the Hamiltonian operator, \hat{H} , formed from the classical Hamiltonian. E represents the energy of the system, which gives the time independent Schrödinger equation. $\psi(x)$ represents the state function, which provides information on the physical properties of the system. The time-independent Schrödinger equation may be generalized to three dimensions as:

$$\frac{-\hbar^2}{2m} \left[\frac{\partial^2 \Psi}{\partial x^2} + \frac{\partial^2 \Psi}{\partial y^2} + \frac{\partial^2 \Psi}{\partial z^2} \right] + V(x, y, z)\Psi(x, y, z) = E\Psi(x, y, z) \quad (2-3)$$

and in spherical polar coordinates as:

$$\frac{-\hbar^2}{2m} \nabla^2 \Psi + V(r, \theta, \phi) \Psi(r, \theta, \phi) = E \Psi(r, \theta, \phi) \quad (2-4)$$

where ∇^2 is a second-order differential operator known as the Laplacian:

$$\nabla^2 = \frac{\partial^2 \Psi}{\partial x^2} + \frac{\partial^2 \Psi}{\partial y^2} + \frac{\partial^2 \Psi}{\partial z^2} \quad (2-5)$$

Schrödinger's equation is currently not solvable for any system larger than that of the hydrogen atom because of interelectronic repulsion creating a three-body problem. However, a number of assumptions and approximations may be used to yield an approximate solution.

The Hamiltonian Operator

A quantum mechanical operator is associated with each measurable parameter in a physical system and the operator associated with the system energy is called the Hamiltonian.

The Hamiltonian operator, \hat{H} is the sum of the kinetic energy, T and potential energy, V

$$\hat{H} = T + V \quad (2-7)$$

where

$$T = \frac{-\hbar^2}{2m} \left[\frac{\partial^2 \Psi}{\partial x^2} + \frac{\partial^2 \Psi}{\partial y^2} + \frac{\partial^2 \Psi}{\partial z^2} \right] \quad (2-7a)$$

$$V = \frac{1}{4\pi\epsilon_0} \sum_l \sum_{m < l} \frac{q_l q_m}{r_{lm}} \quad (2-7b)$$

and where q_l and q_m are the charges on the l^{th} and m^{th} particle with a separation distance of r_{lm} , and ϵ_0 is the permittivity of free space.

A molecule is considered as a system of interacting nuclei and electrons; hence, the Hamiltonian operator for such a system is constructed as follows:

$$\hat{H} = - \sum_{i=1}^N \frac{\hbar^2}{2m_e} \nabla_i^2 - \sum_{A=1}^M \frac{\hbar^2}{2M_A} \nabla_A^2 - \sum_{i=1}^N \sum_{A=1}^M \frac{1}{4\pi\epsilon_0} \frac{Z_A e^2}{r_{iA}} + \sum_{i=1}^{N-1} \sum_{j=i+1}^N \frac{1}{4\pi\epsilon_0} \frac{e^2}{r_{ij}} + \sum_{A=1}^M \sum_{B>A}^M \frac{1}{4\pi\epsilon_0} \frac{Z_A Z_B e^2}{R_{AB}}$$

$$\hat{H} = \hat{H}_{elec}^{kin} + \hat{H}_{nuc}^{kin} + \hat{H}_{elec-nuc}^{pot} + \hat{H}_{elec-elec}^{pot} + \hat{H}_{nuc-nuc}^{pot} \quad (2-8)$$

The equations shown for the Hamiltonian operators of a molecule correspond to the operators for kinetic energy contribution of the electrons, \hat{H}_{elec}^{kin} , the kinetic energy contribution of the nuclei, \hat{H}_{nuc}^{kin} , the potential energy contribution from electron-nuclei interaction, $\hat{H}_{elec-nuc}^{pot}$, the potential energy contribution from electron-electron interaction, $\hat{H}_{elec-elec}^{pot}$, and the potential energy contribution from nuclei-nuclei interaction, $\hat{H}_{nuc-nuc}^{pot}$.

Atomic Units

The results of accurate quantum-mechanical calculations on atoms and molecules are obtained using atomic units (a. u.). Atomic units form a system of natural units, which is used for calculations. They are based on Gaussian units in which the three defining base units are the fundamental natural constants e (electronic charge), m_e (electronic mass), and \hbar . The advantage of using these units is that they bring the electronic Schrödinger equation to its intrinsically

simplest form such that the key atomic properties will have the values of one.^{81,82} In order to obtain a less complicated expression for the Hamiltonian:

$$\hat{H} = -\frac{1}{2} \sum_{i=1}^N \nabla_i^2 - \frac{1}{2} \sum_{A=1}^M \nabla_A^2 - \sum_{i=1}^{N-1} \sum_{j=i+1}^N \frac{1}{r_{ij}} + \sum_{A=1}^M \sum_{B>A}^M \frac{Z_A Z_B}{R_{AB}} \quad (2-9)$$

The atomic unit of energy, $\frac{e^2}{a_0}$, is the hartree (E_h),

$$E_h = \frac{e^2}{4\pi\epsilon_0 a_0} = 27.21138602 \text{ eV} \quad (2-10a)$$

$$a_0 = \frac{\hbar^2}{m_e e^2} = 0.5291177 \text{ \AA} \quad (2-10b)$$

where one hartree is the Coulombic repulsion between two electrons separated by a distance of one Bohr radius, or 0.52911725 Å. It is equivalent to 27.21138602 eV or $4.359744650 \times 10^{-18}$ J.

Born-Oppenheimer Approximation

The Born-Oppenheimer (BO) approximation is one of the basic concepts underlying the description of the quantum states of molecules. The physical idea behind the BO approximation is that the nuclei are much heavier than electrons. As electrons move much faster than nuclei, the nuclei can be considered as fixed with respect to the motion of the electrons. So ignoring relativistic interactions, the molecular Hamiltonian may be written as:

$$\hat{H} = -\frac{\hbar^2}{2} \sum_i m_i \nabla_i^2 - \frac{\hbar^2}{2m_e} \sum_l \nabla^2 + \sum_i \sum_{j>i} \frac{Z_i Z_j e^2}{r_{ij}} - \sum_i \sum_l \frac{Z_l e^2}{r_{li}} + \sum_m \sum_{l>m} \frac{e^2}{r_{lm}} \quad (2-11)$$

where i and j are nuclei and l and m are electrons. The first term of the equation is the kinetic energy operator for the nuclei, and the second term is the kinetic energy operator for electrons.

The third term is the electrostatic energy of repulsion between the nuclei separated by a distance r_{ij} . The fourth is the electrostatic energy for attraction between nucleus i and electron l separated by a distance r_{il} . By separating the nuclear and electronic motions, the problem can be simplified to the electronic Schrödinger equation:

$$\hat{H}_{el}\psi_{el}(q_l q_i) = E_{el}\psi_{el}(q_l q_i) \quad (2-12)$$

The nuclear kinetic energy terms in the molecular Hamiltonian are neglected and the Schrödinger equation for the electronic motion is written as:

$$(\hat{H}_{el} + V_{NN})\psi_{el} = U\psi_{el} \quad (2-13)$$

where the electronic Hamiltonian is

$$\hat{H}_{el} = -\frac{\hbar^2}{2m_e} \sum_i \nabla_i^2 - \sum_i \sum_l \frac{Z_i e^2}{r_{il}} + \sum_m \sum_{l>m} \frac{e^2}{r_{lm}} \quad (2-14)$$

Also, the nuclear repulsion term V_{NN} is given as

$$V_{NN} = \sum_i \sum_{j>i} \frac{Z_i Z_j e^2}{r_{ij}} \quad (2-15)$$

The total energy inclusive of the internuclear repulsion experienced by the nuclei i and j is the energy U . The internuclear distance r_{ij} is fixed at a constant value and hence the electronic wave functions and energies depend parametrically on the nuclear coordinates:

$$\psi_{el} = \psi_{el,n}(q_l, q_i) \quad (2-16)$$

$$U = U_n(q_n) \quad (2-17)$$

The electronic Hamiltonian is dependent on the electronic coordinates and parameterizes the nuclear coordinates. The nuclear repulsion term V_{NN} is constant for a particular nuclear configuration. Hence, V_{NN} can be neglected from the electronic Schrödinger equation giving:

$$\hat{H}_{el}\psi_{el} = E_{el}\psi_{el} \quad (2-18)$$

The purely electronic energy E_{el} is related to the total energy as

$$U = E_{el} + V_{NN} \quad (2-19)$$

The approximation yields reasonable results for the ground electronic states of diatomic molecules.

The Hartree-Fock Self Consistent Field Method

The Hartree-Fock Self-Consistent Field (HF-SCF) method is the basis for the use of atomic and molecular orbitals in many-electrons system. In many-electron systems such as Helium or Lithium, the HF-SCF method is employed to determine the accurate wave functions. The exact wave function for hydrogen can be calculated, however, the wave functions of larger systems can only be obtained if approximations are made. For an n-electron system, the Hamiltonian operator is given as:

$$\hat{H} = -\frac{\hbar^2}{2m_e} \sum_{i=1}^n \nabla_i^2 - \sum_{i=1}^n \frac{Ze^2}{r_i} + \sum_{i=1}^{n-1} \sum_{j=i+1}^n \frac{e^2}{r_{ij}} \quad (2-20)$$

where the first term represents the sum of the kinetic energy for n-electrons, the second term represents the sum of the potential energy for the attractions between the electrons and the nucleus of charge Ze . $Z = n$ for neutral atoms and the third term represents the interelectronic

repulsion term. The restriction $j > i$ rejects counting the same interelectronic repulsion twice and avoids terms like $\frac{e^2}{r_{ii}}$. As an initial approximation, the interelectronic repulsion term may be neglected to obtain a zeroth-order wave function. The zeroth-order wave function may be expressed as a product of n hydrogen-like (one-electron) orbitals:

$$\psi^{(0)} = f_1(r_1\theta_1\phi_1)f_2(r_2\theta_2\phi_2) \dots f_n(r_n\theta_n\phi_n) \quad (2-21)$$

The hydrogen-like wave functions are given as:

$$f = R_{nl}(r)Y_l^m(\theta, \phi) \quad (2-22)$$

$R_{nl}(r)$ represents the radial component of the hydrogen-like orbitals and is given by:⁸³

$$R_{nl}(r) = \left\{ \frac{n-l-1}{2n[n+1]} \right\}^{\frac{1}{2}} \left(\frac{2}{na_0} \right)^{\frac{l+3}{2}} r^l e^{-\frac{r}{na_0}} L_{n-l-1}^{2l+1} \left(\frac{2r}{na_0} \right) \quad (2-23)$$

The $L_{n-l-1}^{2l+1} \left(\frac{2r}{na_0} \right)$ term is associated Laguerre polynomials, while n and l terms are quantum numbers. The spherical harmonic, $Y_l^m(\theta, \phi)$, terms are given by:⁸⁴

$$Y_l^m(\theta, \phi) = \left[\frac{(2l+1)}{4\pi} \frac{l-|m|!}{(l+|m|)!} \right]^{\frac{1}{2}} P_l^{|m|} \cos(\theta) e^{im\phi} \quad (2-24)$$

where $P_l^{|m|} \cos(\theta)$ is the associated Legendre polynomials.

The approximate wave function is qualitatively useful; however, it is quantitatively inaccurate because all electrons experience the same nuclear charge. Therefore, the approximation can be made quantitatively accurate by employing different effective atomic numbers for different orbitals for the screening effect. Hence, there is the need to use a variational function that is not restricted to any form of orbitals. Such a function is written as:

$$\phi = g_1(r_1\theta_1\phi_1)g_2(r_2\theta_2\phi_2) \dots g_n(r_n\theta_n\phi_n) \quad (2-25)$$

The variational integral is then minimized by the functions g_i as shown below:

$$E_1 \leq \frac{\int \phi^* \hat{H} \phi d\tau}{\int \phi^* \phi d\tau} \quad (2-26)$$

where E_1 is the ground state energy for the system.

Generally, an approximation is made in the atomic calculations as:

$$g_i = h_i(r_i)Y_{li}^m(\theta_i\phi_i) \quad (2-27)$$

Hartree introduced the procedure for calculating g_i and it is termed as the Hartree Self-Consistent field (HSCF) method.^{85,86}

Hartree's Procedure

The product wave function is the first step to guess in Hartree's procedure.

$$\phi = s_1(r_1\theta_1\phi_1)s_2(r_2\theta_2\phi_2) \dots s_n(r_n\theta_n\phi_n) \quad (2-28)$$

s_i in the above equation is the normalized function of r multiplied by a spherical harmonic. The primary approximation is the central field approximation where the electrostatic electron-electron repulsion term is averaged. Each electron is considered to interact with a continuous charge distribution where by each electron sees the other electrons as being smeared out to form a static distribution of electric charges through which it moves. The potential energy of interactions between two charges q_1 and q_2 is given as

$$V_{12} = \frac{1}{4\pi\epsilon_0} \frac{q_1 q_2}{r_{12}} \quad (2-29)$$

By considering a charge density (charge per unit volume) ρ and the infinitesimal charge in the infinitesimal volume (dv), the potential energy of interaction of any electron carrying a charge Q with the static continuum is given as

$$V = \frac{Q}{4\pi\epsilon_0} \int \frac{\rho}{r} dv \quad (2-30)$$

where r is the distance between Q and ρ .

The probability density for electron i is $|s_i|^2$, hence

$$\rho = -e|s_i|^2 \quad (2-31)$$

The probability density function of the second electron with $|s_2|$ is

$$V_{12} = \frac{e^2}{4\pi\epsilon_0} \int \frac{|s_2|^2}{r_{12}} dv_2 \quad (2-32)$$

By adding the interaction with other electrons gives

$$V_{12} + V_{13} + \dots + V_{1n} = \sum_{j=2}^n \frac{e^2}{4\pi\epsilon_0} \int \frac{|s_j|^2}{r_{1j}} dv_j \quad (2-33)$$

The potential energy of interaction between an electron and the nucleus gives

$$V(r_1\theta_1\phi_1) = \sum_{j=2}^n \frac{e^2}{4\pi\epsilon_0} \int \frac{|s_j|^2}{r_{1j}} dv_j - \frac{Ze^2}{4\pi\epsilon_0 r_1} \quad (2-34)$$

The effective potential acting on an electron, from the central field approximation, is considered as a function of r only. $V(r_1\theta_1\phi_1)$ is averaged over the angles θ and ϕ to give

$$V_1(r_1) = \frac{\int_0^{2\pi} \int_0^\pi V(r_1 \theta_1 \phi_1) \sin \theta_1 d\theta_1 d\phi_1}{\int_0^{2\pi} \int_0^\pi \sin \theta d\theta d\phi} \quad (2-35)$$

Therefore, $V_1(r_1)$ is substituted in a one electron Schrödinger equation to give:

$$\varepsilon_1 t(1) = \left[-\frac{\hbar^2}{2m_e} \nabla_1^2 + V_1(r_1) \right] t_1(1) \quad (2-36)$$

where ε_1 is the energy of the orbital of electron one and $t(1)$ is the improved orbital of electron one. This procedure is repeated iteratively to improve the orbitals for each electron until the final sets of orbitals give the HSCF wave function. The general form of the differential equation for finding the Hartree-Fock orbitals is given as:

$$\mathcal{F}t_i(i) = \varepsilon_i t_i(i) \quad (2-37)$$

\mathcal{F} is the Hartree-Fock operator where

$$\mathcal{F} = \left[-\frac{\hbar^2}{2m_e} \nabla_1^2 + V_1(r_1) \right] \quad (2-38)$$

The orbital energy in the SCF approximation is calculated by iteratively solving the one electron Schrödinger equation where by the energy of the atom is the sum of the orbital energies minus a correction term. The correction term is introduced to avoid the double counting of the repulsion terms. Hence, the corrected energy is given as

$$E = \sum_{i=1}^n \varepsilon_i - \sum_{i=1}^{n-1} \sum_{j=i+1}^n \iint \frac{e^2}{4\pi\varepsilon_0} \frac{|g_i(i)|^2 |g_j(j)|^2}{r_{ij}} dv_i dv_j \quad (2-39)$$

In the equation, the first term is the sum of orbital's energies and the second term is the sum of potential energy terms counted twice.

There is an improvement on Hartree's method by using the properly antisymmetrized wave function (Slater determinant) instead of simple one-electron wavefunctions.⁸⁷ The method is ideal for a computer, because it is easily written as an algorithm as shown below:

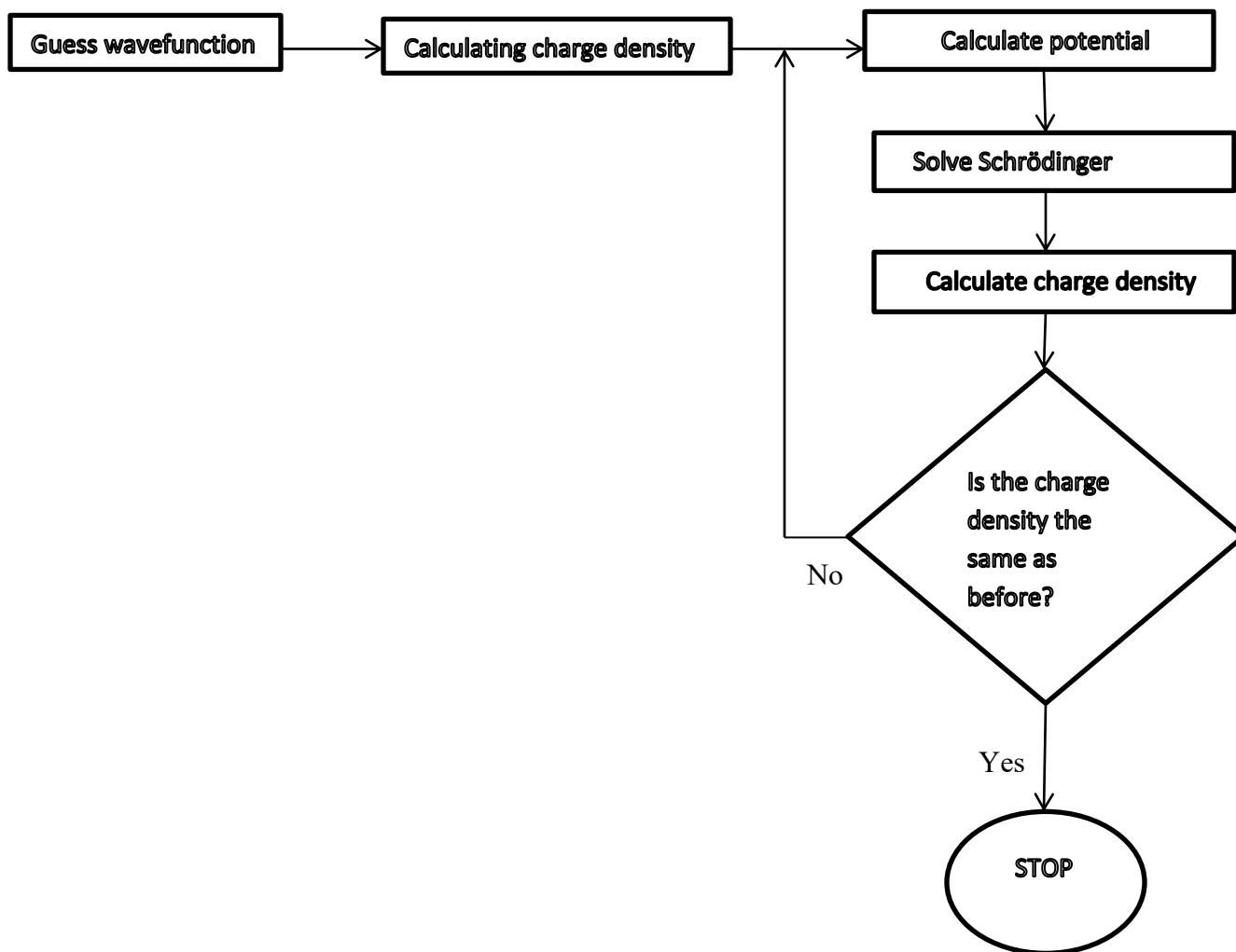


Figure 6: Algorithm for self-consistent field theory

The Wave Function as a Slater Determinant

The two important properties of the electronic wave function Ψ are that the wave function must be normalized and the electron wave function must be anti-symmetric (it changes sign when two electrons are interchanged) because electrons are fermions. The molecular Hartree-Fock (HF) wave function is written as anti-symmetrized and normalized products of spin orbitals, where each spin-orbital being a product of a spatial orbital ϕ_i and a spin function (either α or β).⁸⁸

$$\Psi = \frac{1}{\sqrt{N!}} \begin{vmatrix} \phi_1(1)\alpha_1 & \phi_1(1)\beta_1 & \cdots & \phi_N(1)\alpha_1 & \phi_N(1)\beta_1 \\ \phi_1(1)\alpha_2 & \phi_1(1)\beta_2 & \cdots & \phi_N(1)\alpha_2 & \phi_N(1)\beta_2 \\ \vdots & \vdots & & \vdots & \vdots \\ \phi_1(1)\alpha_N & \phi_1(1)\beta_N & \cdots & \phi_N(1)\alpha_N & \phi_N(1)\beta_N \end{vmatrix} \quad (2-40)$$

The vital assumption in the HF method is that the wave function of an electron, which is not a physical observable, can be represented mathematically as an anti-symmetric product of molecular orbitals. Each electron is assumed to experience an average charge distribution due to other electrons in the system, and not interact explicitly with other electrons.

The Variational Principle

The variational principle is a starting point for almost all methods that seek to find an approximate solution to the Schrödinger equation. The Variational theorem states that the energy determined from any approximate wavefunction will always be greater than the energy for the exact wavefunction. It gives the expression for the HF molecular electronic energy E_{HF} as

$$E_{HF} = \langle \psi | \hat{H}_{el} + V_{NN} | \psi \rangle \quad (2-41)$$

where ψ is the Slater determinant HF wave function, \hat{H}_{el} is the electronic Hamiltonian operator and V_{NN} is the potential energy for nuclear repulsion.

The electronic Hamiltonian gives the sum of one-electron Hamiltonians as

$$f_i = -\frac{1}{2}\nabla_i^2 - \sum_{\alpha} \frac{Z_{\alpha}}{r_{i\alpha}} \quad (2-42)$$

and the two electron operator as

$$g_{ij} = \frac{1}{r_{ij}} \quad (2-43)$$

The HF energy of a diatomic or polyatomic molecule with closed shells only is:⁸⁹

$$E_{HF} = 2 \sum_{i=1}^{n/2} H_{ii}^{core} + \sum_{i=1}^{n/2} \sum_{j=1}^{n/2} (2J_{ij} + K_{ij}) + V_{NN} \quad (2-44)$$

where H_{ii}^{core} is the core Hamiltonian for one-electron, J_{ij} , the coulomb integral and K_{ij} , the exchange integral. The HF method seeks to minimize the variational integral E_{HF} for the orbitals ϕ_i . The orbitals are assumed orthogonal and must satisfy the equation as:

$$\mathcal{F}(1)\phi_i(1) = \varepsilon_i\phi_i(1) \quad (2-45)$$

The orbital energy ε_i for normalized ϕ_i is given as:

$$\varepsilon_i = \int \phi(1)\mathcal{F}(1)\phi_i(1)dv_i \quad (2-46)$$

and by simplifying the equation gives:

$$\varepsilon_i = H_i^{core} + \sum_{j=1}^{n/2} (2J_{ij} - K_{ij}) \quad (2-47)$$

Then, the HF energy is finally obtained as:

$$E_{HF} = 2 \sum_{i=1}^{n/2} \varepsilon_i + \sum_{i=1}^{n/2} \sum_{j=1}^{n/2} (2J_{ij} + K_{ij}) + V_{NN} \quad (2-48)$$

The Roothaan-Hall Equations

Roothaan and Hall independently formulated the HF equations by using non-orthonormal Gaussian type or Slater type basis sets.^{90,91} The Roothaan-Hall equations are obtained as:

$$\sum_{v=1}^{Nbasis} (F_{\mu v} - \varepsilon_i S_{\mu v}) C_{vi} = 0; \quad \mu = 1, 2 \dots Nbasis \quad (2-49)$$

The electronic energy is calculated from the core Hamiltonian matrix $H_{\mu\nu}^{core}$, the Fock matrix $F_{\mu\nu}$ and the one electron density matrix $P_{\mu\nu}$. The Hartree-Fock energy is obtained by adding E_{elec} to the nuclear repulsion energy:

$$E_{HF} = \frac{1}{2} \sum_{\mu=1}^{Nbasis} \sum_{\nu=1}^{Nbasis} P_{\mu\nu} (F_{\mu\nu} + H_{\mu\nu}^{core}) + \sum_{A=1}^M \sum_{A<B}^M \frac{Z_A Z_B}{R_{AB}} \quad (2-50)$$

Figure 7 gives the flowchart summary of the procedure for solving the Roothaan-Hall equations.

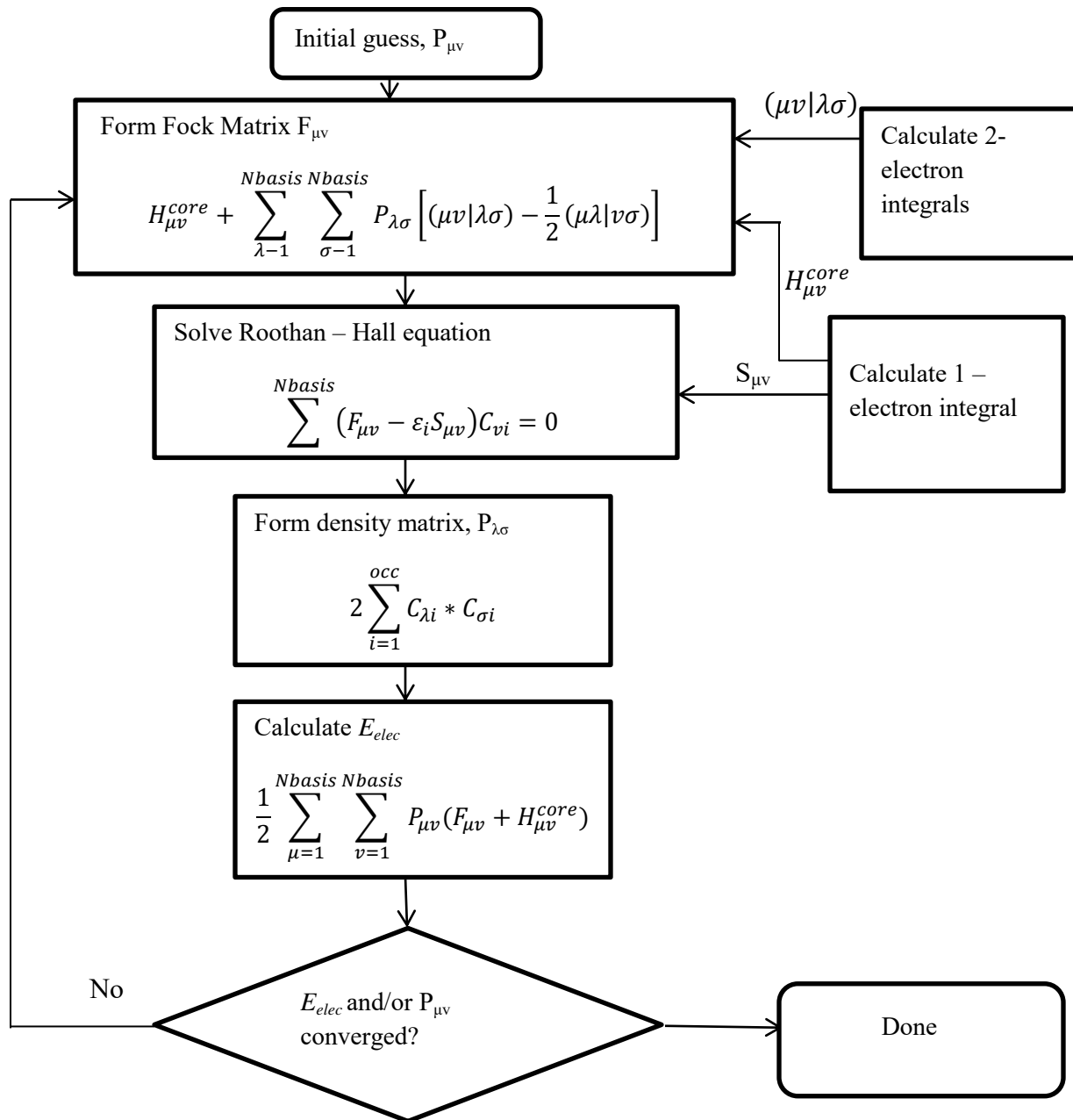


Figure 7: A flowchart summary of the procedure for solving the Roothaan-Hall equations

Restricted and Unrestricted Hartree-Fock Methods

The Restricted Hartree-Fock (RHF) method is a HF-SCF method where an atom or a molecule is a closed-shell system with all spatial orbitals (atomic or molecular) doubly occupied. The RHF method is thus not suitable for an open-shell system. Therefore, to solve this problem, two methods are used; the Restricted Open-Shell Hartree-Fock (ROHF) and the Unrestricted Hartree-Fock method (UHF). The UHF method is the common one used to treat open-shell systems to separate α and β electrons into singly occupied spatial orbitals. It is also used to solve two sets of Roothaan-Hall equations, known as the Pople-Nesbet equations:⁹²

$$F^{\alpha} C^{\alpha} = S C^{\alpha} \epsilon^{\alpha} \quad (2-51a)$$

$$F^{\beta} C^{\beta} = S C^{\beta} \epsilon^{\beta} \quad (2-51b)$$

where F^{α} and F^{β} are the Fock matrices for the α and β orbitals, C^{α} and C^{β} are the coefficient matrices for the α and β orbitals, S is the overlap matrix of the basis functions, and ϵ^{α} and ϵ^{β} are the matrices of orbital energies for the α and β orbitals. However, the disadvantage of using the UHF method is that one-electron Slater determinants for α and β electrons are not satisfactory eigenfunctions of the total spin operator, \hat{S}^2 . As a result, wave functions of higher states contaminate the total wave function. The spin contamination, which is the deviation of the expectation value of the total spin operator, $\langle \hat{S}^2 \rangle$, from $S(S+1)$ gives an indication of the contamination from higher spin states. ROHF uses doubly occupied molecular orbitals as far as possible and then singly occupied orbitals for the unpaired electrons. The ROHF method, unlike UHF, gives a satisfactory eigenfunction of the total spin operator \hat{S}^2 , (that is, it has no spin contamination from higher spin states).

Figure 8 shows a graphical representation of the orbital treatment for RHF, UHF and ROHF methods

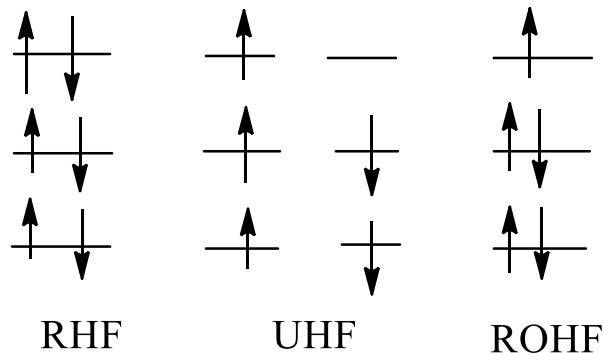


Figure 8: A graphical representation of the orbital treatment for the RHF, UHF and ROHF methods

Møller-Plesset Perturbation Theory (MPPT)

Møller-Plesset Perturbation Theory (MPPT) plays a unique role in quantum chemistry because of its treatment of dynamic electron correlation.⁹³ It is a particular formulation of many body perturbation theory (MBPT) which takes \hat{H}_0 to be the sum of the one-electron Fock operators, and treats electron correlation as the perturbation to the zeroth-order Hamiltonian.

The Hamiltonian operator, \hat{H} in MPPT is divided into two parts:

$$\hat{H} = \hat{H}_0 + \lambda V \quad (2-52)$$

where λV is a small perturbation.

Rayleigh-Schrödinger Perturbation Theory (RSPT) can be used to find the ground state wave function and energy of the system as a power series:

$$\Psi = \Psi^{(0)} + \lambda\Psi^{(1)} + \lambda^2\Psi^{(2)} + \lambda^3\Psi^{(3)} \dots \quad (2-53)$$

$$E = E^{(0)} + \lambda E^{(1)} + \lambda^2 E^{(2)} + \lambda^3 E^{(3)} \dots \quad (2-54)$$

By substituting these equations into the time-independent Schrödinger equation gives:

$$(\hat{H}_0 + \lambda\tilde{V})(\sum_i^n \lambda^i \Psi^{(i)}) = (\sum_i^n \lambda^i E^{(i)})(\sum_i^n \lambda^i \Psi^{(i)}) \quad (2-55)$$

The HF energy, $E_{\text{HF}} = E_{(0)} + E_{(1)}$ and the HF wave function $\Psi(0)$ are obtained for $n = 1$ and for $n = 0$, the sum of the electronic orbital energies \sum_i is also obtained. The corresponding MP n energies are obtained when these equations are used to solve to the n th order, for example, MP2, MP3 and MP4.

Density Functional Theory

The basic principle of Density Functional Theory (DFT) is that the energy of a molecule may be determined from the electron density $\rho(r)$ instead of the approximate many electron wave function ψ .⁹⁴ They are extremely popular and are one of the most used methods in computational chemistry, computational physics, and condensed-matter physics.⁹⁵ In 1927, DFT found its root in the works of Thomas and Fermi. They proposed that “electrons are distributed uniformly in the six dimensional phase space for the motion of an electron at the rate of two for each of volume” and that there is an effective potential field that “is itself determined by the nuclear charge and this distribution of electrons,” the kinetic energy of the system of electrons is approximated in the Thomas-Fermi method as an explicit functional of the density, but neglects exchange and correlation among electrons.⁹⁶ Dirac extended the approximation of Thomas and

Fermi, by formulating the local approximation for exchange, giving rise to the energy functional for electrons in an external potential:

$$E_{TF}[\rho] = E_T[\rho] + E_V[\rho] + E_J[\rho] + E_{XC}[\rho] \quad (2-56)$$

where E_T is the kinetic energy of the electron, E_V is the external potential energy from electron-nuclear interaction and nuclear-nuclear repulsion. E_J and E_{XC} are the electron repulsion term and the exchange correlation term respectively.

Current DFT methods originate from the Hohenberg-Kohn theorem,⁹⁷ which states that all properties of a system defined by an external potential are uniquely determined by the ground state electron density. Hence, the state electron density that gives the minimum total energy is the ground state electron density because of the variational principle.

The Hamiltonian of a given system, and its electronic energy, is divided using the Kohn-Sham approach⁹⁸

$$\begin{aligned} E[\rho(r)] &= E_{Ne}[\rho(r)] + T[\rho(r)] + E_{ee}[\rho(r)] \\ &= \int \rho(r)V_{Ne}dr + F[\rho(r)] \end{aligned} \quad (2-57)$$

where $F[\rho(r)]$ is a functional of the electron density, $\rho(r)$.

The factors of $F[\rho(r)]$ are: the kinetic energy of the non-interacting system with density $T_s[\rho(r)]$, the classical electrostatic electron-electron repulsion energy, $J[\rho(r)]$, and the exchange-correlation energy $E_{xc}[\rho(r)]$.

The DFT approach in Equation 2-57 gives the following expression for the calculation of energy:

$$\begin{aligned}
E[\rho(r) = & \\
& -\frac{1}{2}\sum_i^N \langle \varphi_i | \nabla^2 | \varphi_i \rangle + \frac{1}{2}\sum_i^N \sum_j^N \iint |\varphi_i(r)|^2 \frac{1}{r_{12}} |\varphi_j(r_2)|^2 dr_1 dr_2 - \sum_i^N \int \sum_A^M \frac{Z_A}{r_{1A}} |\varphi_i(r_i)|^2 dr_1 + \\
& E_{XC}[\rho(r)]
\end{aligned} \tag{2-58}$$

However, the exact form of the exchange correlation energy, $E_{XC}[\rho(r)]$, is unknown. Finding the accurate form of $E_{XC}[\rho(r)]$ is still an agendum of modern research in quantum chemical methods.

Logically, E_{XC} is approximated as a local or nearly local functional of the density with⁹⁹

$$E_{XC} = \int dr \rho(r) \varepsilon^{xc}([\rho], r) \tag{2-59}$$

where ε^{xc} is the energy per electron at point r that depend on only ρ . The equation shows that E_{XC} can be calculated locally at a position r and exclusively from the positional value of ρ .

The local density and the Dirac exchange energy produce the exchange energy of a uniform free electron gas as:¹⁰⁰

$$E_{LDA}^X[\rho] = -\frac{3}{2}\alpha K_D = -\frac{9}{8}\alpha \left(\frac{3}{\pi}\right)^{\frac{1}{3}} \int \rho^{\frac{4}{3}}(r) dr \tag{2-60}$$

where K_D represents the Dirac exchange-energy formula and α , an empirical constant which has a value of 2/3 for a uniform free electron gas.

The Kohn-Sham Local-Spin-Density Approximation (KS-LSDA) can correct the shortcomings of the Kohn-Sham Local Density Approximation (KS-LDA) where the LDA for exchange energy functional gives the equation:¹⁰¹

$$E_{LSDA}^X[\rho^\alpha \rho^\beta] = 2^{\frac{1}{2}} C_X \int ((\rho^\alpha)^{\frac{4}{3}} + (\rho^\beta)^{\frac{4}{3}}) dr \tag{2-61}$$

When the spin polarization energy is defined as:

$$\zeta = \frac{\rho^\alpha - \rho^\beta}{\rho} = \frac{\rho^\alpha - \rho^\beta}{\rho^\alpha + \rho^\beta} \quad (2-62)$$

then the exchange energy becomes:

$$E_{LSD}^X = \int \rho \varepsilon^x(\rho, \zeta) dr \quad (2-63)$$

with

$$\varepsilon^x(\rho, \zeta) = \varepsilon_x^0 + [\varepsilon_x^1(\rho) - \varepsilon_x^0(\rho)]f(\zeta) \quad (2-64)$$

where ε_x^0 is the exchange energy density for the spin-compensated homogeneous electron gas and ε_x^1 is the exchange energy for spin-completely-polarized homogeneous electron gas.

Since the exchange energy is the major source of error in LDA, this model has been simplified to give the generalized gradient approximation (GGA).

$$E_{GGA}^X = -\frac{3}{4} \left(\frac{3}{\pi}\right)^{\frac{1}{3}} \int dr \rho^{\frac{1}{3}} F(s) \quad (2-65)$$

with

$$S = \frac{|\nabla\rho(r)|}{2K_F\rho} \quad (2-66)$$

$$K_F = (3\pi^2\rho)^{\frac{1}{3}} \quad (2-67)$$

and

$$F(s) = (1 + 1.296S^2 + 14S^4 + 0.2S^6)^{\frac{1}{15}} \quad (2-68)$$

When the exchange function combines with the correlation functional, it reduces the error on the exchange correlation energy through the exchange functional. An example of a hybrid functional is Becke's three parameter exchange functional combined with the correlation functional of Lee, Yang and Parr (B3LYP)^{102,103} and it is written as:

$$E_{B3LYP}^{XC} = (1 - a)E_{LSDA}^X + aE_{HF}^X + bE_{B88}^X + (1 - c)E_{LSDA}^C + cE_{LYP}^C \quad (2-69)$$

where B88 is the Becke's exchange functional and LYP is the Lee-Young-Parr correlation functional.^{102,103}

The Kohn-Sham theory solves the equation:

$$F(1)\psi = \epsilon\psi \quad (2-70)$$

where

$$F(1) = -\frac{1}{2}\nabla_1^2 - \sum_{\alpha} \frac{Z_{\alpha}}{r_{1\alpha}} + \sum_j J_j(1) + V^{XC} \quad (2-70a)$$

$$V^{XC} = \frac{\partial E^{XC}}{\partial \rho} \quad (2-70b)$$

The electron density is obtained from the sum over the occupied orbitals when the Kohn-Sham orbitals are determined:

$$\rho = \sum_i |\psi_i|^2 \quad (2-71)$$

Hybrid functionals such as BLYP; Becke exchange, Perdew and Wang correlation(B3PW91) and Becke exchange, Perdew correlation (B3P86) have attained great success in the computational chemistry.¹⁰⁴ This is due to the accuracy of the results they give for a large variety of

compounds, particularly organic molecules,¹⁰⁵ the prediction of molecular geometries, and harmonic vibrational frequencies.¹⁰⁴

Basis Sets

A basis set is defined as a set of functions (called basis functions) which are combined in linear combinations to create molecular orbitals. Basis functions are atomic orbitals described by a mathematical function based on spherical or Cartesian coordinates.

$$\varphi_i = \sum_{\mu=1}^{N_{basis}} C_{\mu i} X_{\mu} \quad (2-72)$$

The two most common basis functions are Slater-type orbitals and Gaussian-type orbitals. Historically, Slater-type orbitals (STOs) were used as basis functions of molecular orbitals due to their similarity to the atomic orbitals of the hydrogen atom.

$$\chi_i(\zeta, n, l, m; r, \theta, \phi) = N r^{n-1} e^{-\zeta r} Y_{lm}(\theta, \phi) \quad (2-73)$$

where ζ is an exponent, Y_{lm} is a spherical-harmonic function that describes the shape (the angular momentum part); N is a normalization constant; r , θ , and ϕ are the spherical coordinates and n , l , m are the principal, angular momentum, and magnetic quantum numbers respectively. $e^{-\zeta r}$, the exponential term, represents the energy of electrons near the nucleus. STOs are no longer used because they are difficult to evaluate the resulting secular determinants. Multicenter integrals, which involve more than one nuclear center, are difficult to calculate. This problem may be overcome by using Gaussian-type functions (GTFs)

$$g(\alpha, l, m, n; x, y, z) = N e^{-\alpha(x^2+y^2+z^2)} x^l y^m z^n \quad (2-74)$$

$$= N e^{-\alpha r^2} x^l y^m z^n \quad (2-75)$$

where x , y , and z are spherical coordinates; n , l , m are integral exponents of Cartesian coordinates, and α is the exponent instead.

STO-nG, where n is an integer, is the most common minimal basis set. The n value gives the number of Gaussian primitive functions, which comprise a single basis function. Minimal basis sets give rough results that are insufficient for research-quality publication; however they are much cheaper than their larger counterparts. Examples of commonly used minimal basis sets are: STO-3G, STO-4G, STO-6G and STO-3G*.

The split-valence basis sets describe the inner-shell electron using a single Slater orbital and the valence shell by a sum of Slater orbitals. They have a larger number of basis functions per atom. Two or more sizes of basis functions are given to the valence shells of each atom, which allow the orbitals to change size. The notation for the split-valence basis sets is X-YZg. X represents the number of primitive Gaussians, comprising each core atomic orbital basis function. the Y and Z represent the valence orbitals that are composed of two basis functions each, the first one is a linear combination of Y primitive Gaussian functions and the second one is a linear combination of Z primitive Gaussian functions. The presence of two numbers after the hyphen indicates that the basis set is a split-valence double-zeta basis set. X-YZWg and X-YZWWg are split-valence triple- and quadruple-zeta basis sets respectively.

Polarized basis sets add orbitals with a higher angular momentum than the ground state electronic configuration of each atom at the Hartree-Fock level. These could improve the split valence basis sets by adding orbitals with different shapes. The 6-31G(d) (also called 6-31G*) and the 6-311G(d, p) basis sets are the examples of polarized basis sets.

Basis sets with added diffuse functions are important for systems where electrons are far from the nucleus such as anions, and molecules with lone pairs of electrons. These allow diffuse orbitals to occupy larger regions in space. An example of a diffuse basis set is the 6-311+G(d, p) basis set.

Polarization effects occur when orbitals of higher orbital quantum number are added to the mathematical expression of a given orbital, for example 3d orbital and the 2p orbital. When 3d orbitals are added to the 2p orbital functions for second row elements of the periodic table, an asterisk (*) alternative used to indicate the basis set (as above). Also, a double asterisk indicates that polarization is being added on hydrogen 1s orbitals. 3-21G* is an exception to this in which the asterisk denotes the addition of a d-orbital to the second row atoms, that is, 3-21G(d). Also, when different orbitals are added, the added orbitals are given in parenthesis, that is, 6-31G(d,p) means that extra sets of p and d functions are added to non-hydrogen atoms and p extra functions are added to hydrogen, thus denoting 6-31G**. Examples of commonly used split-valence basis sets are 3-21G, 3-21G* and 6-311G*.

Dunning and coworkers¹⁰⁶ developed the correlation consistence (cc) basis sets such as cc-pVDZ, cc-pVTZ, cc-pVQZ, cc-pV5Z, and cc-pV6Z. They are denoted as cc-pVnZ, where n ranges from 2 to 6. The 'cc-p', stands for 'correlation-consistent polarized', the 'V' indicate that they are valence-only basis sets while Z represents zeta. The Complete Basis Set methods were developed by Petersson and co-workers as a model chemistry.¹⁰⁷⁻¹⁰⁹ They make use of a complete basis set (CBS) extrapolation of the correlation energy based on the asymptotic convergence of pair natural orbital expansions.¹¹⁰⁻¹¹⁴ CBS methods are important in that, at higher and higher levels of correlation, the contribution of the correction to the total energy can be determined to less accuracy than at lower levels of theory. Thus, these methods use relatively

large basis sets for the structure calculation, medium sized basis sets for the second-order correlation correction, and small sized basis sets for higher order correlation corrections. Also, empirical corrections are added as necessary.¹¹⁵

CHAPTER 3

RESULTS AND DISCUSSION

Computational Details

All calculations were carried out using NWChem from the Molecular Sciences Laboratory Software Group of Pacific Northwest National Laboratory.^{116,117} Extensible Computational Chemistry Environment software was used to manage the calculations and generate pictorial representations.¹¹⁸ All geometries of the nitrones were fully optimized at Hartree-Fock (self-consistent field) (HF-SCF) and Density Functional Theory (DFT) with the 6-31G* basis set levels of theory, and the single point calculations were done on the HF-SCF optimized geometries at second-order Møller-Plesset Perturbation Theory (MP2) with the cc-pVDZ, cc-pVTZ and cc-pVQZ basis sets to obtain energies. All equilibrium geometries were characterized by the absence of imaginary frequencies. The geometries of DMPO, PBN and FxBN were fully optimized at DFT/m06/6-31G* and HF/6-31G*. In addition, Milliken population analyzes were used to obtain spin and charge populations.

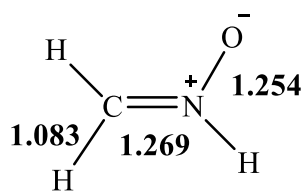
Discussion of the Results

Table 1 shows calculated bond lengths and bond angles for formaldonitrone and the new heteroaryl nitrones at HF/6-31G*. Formaldonitrone is a parent nitrone and has a planar geometry. It has C=N and N-O bond lengths of 1.269 Å and 1.254 Å, respectively. The C-H bond length is 1.083 Å. The CNO bond angle for formaldonitrone is 128.3°. The new heteroaryl substituents considered in this work are 1,2,3-thiadiazol-5-yl, 1,2,4-thiadiazol-3-yl, 1,2,4-thiadiazol-5-yl, furoxan-3-yl, and furoxan-4-yl. When the hydrogen, H attached to the nitrone is substituted by these heteroaryl substituents, the bond lengths and the bond angles shorten or

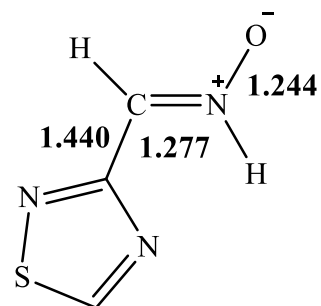
lengthen depending on the nature of the substituents. The C=N bonds lengthen by 0.006 Å - 0.010 Å while the N-O bond lengths shorten by 0.003 Å – 0.013 Å. The C-C_{heteroaryl} bond lengths lengthen in the range of 1.428 Å – 1.440 Å. In addition, there is a decrease in the CNO bond angle in the range of 127.3° - 127.8°. The O atom in the nitrones is highly electronegative because of its higher charge population than the N atom and the C atom. Figure 9 shows the optimized geometry of formaldonitrone and the new heteroaryl nitrones.

Table 1: Calculated bond lengths for formaldonitrone and the new heteroaryl nitrones at HF/6-31G*

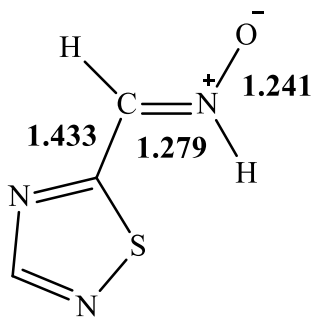
Nitron Spin Trap	Calculated bond lengths (Å)			Calculated bond angles (deg.)
	C=N	N-O	C-C _{heteroaryl}	CNO
Formaldonitrone	1.269	1.254	1.083	128.3
1,2,4-thiadiazol-3-yl nitron	1.277	1.244	1.440	127.8
1,2,4-thiadiazol-5-yl nitron	1.279	1.241	1.433	127.5
Furoxan-4-yl nitron	1.277	1.242	1.436	127.5
Furoxan-3-yl nitron	1.275	1.251	1.428	127.3
1,2,3-thiadiazol-5-yl nitron	1.278	1.246	1.433	127.3



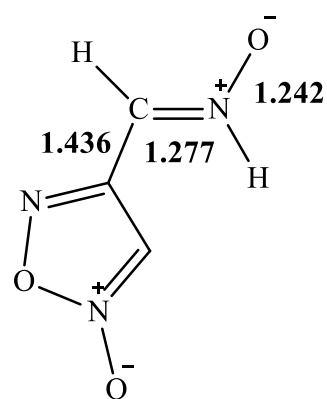
formaldonitrone



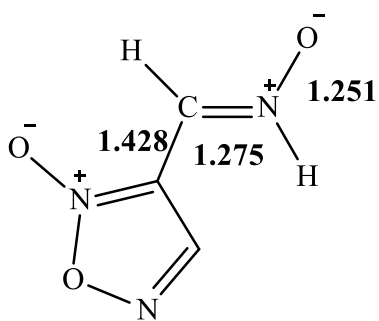
1,2,4 - thiadiazol - 3 - yl nitrone



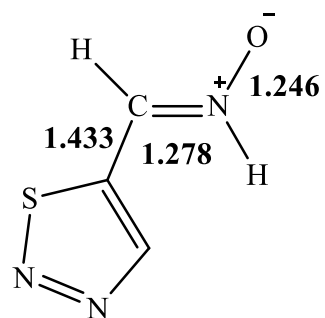
1,2,4 - thiadiazol - 5 - yl nitrone



furoxan - 4 - yl nitrone



furoxan - 3 - yl nitrone



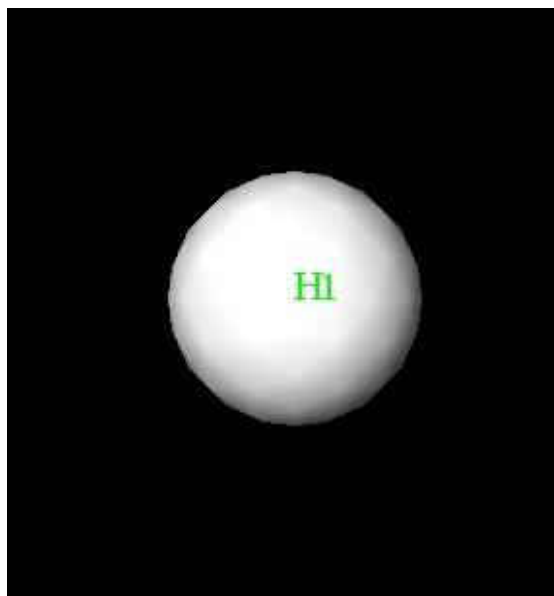
1,2,3 - thiadiazol - 5 - yl nitrone

Figure 9: The optimized geometry of formaldonitrone and the new heteroaryl nitrones. All bond lengths are in Å

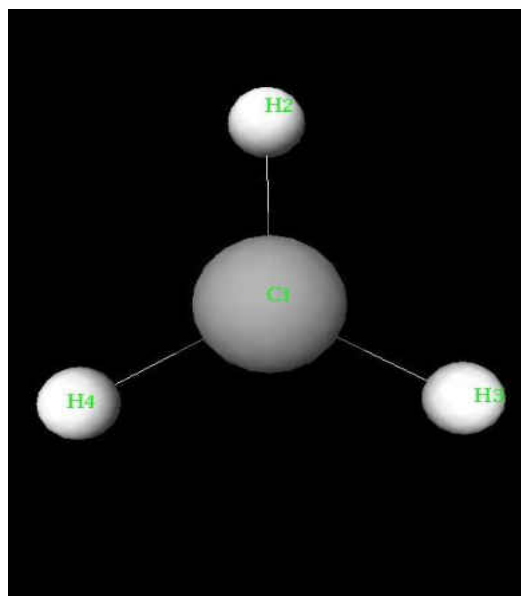
Table 2 shows the total energies of selected biologically relevant radicals, $\bullet\text{H}$, $\bullet\text{CH}_3$, $\bullet\text{OH}$, and their dipole moments. Among the three radicals, $\bullet\text{OH}$ radical has the highest polarity of 1.94 D. It also has the lowest energy. The $\bullet\text{CH}_3$ radical has no polarity because its molecular geometry is trigonal planar. The optimized geometries for the radicals are shown in Figure 10. The order of increasing reactivity for radical addition to nitrones is $\bullet\text{H} < \bullet\text{CH}_3 < \bullet\text{OH}$, which correlates with the inductive effect of each radical as well as the radical's reduction potential.¹¹⁹ The spin and charge populations of each radical give insights into the reactivity to nitrones.

Table 2: Energies of selected biologically relevant radicals and their dipole moments

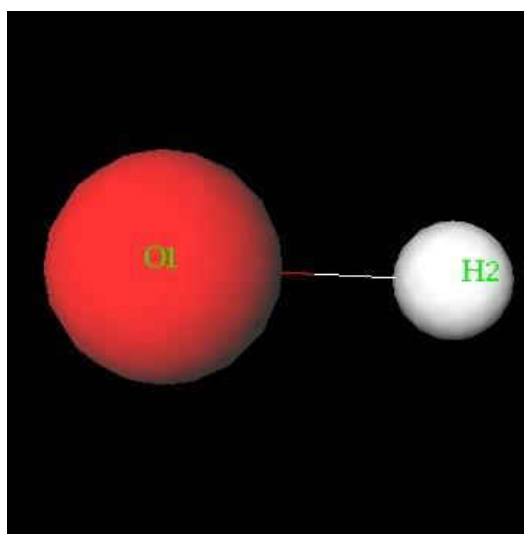
Radical	Energy (E_h) HF/6-31G*	Energy (E_h) DFT/m06/6-31G*	Dipole Moment (D)	Reduction Potential (V)
$\bullet\text{H}$	-0.49820	-0.49792	0	0
$\bullet\text{CH}_3$	-39.63860	-39.79542	0	1.90
$\bullet\text{OH}$	-75.22340	-75.64294	1.94	2.31



Hydrogen Radical



Methyl Radical



Hydroxyl Radical

Figure 10: NWChem optimized geometries of biologically relevant radicals

Table 3 shows the relative energies of formaldonitrone and new heteroaryl nitrones at the HF/6-31G*, MP2/cc-pVDT, MP2/cc-pVTZ, MP2/cc-pVQZ, the MP2 CBS limit, and DFT/m06/6-31G* levels of theory (from HF/6-31G* optimized structures), as well as the dipole moments obtained at HF/6-31G*. The relative energies show that the new heteroaryl nitrones are more stable due to the electronic effects of new heteroaryl substituents. Because of the high stability of the new heteroaryl nitrones, the nitrones show a great capacity to scavenge free radicals.^{63,64} Thus the order of increasing stability of the spin traps is formaldonitrone < furoxanyl nitrone < thiadiazoyl nitrone. Also, the polarity of the spin traps is decreasing in the order: 1,2,4-thiadiazol-3-yl nitrone > furoxan-3-yl nitrone > 1,2,4-thiadiazol-5-yl nitrone > furoxan-4-yl nitrone > 1,2,3-thiadiazol-5-yl nitrone.

Table 3: Energies of formaldonitrone and the new heteroaryl nitrones at the HF/6-31G*, MP2/cc-pVDT, MP2/cc-pVTZ, MP2/cc-pVQZ, the MP2 CBS limit, and DFT/m06/6-31G* levels of theory. The dipole moments were calculated at the HF/6-31* level

Nitrone Spin Trap	HF/6-31G* (E _h)	MP2/cc-pVDT (E _h)	MP2/cc-pVTZ (E _h)	MP2/cc-pVQZ (E _h)	E _{CBS} (E _h)	DFT/m06/6-31G* (E _h)	Dipole moment (D)
Formaldonitrone	-168.80921	-169.32379	-169.50071	-169.55895	-169.59220	-169.69089	4.47
1,2,4-thiadiazol-3-yl nitrone	-750.95291	-752.19826	-752.60343	-752.73909	-752.81677	-753.46128	5.65
1,2,4-thiadiazol-5-yl nitrone	-750.94373	-752.1917	-752.59696	-752.73268	-752.81040	-753.45461	1.97
Furoxan-4-yl nitrone	-502.97481	-504.49516	-504.96856	-505.13299	-505.22777	-505.53385	1.76
Furoxan-3-yl nitrone	-502.97470	-504.47422	-504.96811	-505.13295	-505.22729	-505.53513	4.26
1,2,3-thiadiazol-5-yl nitrone	-750.89840	-752.15743	-752.56122	-752.69673	-752.77436	-753.41851	0.26

As may be seen in Tables 4 and 5, the reaction of biologically relevant radicals with the new heteroaryl nitrones at the C- and O-sites shows that, generally, the spin trapping of biologically relevant radicals by the new heteroaryl nitrones at the C-sites is more exothermic than the spin trapping at the O-sites. This is because the N-O bond of the spin adducts at the C-site serves as a resonance contributor. This is due to the high spin populations of N and O for the spin adducts at the C-sites. However, at the O-sites of the spin adducts, the C atom of the spin adduct carries the higher spin population than N and O, hence the N-O bond does not serve as a resonance contributor. From Table 4, thermodynamically, the reactions of •OH with the new heteroaryl nitrones have the highest exothermicities as compared to the reactions of •H and •CH₃. Hence, the spin adducts formed from the spin trapping reactions with •OH have the highest stability. The furoxan-3-yl spin adduct with •OH has the largest energy change (most negative) of -671.99673 kJ/mol and it is the most stable spin adduct for HF/6-31G*, while furoxan-4-yl has the largest change (-379.41101 kJ/mol) for DFT/m06/6-31G*.

Also from Table 5, the spin trapping reactions of $\bullet\text{CH}_3$ are endothermic in contrast to those for $\bullet\text{H}$ and $\bullet\text{OH}$. However, from Table 5b, the spin trapping reactions of $\bullet\text{OH}$ with the new heteroaryl nitrones, except 1,2,4-thiadiazol-3-yl nitron, are less exothermic as compared to the spin trapping reactions of $\bullet\text{H}$ and $\bullet\text{CH}_3$. Thus, the spin trapping reactions of $\bullet\text{H}$ by the new heteroaryl nitrones at the O-sites give the highest exothermicities, hence the reactions produce the most stable spin adducts.

Table 4: Energies of the spin trapping reactions of selected radicals with formaldonitrone and the new heteroaryl nitrones at the C-site for (a) HF/6-31G* and (b) DFT/m06/6-31G*

(a)

Spin Trap	ΔE (kJ/mol) ^a		
	•H	•CH ₃	•OH
Formaldonitrone	-305.66071	-39.96011	-641.40965
1,2,4-thiadiadozol-3-yl nitrone	-273.83965	-13.62635	-615.33844
1,2,4-thiadiazol-5-yl nitrone	-302.35258	-32.81875	-647.00197
Furoxan-4-yl nitrone	-330.78675	-60.62280	-670.63147
Furoxan-3-yl nitrone	-335.40763	-63.79965	-671.99673
1,2,3-thiadiazol-5-yl nitrone	-303.06147	-33.71142	-654.09082

(b)

Spin Trap	ΔE (kJ/mol) ^a		
	•H	•CH ₃	•OH
Formaldonitrone	-274.86360	-241.23094	-372.08586
1,2,4-thiadiadozol-3-yl nitrone	-235.27106	-207.62454	-336.56285
1,2,4-thiadiazol-5-yl nitrone	-250.05262	-222.45862	-377.67818
Furoxan-4-yl nitrone	-265.88439	-230.28261	-379.41101
Furoxan-3-yl nitrone	-261.63108	-230.67643	-378.25579
1,2,3-thiadiazol-5-yl nitrone	-247.95222	-317.23917	-367.17618

^a ΔE = energy change for gas phase species at equilibrium bond lengths at 0K

$$\Delta E = E_{\text{adduct}} - [E_{\text{spin}} + E_{\text{radical}}]$$

Spin trap and adduct energies are listed in the Appendix.

Table 5: Energies of the spin trapping reactions of biologically relevant radicals with the new heteroaryl nitrones the O-site for (a) HF/6-31G* and (b) DFT/m06/6-31G*

(a)

Spin Trap	ΔE (kJ/mol) ^a		
	•H	•CH ₃	•OH
Formaldonitrone	-125.18384	158.71148	-214.63463
1,2,4-thiadiadazol-3-yl nitrone	-180.81819	54.584145	-337.14046
1,2,4-thiadiazol-5-yl nitrone	-261.44729	31.007155	-351.13437
Furoxan-4-yl nitrone	-293.11082	-0.84016	-387.94388
Furoxan-3-yl nitrone	-241.70353	55.266775	-311.06924
1,2,3-thiadiazol-5-yl nitrone	-280.29838	12.261085	- ^b

(b)

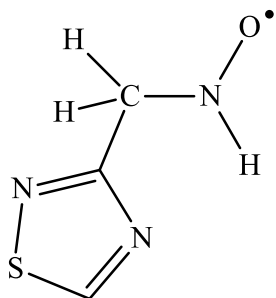
Spin Trap	ΔE (kJ/mol) ^a		
	•H	•CH ₃	•OH
Formaldonitrone	-102.31574	-51.03972	26.93763
1,2,4-thiadiadazol-3-yl nitrone	-159.23658	-134.24182	-164.04124
1,2,4-thiadiazol-5-yl nitrone	-216.91881	-148.55079	-107.01538
Furoxan-4-yl nitrone	-206.15426	-143.74613	-98.95510
Furoxan-3-yl nitrone	-171.99651	-111.11116	-24.18086
1,2,3-thiadiazol-5-yl nitrone	-217.44391	-154.37940	-107.96056

^a ΔE = energy change for gas phase species at equilibrium bond lengths at 0K

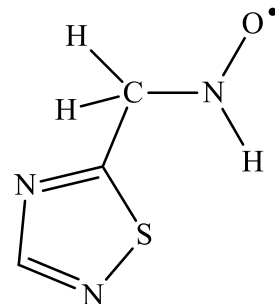
$$\Delta E = E_{\text{adduct}} - [E_{\text{spin}} + E_{\text{radical}}]$$

Spin trap and adduct energies are listed in the Appendix.

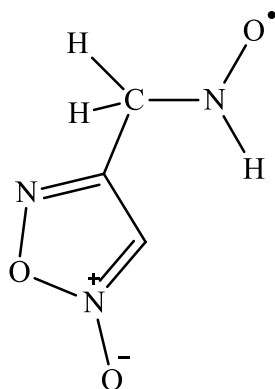
^bStructure optimized with an O-O bond length beyond accepted covalent bond length



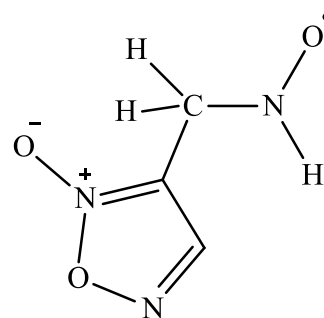
1,2,4-thiadiazol-3-yl spin adduct



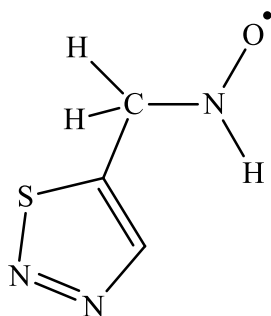
1,2,4-thiadiazol-5-yl spin adduct



furoxan-4-yl spin adduct

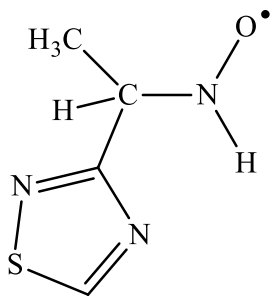


furoxan-3-yl spin adduct

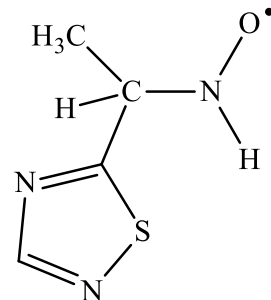


1,2,3-thiadiazol-5-yl spin adduct

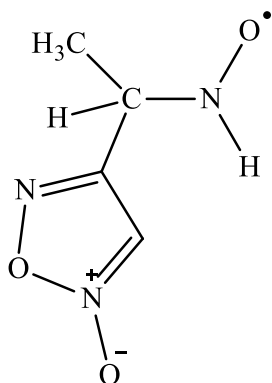
Figure 11: ChemDraw[®] representations of the new heteroaryl spin adducts with •H added the C-site carbon



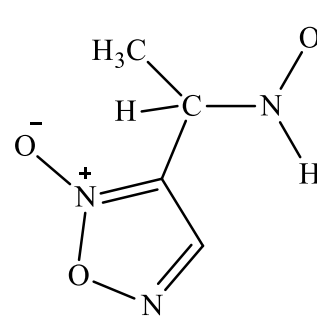
1,2,4-thiadiazol-3-yl spin adduct



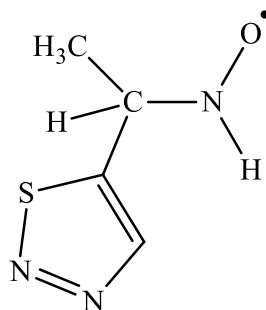
1,2,4-thiadiazol-5-yl spin adduct



furoxan-4-yl spin adduct

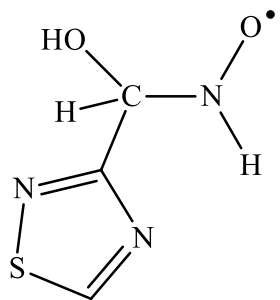


furoxan-3-yl spin adduct

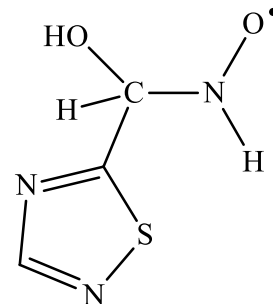


1,2,3-thiadiazol-5-yl spin adduct

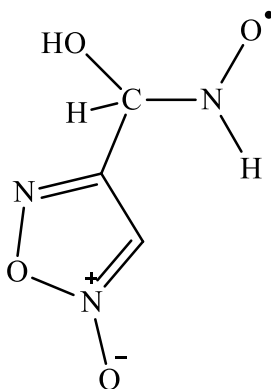
Figure 12: ChemDraw[®] representations of the new heteroaryl spin adducts with •CH₃ added at the C-site carbon



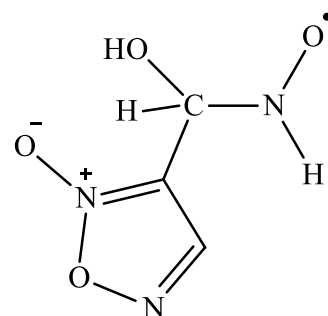
1,2,4-thiadiazol-3-yl spin adduct



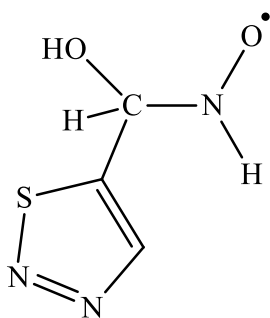
1,2,4-thiadiazol-5-yl spin adduct



furoxan-4-yl spin adduct

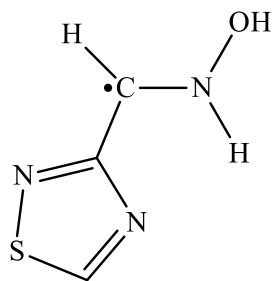


furoxan-3-yl spin adduct

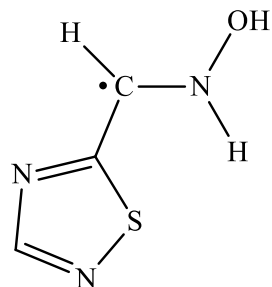


1,2,3-thiadiazol-5-yl spin adduct

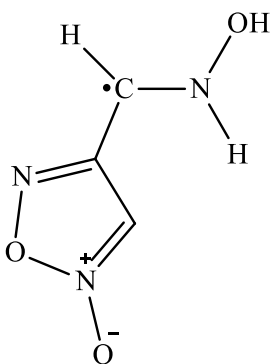
Figure 13: ChemDraw[®] representations of the new heteroaryl spin adducts with •OH added at the C-site carbon



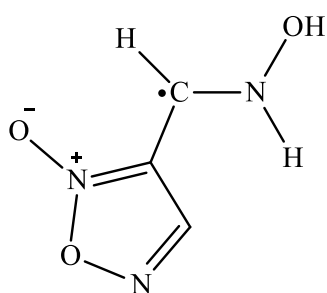
1,2,4-thiadiazol-3-yl spin adduct



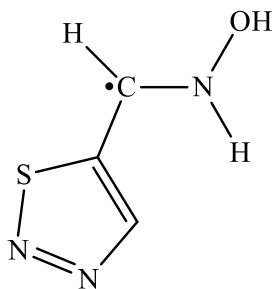
1,2,4-thiadiazol-5-yl spin adduct



furoxan-4-yl spin adduct

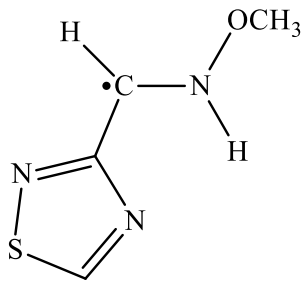


furoxan-3-yl spin adduct

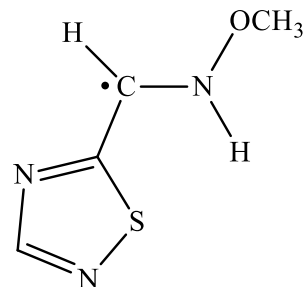


1,2,3-thiadiazol-5-yl spin adduct

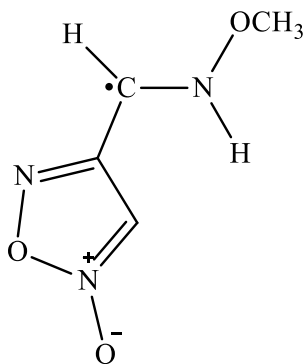
Figure 14: ChemDraw[®] representations of the new heteroaryl spin adducts with •H added at the O-site oxygen



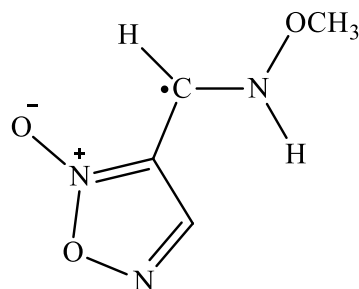
1,2,4-thiadiazol-3-yl spin adduct



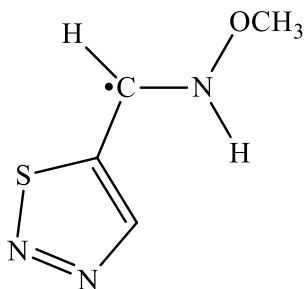
1,2,4-thiadiazol-5-yl spin adduct



furoxan-4-yl spin adduct

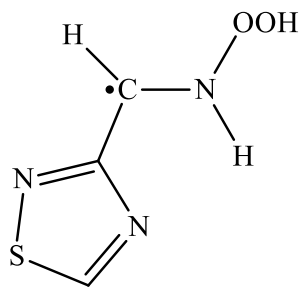


furoxan-3-yl spin adduct

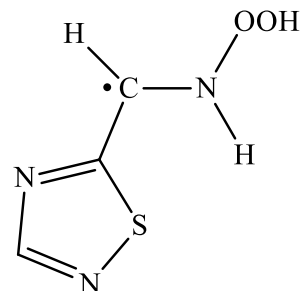


1,2,3-thiadiazol-5-yl spin adduct

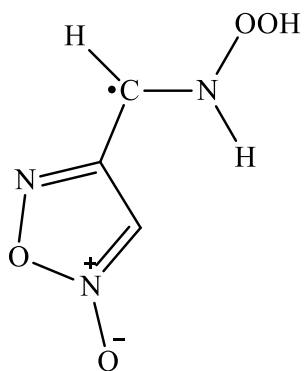
Figure 15: ChemDraw[®] representations of the new heteroaryl spin adducts with •CH₃ added at the O-site oxygen



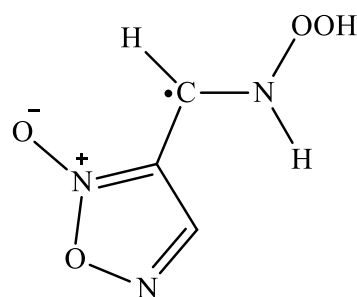
1,2,4-thiadiazol-3-yl spin adduct



1,2,4-thiadiazol-5-yl spin adduct

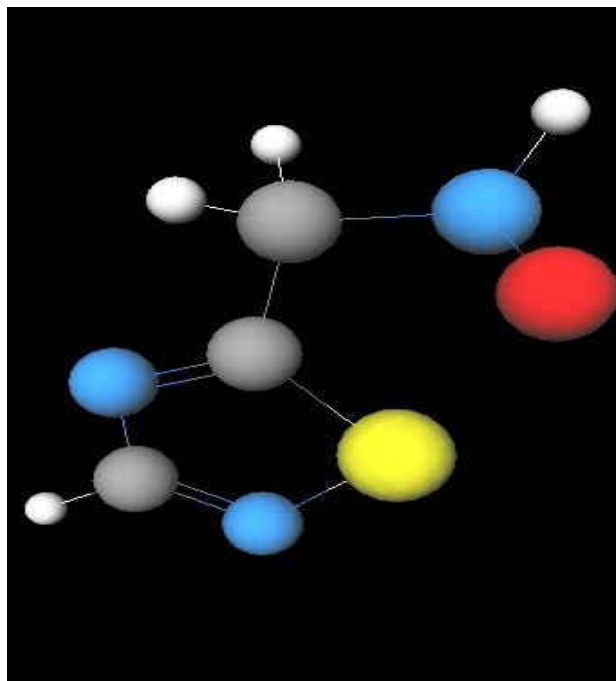


furoxan-4-yl spin adduct

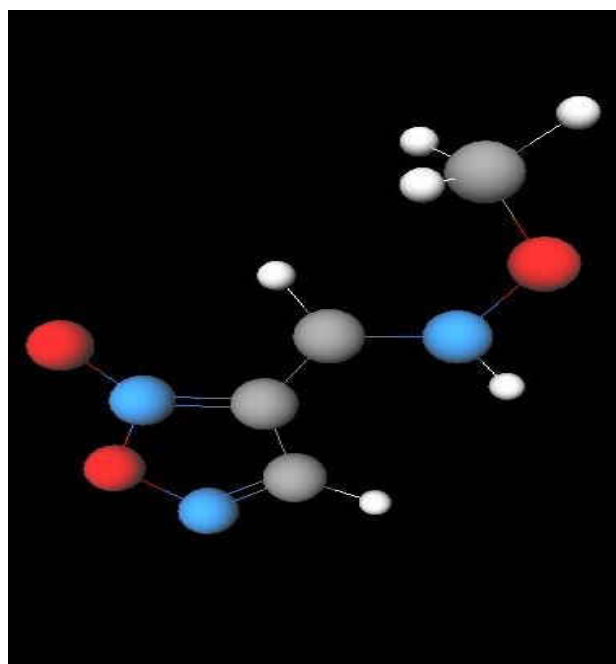


furoxan-3-yl spin adduct

Figure 16: ChemDraw[®] representations of the new heteroaryl spin adducts with $\bullet\text{OH}$ added at the O-site oxygen



a) Hydrogen radical at the C-site of 1,2,4-thiadiazol-5-yl nitrone



b) Methyl radical at the O-site of furoxan-3-yl nitrone

Figure 17: NWChem optimized geometries of example new heteroaryl spin adducts at the C- and O-sites. The colors follow standard colors: red - oxygen, hydrogen - white, grey - carbon, blue - nitrogen, and yellow - sulfur

The energetics of the spin trapping reactions of biologically relevant radicals with the new heteroaryl nitrones at both the C- and O-sites are shown in Tables 6, 7, and 8.

Thermodynamically, the spin trapping reactions of di •OH are highly exothermic, hence their diadducts are very stable. The spin trapping reactions of di •CH₃ with the new heteroaryl nitrones have the least exothermicities as compared to di •H and di •OH. In addition, the diadducts are more stable than the mono spin adducts at the C-sites and the mono spin adduct at the O-sites. The double spin adducts are known to occur experimentally^{120,121} having been observed using liquid chromatography and mass spectroscopy.¹²² Even though the double spin adducts are generally stable, they are EPR inactive because they are diamagnetic.

Table 6: Energies of the spin trapping reactions of •H with formaldonitrone and the new heteroaryl nitrones at both C- and O-sites at (a) HF/6-31G* and (b) DFT/m06/6-31G*

(a)

Spin Trap	Energy (E_h)		ΔE	
	Parent	Diadduct	E_h	kJ/mol
Formaldonitrone	-168.80921	-170.01157	-0.20596	-540.74798
1,2,4-thiadiadozol-3-yl nitrone	-750.95291	-752.14573	-0.19642	-515.70071
1,2,4-thiadiazol-5-yl nitrone	-750.94373	-752.14639	-0.20626	-541.53563
Furoxan-4-yl nitrone	-502.97481	-504.17685	-0.20564	-539.90782
Furoxan-3-yl nitrone	-502.97470	-504.17701	-0.20591	-540.61671
1,2,3-thiadiazol-5-yl nitrone	-750.89840	-752.10158	-0.20678	-542.90089

(b)

Spin Trap	Energy (E_h)		ΔE	
	Parent	Diadduct	E_h	kJ/mol
Formaldonitrone	-168.80921	-170.91393	-0.22720	-596.51360
1,2,4-thiadiadozol-3-yl nitrone	-750.95291	-754.67003	-0.21291	-558.99521
1,2,4-thiadiazol-5-yl nitrone	-750.94373	-754.67160	-0.22115	-580.62933
Furoxan-4-yl nitrone	-502.97481	-506.75566	-0.22597	-593.28424
Furoxan-3-yl nitrone	-502.97470	-506.75056	-0.21959	-576.53355
1,2,3-thiadiazol-5-yl nitrone	-750.89840	-754.63406	-0.21971	-576.84861

Table 7: Energies of the spin trapping reactions of $\bullet\text{CH}_3$ with formaldonitrone and the new heteroaryl nitrones at both C- and O-sites at (a) HF/6-31G* and (b) DFT/m06/6-31G*

(a)

Spin Trap	Energy (E_h)		ΔE	
	Parent	Diadduct	E_h	kJ/mol
Formaldonitrone	-168.80921	-248.0778	0.00861	22.60556
1,2,4-thiadiadozol-3-yl nitrone	-750.95291	-830.21125	0.01886	49.51693
1,2,4-thiadiazol-5-yl nitrone	-750.94373	-830.21313	0.00780	20.47890
Furoxan-4-yl nitrone	-502.97481	-582.24307	0.00894	23.47197
Furoxan-3-yl nitrone	-502.97470	-582.24686	0.00504	13.23252
1,2,3-thiadiazol-5-yl nitrone	-750.89840	-830.16683	0.00877	23.02564

(b)

Spin Trap	Energy (E_h)		ΔE	
	Parent	Diadduct	E_h	kJ/mol
Formaldonitrone	-168.80921	-249.47214	-0.19041	-499.92146
1,2,4-thiadiadozol-3-yl nitrone	-750.95291	-833.22912	-0.17700	-464.71350
1,2,4-thiadiazol-5-yl nitrone	-750.94373	-833.23218	-0.18673	-490.25962
Furoxan-4-yl nitrone	-502.97481	-585.30874	-0.18405	-483.22328
Furoxan-3-yl nitrone	-502.97470	-585.31344	-0.18747	-492.20249
1,2,3-thiadiazol-5-yl nitrone	-750.89840	-833.19462	-0.18527	-486.42639

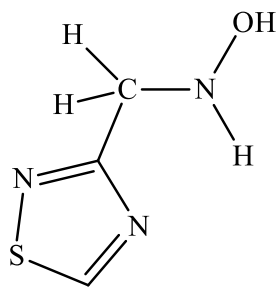
Table 8: Energies of the spin trapping reactions of •OH with formaldonitrone and the new heteroaryl nitrones at both C- and O-sites at (a) HF/6-31G* and (b) DFT/m06/6-31G*

(a)

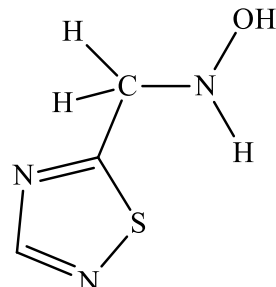
Spin Trap	Energy (E_h)		ΔE	
	Parent	Diadduct	E_h	kJ/mol
Formaldonitrone	-168.80921	-319.62732	-0.37131	-974.87441
1,2,4-thiadiazol-3-yl nitrone	-750.95291	-901.76282	-0.36311	-953.345305
1,2,4-thiadiazol-5-yl nitrone	-750.94373	-901.76535	-0.37482	-984.08991
Furoxan-4-yl nitrone	-502.97481	-653.79778	-0.37617	-987.63434
Furoxan-3-yl nitrone	-502.97470	-653.79602	-0.37452	-983.30226
1,2,3-thiadiazol-5-yl nitrone	-750.89840	-901.72202	-0.37682	-989.34091

(b)

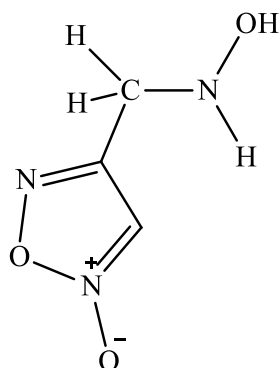
Spin Trap	Energy (E_h)		ΔE	
	Parent	Diadduct	E_h	kJ/mol
Formaldonitrone	-168.80921	-320.2125	-0.23573	-618.90912
1,2,4-thiadiazol-3-yl nitrone	-750.95291	-904.965539	-0.21838	-573.35406
1,2,4-thiadiazol-5-yl nitrone	-750.94373	-904.96419	-0.22370	-587.32435
Furoxan-4-yl nitrone	-502.97481	-657.04745	-0.22772	-597.87886
Furoxan-3-yl nitrone	-502.97470	-657.04763	-0.22662	-594.99081
1,2,3-thiadiazol-5-yl nitrone	-750.89840	-904.92959	-0.22520	-591.26260



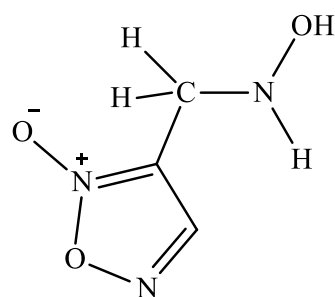
1,2,4-thiadiazol-3-yl double adduct



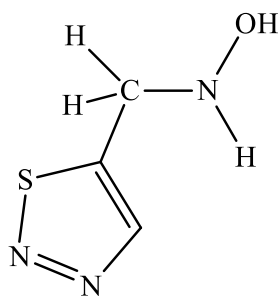
1,2,4-thiadiazol-5-yl double adduct



furoxan-4-yl double adduct

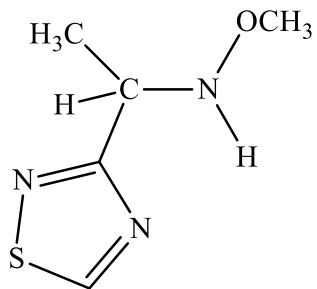


furoxan-3-yl double adduct

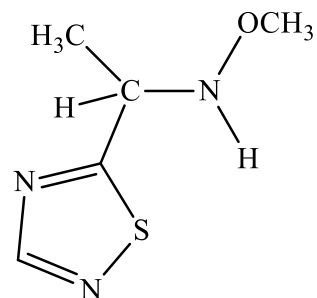


1,2,3-thiadiazol-5-yl double adduct

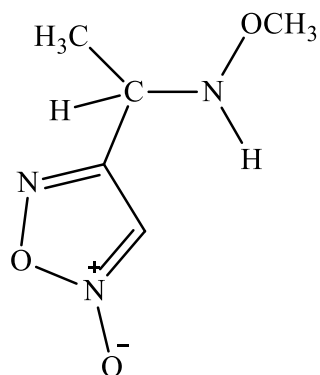
Figure 18: ChemDraw[®] representations of the new heteroaryl diadducts with •H added at both the C-site carbon and the O-site oxygen



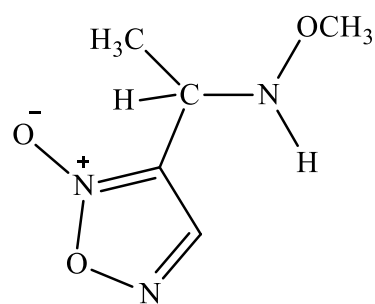
1,2,4-thiadiazol-3-yl double adduct



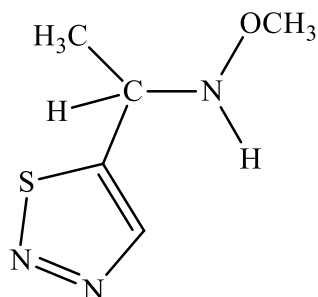
1,2,4-thiadiazol-5-yl double adduct



furoxan-4-yl double adduct

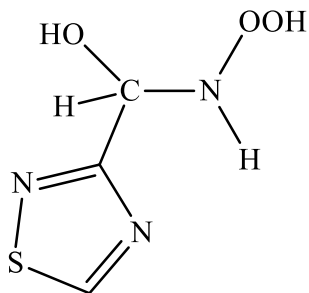


furoxan-3-yl double adduct

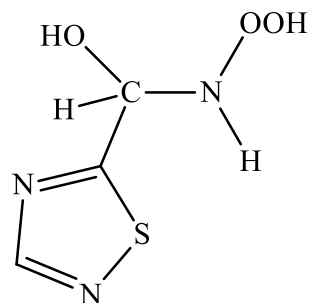


1,2,3-thiadiazol-5-yl double adduct

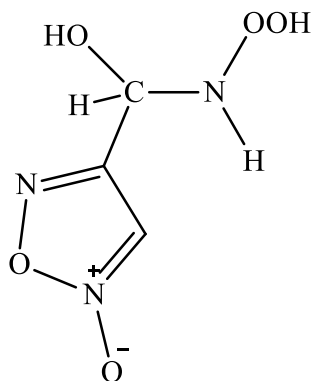
Figure 19: ChemDraw[®] representations of the new heteroaryl diadducts with $\bullet\text{CH}_3$ added at both the C-site carbon and the O-site oxygen



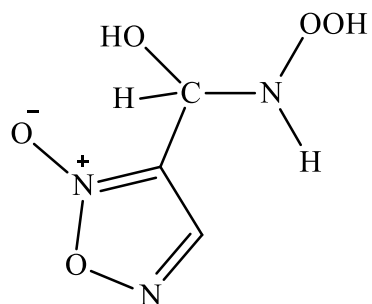
1,2,4-thiadiazol-3-yl spin adduct



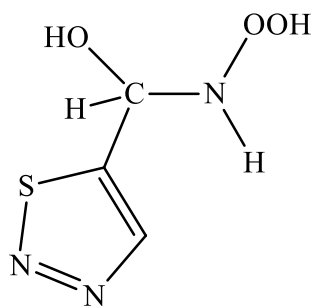
1,2,4-thiadiazol-5-yl spin adduct



furoxan-4-yl spin adduct



furoxan-3-yl spin adduct



1,2,3-thiadiazol-5-yl spin adduct

Figure 20: ChemDraw[®] representations of the new heteroaryl diadducts with •OH added at both the C-site carbon and the O-site oxygen

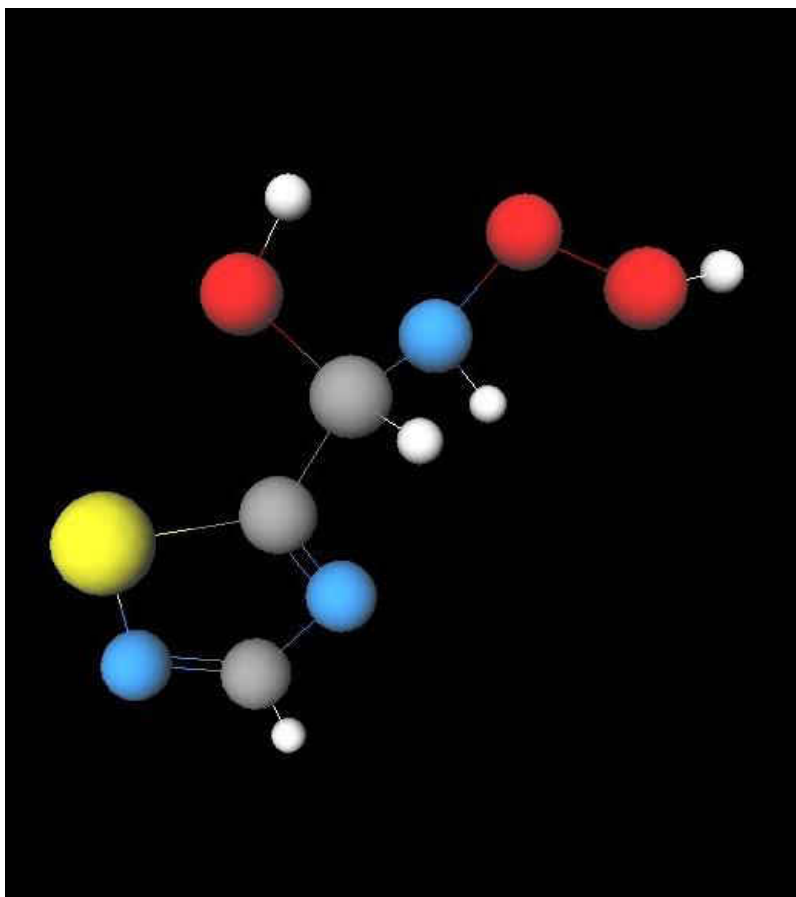


Figure 21: NWChem optimized geometry of the most stable diadduct thermodynamically of 1,2,3-thiadiazol-5-yl nitron with di \bullet OH at added both the C- and O-sites. The colors follow standard colors: red - oxygen, hydrogen - white, grey - carbon, blue - nitrogen, and yellow - sulfur

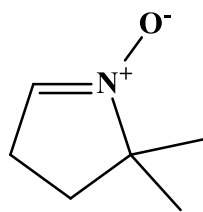
From Table 9, the reaction of PBN with \bullet OH is highly endothermic for both the mono spin adduct and the diadduct while the reactions of DMPO and FxBN with \bullet OH are exothermic. The reactivity of FxBN with \bullet OH is highly exothermic and shows the highest stability for both the mono and diadduct, with the diadduct being the most stable all the spin adducts. This is rationalized by the presence of intramolecular hydrogen bonding in both the mono and diadduct of FxBN with \bullet OH, which makes them very stable. The order of increasing stability of the spin

adducts of PBN, DMPO, and FxBN follows the same trend with the experimental half-lives and the spin trapping rate constants, obtained by Barriga *et al.*⁶⁴ Experimental studies have shown that the new heteroaryl nitron, FxBN, is more sensitive to trapping the hydroxyl radical than DMPO in competition assays and is known to possess spin trapping capability in biological system because of its low toxicity.⁶⁴ The EPR experiments have also shown that the presence of a heteroaryl substituent in the nitron increases the stability of the spin adduct formed.⁶²

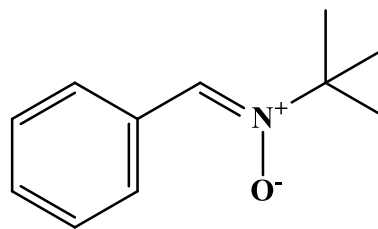
Data obtained for the new heteroaryl nitrones, mono spin adducts, and diadducts at the DFT/m06/6-31G* level of theory provide lower energies than data obtained at HF/6-31G*. DFT is well known to be a reliable method for the computation of molecular structures, vibrational frequencies and energy studies. The energy changes from DFT and HF are comparable. Thermodynamically, DFT indicates that the monoadduct of DMPO is more stable than the diadduct. However, from HF, the diadduct of DMPO is more stable than the mono spin. The mono spin adduct and diadduct of PBN at HF/6-31G* are more stable than at DFT/mo6/6-31G*. The present results by DFT and HF all indicate that FxBN for both the mono spin adduct and the diadduct are highly exothermic and are more stable than those of DMPO and PBN. In addition, the energy changes of the mono spin adduct and diadduct of FxBN at DFT/m06/6-31G* are lower than the energy changes of at HF/6-31G*.

Table 9: Energies of the addition of •OH to DMPO, PBN and FxBN at the DFT/m06/6-31G* and HF/6-31* levels of theory

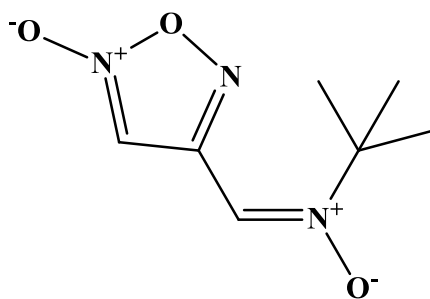
Nitron	ΔE (kJ/mol)				$t_{1/2}$ (s)	$k_{ST} \cdot 10^9$ ($\text{dm}^3 \text{mol}^{-1} \text{s}^{-1}$)
	DFT		HF			
	Monoadduct	Diadduct	Monoadduct	Diadduct		
DMPO	-1123.81	-571.73	-628.14	-935.92	3300.0	3.6
PBN	+5940.85	+5739.95	+5471.65	+5195.04	36.0	2.6
FxBN	-1548.71	-1847.18	-698.44	-979.83	7560.0	12.2



DMPO - 5,5-dimethylpyrroline-N-oxide



PBN - phenyl-N-t-butyl nitron



FxBN - (Z)-(3-methylfuroxan-4-yl)-N-tert-butyl nitron

Figure 22: ChemDraw[®] representations of 5,5-dimethylpyrroline-N-oxide, phenyl-N-tert-butyl nitron and (Z)-(3-methylfuroxan-4-yl)-N-tert-butyl nitron

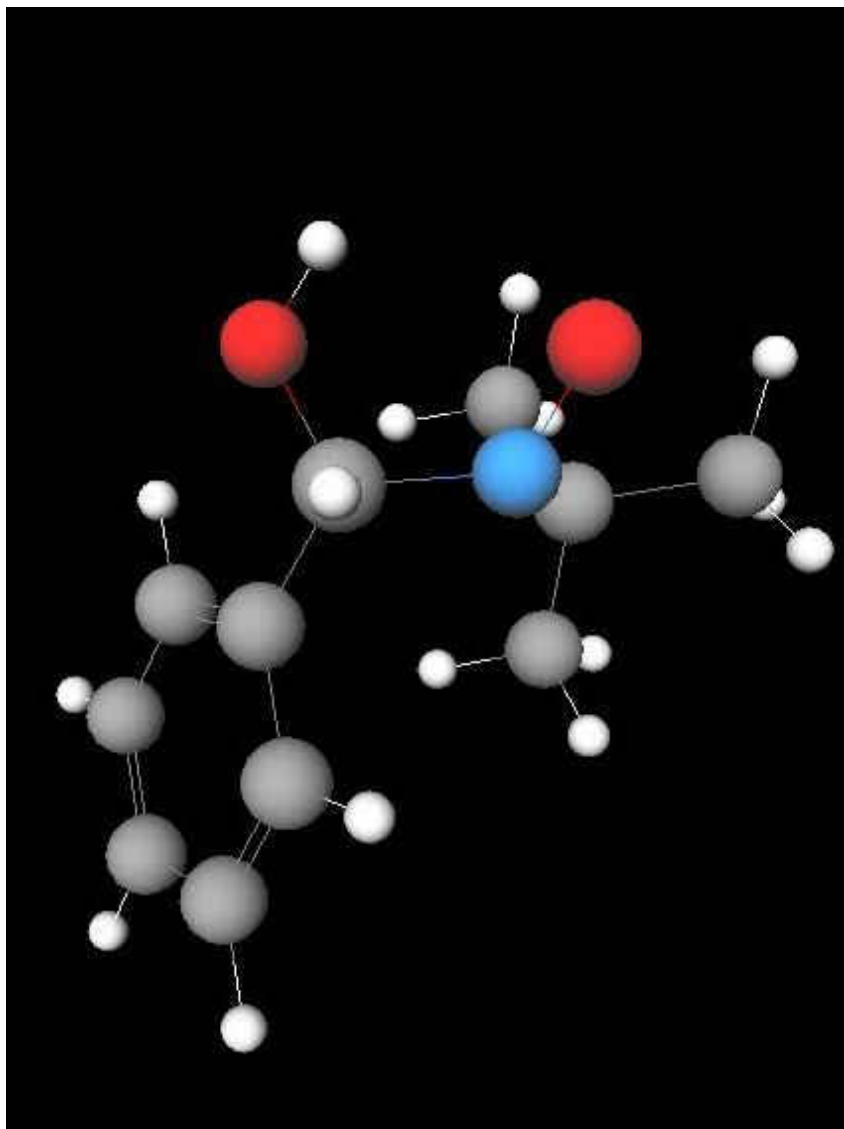


Figure 23: NWChem optimized geometry of the spin adduct of PBN with $\bullet\text{OH}$ radical at C- site. The colors follow standard colors: red - oxygen, hydrogen - white, grey - carbon, and blue - nitrogen

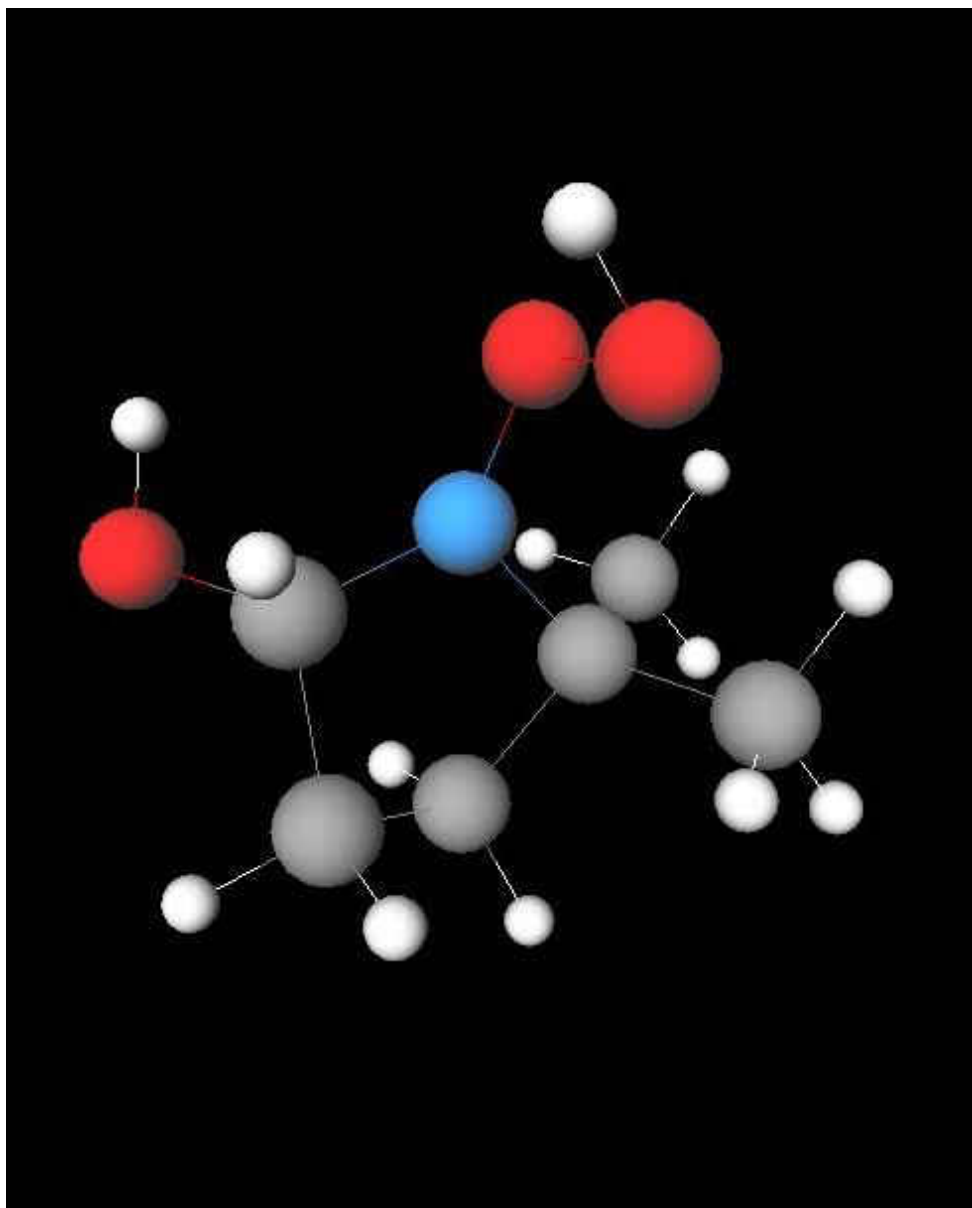
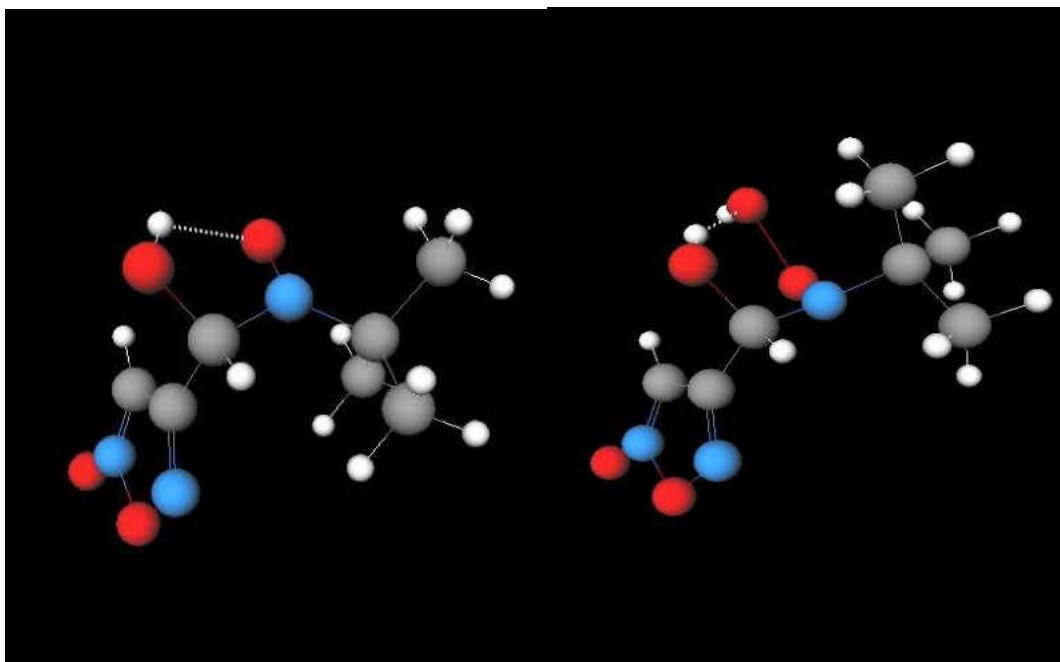


Figure 24: NWChem optimized geometry of diadduct of DMPO with di \bullet OH at both the C- and O- sites. The colors follow standard colors: red - oxygen, hydrogen - white, grey - carbon, and blue - nitrogen



a

b

Figure 25: NWChem optimized geometries of a) the spin adduct of FxBN with $\bullet\text{OH}$ at C-site and b) the diadduct of FxBN with di $\bullet\text{OH}$ at both C- and O- sites. The intramolecular hydrogen bonds are present in both a) and b). The colors follow standard colors: red - oxygen, hydrogen - white, grey - carbon, and blue - nitrogen

CHAPTER 4

CONCLUSIONS

The connectivity, the nature, and the position of the new heteroaryl substituents in the parent nitronne may affect the chemical and biological properties of the nitronyl group. New heteroaryl nitrones are the most stable spin traps due to the electronic effects of new heteroaryl substituents. The addition reaction between the new heteroaryl nitrones and the radicals at the C-site is more exothermic than at the O-site. This is due to the presence of resonance stabilization occurring at the C-site adduct. Generally, diadducts are thermodynamically more stable than mono spin adducts. The reactions of di $\bullet\text{OH}$ with the nitrones at both the C- and O- sites show the highest exothermicities with 1,2,3-thiadiazol-5-yl diadduct being the most thermodynamically stable compound. The new heteroaryl nitronne, FxBN, is the most stable spin trap adducts for the $\bullet\text{OH}$ radical compared to DMPO and PBN.

REFERENCES

1. Karlsson, J. Introduction to Nutraology and Radical Formation. In *Antioxidants and Exercise*; Illinois: Human Kinetics Press, 1997, 1-143.
2. Betteridge, D. J. What is Oxidative Stress? *Metabolism* **2000**, *49*, 3-8.
3. Halliwell, B. Free Radicals and Other Reactive Species in Disease. *Encyclopedia of Life Sciences* **2015**, 1-9.
4. Tegeli, V.; Karpe, P.; Katve V. Importance of Free Radical and Antioxidant on Human Health. *International Journal of Pharmaceutical, Chemical and Biological sciences* **2014**, *4*, 1038-1050.
5. Ebadi M. Antioxidants and Free Radicals in Health and Disease: An Introduction to Reactive Oxygen Species, Oxidative Injury, Neuronal Cell Death and Therapy in Neurodegenerative Diseases. **2001**, 13-5.
6. Bagchi, K.; Puri, S. Free Radicals and Antioxidants in Health and Disease. *East Mediterranean Health Journal* **1998**, *4*, 350-360.
7. Halliwell, B.; Erchabach, R. A.; Lologer, J.; Aruoma, O. I. The Characterization of Antioxidants. *Food Chem Toxicol.* **1995**, *33*, 601-617.
8. Buettner, G. R.; Jurkiewicz, B. A. Ascorbate free radical as a marker of oxidative stress: an ERR study. *Free Radical Biology and Medicine* **1993**, *14*, 49-55
9. Esme, H.; Cemek, M.; Sezer, M.; Soglam, H.; Demir, A.; Melek, H.; Unlu, M. High Levels of Oxidative Stress in Patients with Advanced Lung Cancer. *Respirology* **2008**, *13*, 112-116.

10. Weisel, R. D.; Mickle, D. A.; Finkle, C. D.; Tumiati, L. C.; Madonik, M.; Ivanov, J.; Burtaon, G. W.; Ingold, K. U. Myocardial Free-Radical Injury after Cardioplegia. *Circulation* **1989**, *80*, III14-8.
11. Kenhrer, J. P. Free Radicals as Mediators of Tissue Injury and Disease. *Critical reviews in toxicology* **1993**, *23*, 21-48.
12. Droge, W. Free Radicals in the Physiological Control of Cell Function. *Physiological reviews* **2002**, *82*, 47-95
13. Janzen, E. G. Spin trapping. *Acc. Chem. Res.* **1971**, *4*, 31-40.
14. Eaton, G. R.; Eaton S. S.; Salikhov, K. M. *Foundations of modern EPR: World Scientific*; Singapore, **1998**.
15. Zweier, J. L.; Flaherty, J. T.; Weisfeldt, M. L. Direct Measurement of Free Radical Generation following Reperfusion of Ischemic Myocardium. *Proc. Natl. Acad. Sci.* **1987**, *84*, 1404.
16. Zweier, J. L.; Kuppusamy, P.; Lutty, G. A. Measurement of Endothelial Cell Free Radical Generation: Evidence for A Central Mechanism of Free Radical Injury in Postischemic Tissues. *Proc. Natl. Acad. Sci.* **1988**, *85*, 4046.
17. Floyd, R. A.; Kopke, R. D.; Choi, C-H; Foster, S. B.; Doblas, S.; Towner, R. A. Nitrones as Therapeutics. *Free Radical Biology and Medicine* **2008**, *45*, 1361.
18. Feuer H., Ed. Nitrile Oxides, Nitrones and Nitronates. In *Organic Synthesis: Novel Strategies in Synthesis*. John Wiley & Sons: Hoboken, N.J., 2008.
19. Floyd, R. A.; Towner, R. A.; He, T.; Hensley, K.; Maples, K. R. Theory and Biological Application of the Electron Spin Resonance Technique of Spin Trapping. *Free Radical Biol. Med.* **2011**, *51*, 931.

20. Villamena, F. A.; Zweier, J. L. Detection of Reactive Oxygen and Nitrogen Species by EPR Spin Trapping. *Antioxidant Redox Signaling* **2004**, *6*, 619.
21. Rosen, G. M.; Britigan, B. E.; Halpern, H. J.; Pou, S.; Biology and Detection by Spin Trapping: Free Radicals; Oxford University Press, N.Y., 1999.
22. Rhodes, C. J. *The Critical Role of Free Radicals: Toxicology of the human environment*; Taylor & Francis, London, 2000.
23. Thornalley, P. J. Theory and biological Application of the Electron Spin Resonance Technique of Spin Trapping. *Life Chemistry Reports* **2010**, 1–56.
24. Janzen, E. G. Critical Review of Spin Trapping in Biological Systems In: *Free Radicals in Biology* Academic Press, New York, **1980**, 115–154.
25. Novelli, G.; Angiolini, P.; Cansales, G.; Lippi, R.; Tani, R.; Anti-Shock Action of Phenyl-t-butyl-nitron, A Spin trapper **1986**, 119–124.
26. Novelli, G. P.; Angiolini, P.; Tani, R.; Consales, G.; Bordi, L. Phenyl-t-butyl-nitron is Active against Traumatic Shock in Rats. *Free Radic. Res. Commun.* **1985**, *1*, 321–327.
27. Novelli, G. P.; Angiolini, P.; Tani, R. The Spin Trap Phenyl Butyl Nitron Prevents Lethal Shock in the Rat. In *Free Radicals in Liver Injury*; Poll, G.; Cheeseman, K. H.; Dianzani, M. U.; Slater T. F., Eds. IRL Press Limited: Oxford, 1986, pp 225–228.
28. Bosnjakovic, A.; Kadirov, M. K.; Schlick, S. Using ESR Spectroscopy to Study Radical Intermediates in Proton-Exchange Membranes Exposed to Oxygen Radicals. *Res. Chem. Intermed.* **2007**, *33*, 677.
29. Bosnjakovic, A.; Schlick, S. Spin Trapping by 5, 5-dimethylpyrroline-N-oxide in Fenton Media in the Presence of Nafion Perfluorinated Membranes: Limitations and Potential. *J. Phys. Chem. B.* **2006**, *110*, 10720–10728.

30. Danilczuk, M.; Bosnjakovic, A.; Kadirov, M. K.; Schlick, S. J. Direct ESR and Spin Trapping Methods for the Detection and Identification of Radical Fragments in Nafion Membranes and Model Compounds exposed to Oxygen Radicals. *Power Sources* **2007**, *172*, 78.
31. Dodd, N. J.; Jha A. N. Photoexcitation of Aqueous Suspensions of Titanium Dioxide Nanoparticles: An Electron Spin Resonance Spin Trapping Study of Potentially Oxidative Reactions. *Photochem. Photobiol.* **2011**, *87*, 632-640.
32. Ionita, P.; Conte, M.; Gilbert, B. C.; Chechik, V. Gold Nanoparticle-Initiated Free Radical Oxidations and Halogen Abstractions. *Org. Biomol. Chem.* **2007**, *5*, 3504-3509
33. Fu, H.; Zhang, L.; Zhang, S.; Zhu, Y.; Zhao, J. Electron Spin Resonance Spin-trapping Detection of Radical Intermediates in N-doped TiO₂-assisted Photodegradation of 4-Chlorophenol. *J. Phys. Chem. B.* **2006**, *110*, 3061-3065.
34. Xiao, G.; Wang, X.; Li, D.; Fu, X. InVO 4-sensitized TiO₂ Photocatalysts for Efficient Air Purification with Visible Light. *J. Photochem. Photobiol., A.* **2008**, *193*, 213-221.
35. Mroz, P.; Pawlak, A.; Satti, M.; Lee, H.; Wharton, T.; Gali, H.; Sarna, T.; Hamblin, M. R. Functionalized Fullerenes Mediate Photodynamic Killing of Cancer Cells: Type I versus Type II Photochemical Mechanism. *Free Radical Biol. Med.* **2007**, *43*, 711.
36. Rajendran, M.; Inbaraj, J. J.; Gandhidasan, R.; Murugesan, R. Photogeneration of Reactive Oxygen Species by 3-arylcoumarin and flavanocoumarin derivatives. *J. Photochem. Photobiol. A.* **2006**, *182*, 67.
37. Zeng, Z.; Zhou, J.; Zhang, Y.; Qiao, R.; Xia, S.; Chen, J.; Wang, X.; Zhang, B. Photodynamic Properties of Hypocrellin A, Complexes with Rare Earth Trivalent Ions: Role of the Excited State Energies of the Metal Ions. *J. Phys. Chem. B.* **2007**, *111*, 2688.

38. Janzen, E. G.; Liu, J. I.-P. J. Radical Addition Reactions of 5, 5-dimethyl-1-pyrroline-1-oxide. ESR Spin Trapping with A Cyclic Nitron. *Magn. Reson.* **1973**, *9*, 510.
39. Timmins, G. S.; Liu, K. J.; Bechara, E. J.; Kotake, Y.; Swartz, H. M. Trapping of Free Radicals with Direct in vivo EPR Detection: A Comparison of 5, 5-dimethyl-1-pyrroline-N-oxide and 5-diethoxyphosphoryl-5-methyl-1-pyrroline-N-oxide as Spin Traps for HO• and SO₄^{•-}. *Free Radical Biol. Med.* **1999**, *27*, 329.
40. Kotake, Y.; Janzen, E. G. Decay and Fate of the Hydroxyl Radical Adduct of alpha-phenyl-N-tert-butyl nitron (PBN) in Aqueous Media. *J. Am. Chem. Soc.* **1991**, *113*, 9503.
41. Floyd, R. A.; Hensley, K.; Forster, M. J.; Kelleher-Andersson, J. A.; Wood, P. L. Nitrones, Their Value as Therapeutics and Probes to Understand Aging. *Mech. Ageing Dev.* **2002**, *123*, 1021.
42. Dikalova, A.E.; Kadiiska, M.B.; Mason, R.P. An In Vivo ESR Spin-Trapping Study: Free Radical Generation in Rats from Formate Intoxication—Role of the Fenton Reaction. *Proc. Natl. Acad. Sci.* **2001**, *98*, 13549-13553.
43. Kadiiska, M. B.; Burkitt, M. J.; Xiang, Q. H.; Mason, R. P. Iron Supplementation generates Hydroxyl Radical In Vivo. An ESR Spin-Trapping Investigation. *J. Clin. Invest.* **1995**, *96*, 1653-1657.
44. Hensley, K.; Carney, J. M.; Stewart, C. A.; Tabatabaie, T.; Pye, Q.; Floyd, R. A. *Int. Rev. Neurobiol.* **1997**, *40*, 299.
45. Kotake, Y. Pharmacologic Properties of Phenyl N-tert-butyl nitron. *Antioxid. Redox Signal.* **1999**, *1*, 481.

46. Li, P. A.; He, Q. P.; Nakamura, L.; Csiszar, K. Free Radical Spin Trap α -phenyl-N-tert-butyl-nitron inhibits Caspase-3 Activation and reduces Brain Damage following A Severe Forebrain Ischemic Injury. *Free Radical Biol. Med.* **2001**, *31*, 1191.
47. Durand, G.; Polidori, A.; Salles, J. P.; Prost, M.; Durand, P.; Pucci, B. Synthesis and Antioxidant Efficiency of A New Amphiphilic Spin-Trap derived from PBN and Lipoic Acid. *Bioorg. Med. Chem. Lett.* **2003**, *13*, 2673.
48. Floyd, R. A.; Kopke, R. D.; Choi, C.-H.; Foster, S. B.; Doblas, S.; Towner, R. A. Nitrones as Therapeutics. *Free Radical Biol. Med.* **2008**, *45*, 1361.
49. Fréjaville, C.; Karoui, H; Tuccio, B.; Moigne, F. L.; Culcasi, M.; Pietri, S.; Lauricella, R.; Tordo, P. 5-(Diethoxyphosphoryl)-5-methyl-1-pyrroline N-oxide: A New Efficient Phosphorylated Nitron for the In Vitro and In Vivo Spin Trapping of Oxygen-Centered Radicals. *J. Med. Chem.*, **1995**, *38* 258-265.
50. Olive, G.; Mercier, A.; Moigne, F.; Rockenbauer, A.; Tordo, P. 2-ethoxycarbonyl-2-methyl-3, 4-dihydro-2H-pyrrole-1-oxide: Evaluation of the Spin Trapping Properties. *Free Radical Biol. Med.* **2000** *28*, 403-408.
51. Zhao, H.; Joseph, J.; Zhang, H.; Karoui, H.; Kalyanaraman, B. Synthesis and Biochemical Applications of a Solid Cyclic Nitron Spin Trap: A Relatively Superior Trap for Detecting Superoxide Anions and Glutathyl Radicals. *Free Radical Biol. Med.* **2001**, *31* 599-606.
52. Stolze, K.; Rohr-Udilova, N.; Rosenau, T.; Hofingerc, A.; Nohl, H. Free Radical Trapping Properties of Several Ethyl-substituted derivatives of 5-ethoxycarbonyl-5-methyl-1-pyrroline N-oxide (EMPO). *Bioorg. Med. Chem.* **2007**, *15*, 2827.

53. Stolze, K.; Rohr-Udilova, N.; Hofinger, A.; Rosenau, T. Spin Trapping Experiments with Different Carbamoyl-substituted EMPO derivatives. *Bioorg. Med. Chem.* **2008**, *16*, 8082.
54. Villamena, F. A.; Rockenbauer, A.; Gallucci, J.; Velayutham, M.; Hadad, C. M.; Zweier, J. L. Spin Trapping by 5-carbamoyl-5-methyl-1-pyrroline N-oxide (AMPO): Theoretical and Experimental Studies. *J. Org. Chem.*, **2004**, *69*, 7994-8004.
55. Villamena, F. A.; Xia, S.; Merle, J. K.; Lauricella, R.; Tuccio, B.; Hadad, C. M.; Zweier, J. L. Reactivity of Superoxide Radical Anion with Cyclic Nitrones: Role of Intramolecular H-bond and Electrostatic Effects. *J. Am. Chem. Soc.* **2007**, *129*, 8177-8191.
56. Terabe, S.; Konaka, R. Electron Spin Resonance Studies on Oxidation with Nickel Peroxide. Spin Trapping of Free-Radical Intermediates." *J. Am. Chem. Soc.* **1969**, *91*, 5655–5657.
57. Bardelang, D.; Charles, L.; Finet, J.P.; Jicsinszky, L.; Karoui, H.; Marque, S.R., et al. α -Phenyl-N-tert-butylnitron-Type Derivatives Bound to β -Cyclodextrins: Syntheses, Thermokinetics of Self-Inclusion and Application to Superoxide Spin-Trapping. *Chemistry* **2007**, *13* 9344–9354.
58. Terabe, S.; Konaka, R. Electron Spin Resonance Studies on Oxidation with Nickel Peroxide. Spin Trapping of Free-Radical Intermediates. *J. Am. Chem. Soc.* **1969**, *91*, 5655– 5657.
59. Bardelang, D.; Charles, L.; Finet, J. P.; Jicsinszky, L.; Karoui, H.; Marque, S. R.; et al. Alpha-phenyl-N-tertbutylnitron-type derivatives bound to beta-cyclodextrins: Syntheses, Thermokinetics of Selfinclusion and Application to Superoxide Spin-Trapping. *Chemistry*. **2007**, *13*, 9344–9354.

60. Sankuratri, N.; Kotake, Y.; Janzen, E. G. Studies on the Stability of Oxygen Radical Spin Adducts of a New Spin Trap: 5-methyl-5-phenylpyrroline-1-oxide (MPPO). *Free Radical Biol. Med.* **1996**, *21*, 889.
61. Tsai, P.; Ichikawa, K.; Mailer, C.; Pou, S.; Halpern, H. J.; Robinson, B. H.; Nielsen, R.; Rosen, G. M. Esters of 5-carboxyl-5-methyl-1-pyrroline N-oxide: A Family of Spin Traps for superoxide. *J. Org. Chem.* **2003**, *68*, 7811.
62. Goldstein, S.; Lestage, P. Chemical and Pharmacological Aspects of Heteroaryl-nitrones. *Current Medicinal Chemistry* **2000**, *7*, 1255-1267.
63. Porcal, W.; Hernández, P.; González, M.; Ferreira, A.; Olea-Azar, C.; Cerecetto, H.; Castro, A. Heteroaryl nitrones as Drugs for Neurodegenerative Diseases: Synthesis, Neuroprotective Properties, and Free Radical Scavenger Properties. *J. Med. Chem.* **2008**, *51*, 6150–6159.
64. Barriga, G.; Olea-Azar, C.; Norambuena, E.; Castro, A.; Porcal, W.; Gerpe, A.; González, M.; Cerecetto, H. New Heteroaryl Nitrones with Spin Trap Properties: Identification of a 4-furoxanyl derivative with Excellent Properties to be used in Biological Systems. *Bioorganic & Medicinal Chemistry* **2010**, *18*, 795–802.
65. Boyd, S. L.; Boyd, R. J. A Theoretical Study of Spin Trapping by Nitron: Trapping of Hydrogen, Methyl, Hydroxyl, and Peroxyl Radicals. *J. Phys. Chem.* **1994**, *98*, 11705 – 11713.
66. Young, D. *Computational Chemistry: A Practical Guide for Applying Techniques to Real World Problems*, John Wiley & Sons, **2001**.
67. Pacheco, B. A. *Introduction to Computational Chemistry*, LONI workshop series, Tulane University, New Orleans, **2011**, 4.

68. Lavery, D. R. "Mathematical Challenges from Theoretical/Computational Chemistry."
National Academy of Sciences – National Research Council 2101 Constitution Avenue
20418
69. Mathematical Challenges from Theoretical/Computational Chemistry, Committee on
Mathematical Challenges from Computational Chemistry, National Research Council,
1995, 1-144.
70. Leach, A. R. Principles and Applications: In *Molecular Modelling*, Ed., Prentice Hall:
Harlow, England. 2001.
71. Lewars E. *Introduction to the Theory and Applications of Molecular and Quantum
Mechanics*, Klumer Academic Publishers, **2004**, 2-3.
72. Anslyn, E. V.; Dennis, A. D. *Modern Physical Organic Chemistry*, University Science
Books, **2006**
73. Allinger, N. L. Conformational Analysis. 130. MM2. A Hydrocarbon Force Field
Utilizing V1 and V2 Torsional Terms. *J. Am. Chem. Soc.* **1997**, 99, 8127-8134
74. Rappe, K. A.; Casewit C. J.; Colwell K. S.; Goddardlii, W. A.; Skiff, W. M. UFF, A Full
Periodic Table Force Field for Molecular Mechanics and Molecular Dynamics
Simulations. *J. Am. Chem. Soc.* **1992**, 114, 10024-10035.
75. Levine, I. N. *Quantum Chemistry*. Prentice Hall: Englewood Cliffs, N. J., **1991**, 455–
544.
76. Dewar, J. S.; Zoebisch, E. G.; Healy, E. F.; Stewart, J. P. Development and Use of
Quantum Mechanical Molecular Models. 76. AM1: A New General Purpose Quantum
Mechanical Molecular Model. *J. Am. Chem. Soc.* **1985**, 107, 3902.

77. Kohn, W.; Becke, A. D.; Parr, R. G. Density Functional Theory of Electronic Structure. *J. Phys. Chem.* **1996**, *100*, 12974.
78. Alder, B. J.; Wainwright, T. E. Studies in Molecular Dynamics. I. General Method. *J. Chem. Phys.* **1959**, *31*, 459
79. Schrödinger, E. Quantisierung als eigenwertproblem. *Ann. Phys.* **1926**, *79*, 361.
80. Schrödinger, E. An Undulatory Theory of the Mechanics of Atoms and Molecules. *Phys. Rev.* **1926**, *28*, 1049.
81. Hartree, D. R. The Wave Mechanics of an Atom with a Non-Coulomb Central Field II: Some Results and Discussion. *Proc. Cambridge Phil. Soc.* **1927**, *24*, 111.
82. McWeeny, R. Natural Units in Atomic and Molecular Physics. *Nature* **1973**, *243*, 196.
83. Teschl, G. Mathematical Methods in Quantum Mechanics; With Applications to Schrödinger Operators, American Mathematical Society, **2009**.
84. Courant, R.; Hilbert, D. Methods of Mathematical Physics, **1962**, Volume I, Wiley-Interscience.
85. Fock, V. Näherungsmethode zur Lösung des Quantenmechanischen Mehrkörperproblems. *Z. Phys.* **1930**, *61*, 126.
86. Hartree, D. R. The Wave Mechanics of an Atom with a Non-Coulomb Central Field. Part I. Theory and Methods. *Proc. Cambridge Phil. Soc.* **1928**, *24*, 426.
87. Slater, J.; Verma, H. C. The Theory of Complex Spectra. *Physical Review*, **1929**, *34*, 1293-1322.
88. Atkins, P.W. An Introduction to Quantum Chemistry: In *Molecular Quantum Mechanics Parts I and II*, Oxford University Press. 1977.
89. Levine, I. N. *Quantum Chemistry*. Eds., Pearson Education Inc., 2014, 409-411.

90. Roothaan, C. C. J. New Developments in Molecular Orbital Theory. *Rev. Mod. Phys.* **1951**, 23, 69.
91. Hall, G. G. The Molecular Orbital Theory of Chemical Valency. VIII. A Method of Calculating Ionization Potentials. *Proc. Roy. Soc.* **1951**, A205, 541.
92. Pople, J. A.; Nesbet, R. K. Self-Consistent Orbitals for Radicals. *J. Chem. Phys.* **1954**, 22, 571.
93. Møller, C.; Plesset, M. S. Note on an Approximation Treatment for Many-Electron Systems. *Phys. Rev.* **1934**, 46, 618.
94. Kohn, W.; Becke, A. D.; Parr, R. G. Density Functional Theory of Electronic Structure. *J. Phys. Chem.* **1996**, 100, 12974.
95. Geerlings, P.; De Proft F.; Langenaeker, W. Conceptual Density Functional Theory. *Chem. Rev.* **2003**, 103, 1793-1874.
96. Parr R. G., Yang, W; *Density Functional Theory of Atoms and Molecules*, Oxford New York, **1989**, 185-187.
97. Hohenberg, P.; Kohn, W. Inhomogeneous electron gas. *Phys. Rev.* **1964**, 136, B864.
98. Kohn, W.; Sham, L. J. Self-Consistent Equations including Exchange and Correlation Effects. *Phys. Rev.* **1965**, 140, A1133.
99. Levine, I. N. *Quantum Chemistry*. Eds.; Pearson Education Inc., 2014, 559.
100. Levine, I. N. *Quantum Chemistry*. Eds.; Pearson Education Inc., **2014**, 560.
101. Kohn, W.; Sham, J. L. Self-Consistent Equations including Exchange and Correlation Effects. *Phys. Rev.*, **1965**, 140, A1133.
102. Kim, K.; Jordan, K. D. Comparison of Density Functional and MP2 Calculations on the Water Monomer and Dimer. *J. Phys. Chem.* **1994**. 98, 10089–10094.

103. Stephens, P. J.; Devlin, F. J.; Chabalowski, C. F.; Frisch, M. J. *Ab initio* Calculation of Vibrational Absorption and Circular Dichroism Spectra using Density Functional Force Fields. *J. Phys. Chem.*, **1994**, *98*, 11623–11627.
104. Raghavachari, K. Perspective on “Density Functional Thermochemistry. III. The Role of Exact Exchange. *Theor. Chem. Acc.* **2000**, *103*, 361.
105. Young, D. C, A Practical Guide for Applying Techniques to Real World Problem: In *Computational Chemistry*; John Wiley & Sons Inc., **2001**, 45.
106. Dunning, T. H. Gaussian Basis Sets for Use in Correlated Molecular Calculations. I. The Atoms Boron through Neon and Hydrogen. *J. Chem. Phys.* **1989**, *90*, 1007–1023.
107. Peterson, G. A.; Malick, D. K., Wilson, G. W., Ochterski, J. W., Montgomery, J. J. A.; Frisch, M. J. Calibration and Comparison of the Gaussian-2, Complete Basis Set, and Density Functional Methods for Computational Thermochemistry. *J. Chem. Phys.* **1998**, *109*, 10570.
108. Peterson, G. A.; Al-Laham, M. A. A Complete Basis Set Model Chemistry. II. Open-Shell Systems and the Total Energies of the First-Row Atoms. *J. Chem. Phys.* **1991**, *94*, 6081.
109. Peterson, G. A.; Bennett, A.; Tensfeldt, T. G.; Al-Laham, M. A.; Shirley, W. A.; Mantzaris, J. A Complete Basis Set Model Chemistry. I. The Total Energies of Closed-Shell Atoms and Hydrides of the First-Row Elements. *J. Chem. Phys.* **1988**, *89*, 2193.
110. Lowdin, P. O. Quantum Theory of Many-Particle Systems. I. Physical Interpretations by Means of Density Matrices, Natural Spin-Orbitals, and Convergence Problems in the Method of Configurational Interaction. *Phys. Rev.* **1955**, *97*, 1474.

111. Shull, H.; Lowdin, P. O. Role of the Continuum in Superposition of Configurations. *J. Chem. Phys.* **1955**, *23*, 1362.
112. Lowdin, P. O.; Shull, H. Natural Orbitals in the Quantum Theory of Two-Electron Systems. *Phys. Rev.* **1956**, *101*, 1730.
113. Shull, H.; Lowdin, P. O. Superposition of Configurations and Natural Spin Orbitals. Applications to the He Problem. *J. Chem. Phys.* **1959**, *30*, 617.
114. Shull, H. Natural Spin Orbital Analysis of Hydrogen Molecule Wave Functions. *J. Chem. Phys.* **1959**, *30*, 1405.
115. Ochterski, J. W.; Petersson, G. A.; Montgomery Jr, J. A.; A Complete Basis Set Model Chemistry. V. Extensions to Six or More Heavy Atoms. *J. Chem. Phys.* **1996**, *104*, 2598-2619.
116. Valiev, M. ; Bylaska, E.J. ; Govind, N.; Kowalski, K.; Straatsma, T.P.; van Dam, H.J.J.; Wang, D.; Nieplocha, J.; Apra, E.; Windus, T. L.; de Jong, W.A.; "NWChem: a comprehensive and scalable open-source solution for large scale molecular simulations" *Comput. Phys. Commun.* **2010**, *181*, 1477.
117. Apra, E.; Bylaska, E. J.; de Jong, W. A.; Govind, N.; Kowalski, K.; Straatsma, T. P.; Valiev, M.; van Dam, H. J. J.; Wang, D.; Windus, T. L. et al. "NWChem, A computational Chemistry package for parallel computers. Version 6.3", Pacific Northwest National Laboratory, Richland, Washington 993 52-0999, USA, **2013**.
118. "Extensible Computational Chemistry Environment (ECCE), A Problem Solving Environment for Computational Chemistry, Software Version 7.0" (2013), as developed and distributed by Pacific Northwest National Laboratory, P.O. Box 999,

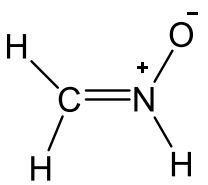
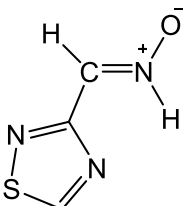
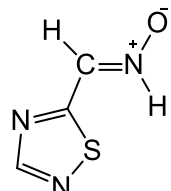
Richland, Washington 99352, USA, and funded by the U.S. Department of Energy, was used to obtain some of these results.

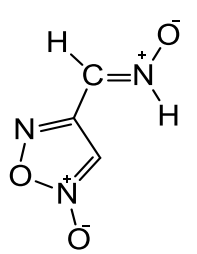
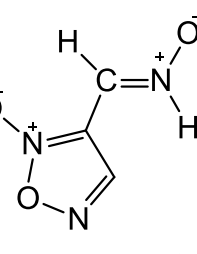
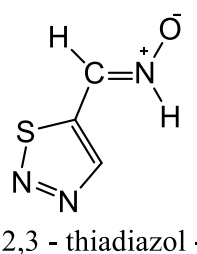
119. Buettner, G. R. The Pecking Order of Free Radicals and Antioxidants: Lipid Peroxidation, α -Tocopherol, and Ascorbate. *Arch. Biochem. Biophys.* **1993**, *300*, 535-543.
120. Iwamura, M.; Inamoto, N. Novel Radical 1,3-Addition to Nitrones. *Bull. Chem. Soc. Jpn.* **1967**, *40*, 702-703.
121. Iwamura, M.; Inamoto, N. Reactions of Nitrones with Free Radicals. I. Radical 1,3-Addition to Nitrones. *Bull. Chem. Soc. Jpn.* **1970**, *43*, 856-860.
122. Janzen, E. G.; Krygsmann, P. H.; Lindsay, D. A.; Haire, D. L. Detection of Alkyl, Alkoxy, and Alkylperoxy Radicals from The Thermolysis of Azobis(isobutyronitrile) by ESR/Spin Trapping. Evidence for Double Spin Adducts from Liquid-Phase Chromatography and Mass Spectroscopy. *J. Am. Chem. Soc.* **1990**, *112*, 8279.

APPENDIX

Tables of Additional Data from the Calculations

Table A1: The parent nitron spin traps

Optimized Species ^a	Selected Parameters		^b Charge Population	Energy (E _h) ^c	Dipole Moment (D)
	Bond lengths (Å)	Bond angles (deg)			
 formaldonitron	CN 1.269 NO 1.254	CNO 128.3 CNH ₁ 116.5 NCH ₂ 118.9	C -0.223 O -0.593 N -0.016 H ₁ +0.393	SCF -168.80921 MP2 ₁ -169.32379 MP2 ₂ -169.50071 MP2 ₃ -169.55895 DFT -169.69089	4.47
 1,2,4 - thiadiazol - 3 -yl nitron	CN 1.277 NO 1.244	CNO 127.8 CNH ₁ 116.1 NCS 120.0	C -0.017 O -0.557 N -0.072 H ₁ +0.433	SCF -750.95291 MP2 ₁ -752.19826 MP2 ₂ -752.60343 MP2 ₃ -752.81677 DFT -753.46128	5.65
 1,2,4 - thiadiazol - 5 - yl nitron	CN 1.279 NO 1.241	CNO 127.5 CNH ₁ 117.9 NCS 123.0	C +0.027 O -0.538 N -0.081 H ₁ +0.417	SCF -750.94373 MP2 ₁ -752.19170 MP2 ₂ -752.59696 MP3 -752.81040 DFT -753.45461	1.97

 furoxan - 4 - yl nitronium	CN 1.277 NO 1.242	CNO 127.5 CNH ₁ 117.7 NCS 122.1	C +0.021 O -0.540 N -0.083 H ₁ +0.411	SCF -502.97481 MP2 ₁ -504.49516 MP2 ₂ -504.96856 MP2 ₃ -505.13295 DFT -505.53385	1.76
 furoxan - 3 - yl nitronium	CN 1.275 NO 1.251	CNO 127.3 CNH ₁ 118.0 NCS 122.5	C +0.054 O -0.556 N -0.106 H ₁ +0.404	SCF -502.97470 MP2 ₁ -504.47422 MP2 ₂ -504.96811 MP2 ₃ -505.13295 DFT -505.53513	4.26
 1,2,3 - thiadiazol - 5 - yl nitronium	CN 1.278 NO 1.246	CNO 127.3 CNH ₁ 117.6 NCS 122.8	C +0.035 O -0.548 N -0.083 H ₁ +0.413	SCF -750.89840 MP2 ₁ -752.15743 MP2 ₂ -752.56122 MP2 ₃ -752.69673 DFT -753.41851	0.26

^aAll structures were optimized at the HF/6-31G* level and have no imaginary frequencies

^bMulliken population analysis

^c1 au = 2625.5 kJ/mol. The MP2₁, MP2₂ and MP2₃ energies are single point energies obtained with the cc-pVDZ, cc-pVTZ and cc-pVQZ basis sets respectively using the 6-31G* optimized geometry, *i.e.* MP2/cc-pVDZ//HF/6-31G*, MP2/cc-pVTZ//HF/6-31G* and MP2/cc-pVQZ//HF/6-31G* respectively.

Table A2: Selected biological relevant radicals

Optimized Radical ^a	Selected Parameters		Spin Population	^b Charge Populations	^c Energy (E _h)	Dipole (D)
	Bond lengths (Å)	Bond angles (deg)				
•H					SCF -0.49820 MP2 ₁ -0.49927 MP2 ₂ -0.49980 DFT -0.49792	0
•CH ₃	CH 1.073	HCH 120.0	C +1.294 H -0.098	C -0.530 H +0.175	SCF -39.63860 MP2 ₁ -39.69002 MP2 ₂ -39.73568 DFT -39.79542	0
•OH	OH 0.958		O +1.056 H -0.056	O -0.457 H +0.457	SCF -75.22340 MP2 ₁ -75.36660 MP2 ₂ -75.46843 DFT -75.64294	1.94

^aAll structures were optimized at the HF/6-31G* level and have no imaginary frequencies

^bMulliken population analysis

^c1 au = 2625.5 kJ/mol. The MP2₁ and MP2₂ energies are single point energies obtained with the cc-pVDZ and cc-pVTZ basis sets respectively using the 6-31G* optimized geometry, *i.e.* MP2/cc-pVDZ//HF/6-31G* and MP2/cc-pVTZ//HF/6-31G* respectively.

Table A3: The reaction of new heteroaryl nitrones with •H at the C-site carbon and the O-site oxygen

Table A3a: 1,2,4-thiadiazol-3-yl nitron

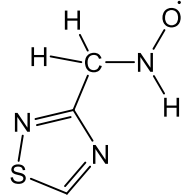
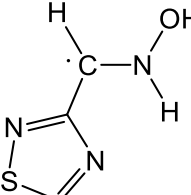
Optimized adducts ^a	Selected parameters			Spin populations	^b Charge populations	Energy ^c (a.u.)	ΔE^d (kJ/mol)	Dipole moments (D)
	Bond lengths (Å)	Bond angles (deg)	Dihedral angles (deg)					
	CN 1.441	CNO 119.5	ONCH ₁ +180.0	C -0.069	C -0.119	SCF -751.55541	SCF -273.83965	4.53
	NO 1.258	CNH ₁ 121.6	ONCH ₃ +59.0	N +0.361	N -0.310	MP2 ₁ -752.77293	MP2 ₁ -197.9627	
		NCH ₃ 109.7	ONCH ₂ -59.0	O +0.687	O -0.350	MP2 ₂ -753.17996	MP2 ₂ -201.43099	
		NCH ₂ 109.7	ONCS +180.0	H ₁ +0.034	H ₁ +0.412	DFT -754.04881	DFT -235.27106	
		NCS 111.5						
	CN 1.352	CNO 123.0	ONCH ₁ +180.0	C +0.748	C -0.013	SCF -751.51998	SCF -180.81819	0.62
	NO 1.378	CNH ₁ 124.8	ONCH ₃ 0.0	N +0.208	N -0.384	MP2 ₁ -752.7280	MP2 ₁ -79.99899	
	OH ₂ 0.948	NCH ₃ 118.1	ONCS +180.0	O -0.012	O -0.577	MP2 ₂ -753.13914	MP2 ₂ -94.25808	
		NCS 121.7	CNOH ₁ +180.0	H ₁ -0.025	H ₁ +0.428	DFT -754.01985	DFT -159.23658	
		NOH ₂ 106.9		H ₂ -0.0006	H ₂ +0.464			

Table A3b: 1,2,4-thiadiazol-5-yl nitron

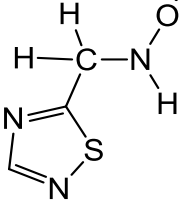
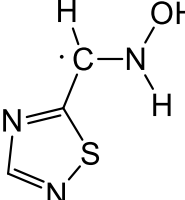
Optimized adducts ^a	Selected parameters			Spin populations	^b Charge populations	Energy ^c (a.u.)	ΔE^d (kJ/mol)	Dipole moments (D)
	Bond lengths (Å)	Bond angles (deg)	Dihedral angles (deg)					
	CN 1.445	CNO 118.0	ONCH ₁ +146.1	C -0.033	C -0.141	SCF -751.55709	SCF -302.35258	3.76
	NO 1.271	CNH ₁ 118.3	ONCH ₃ +166.9	N +0.254	N -0.330	MP2 ₁ -752.76984	MP2 ₁ -207.07319	
		NCH ₃ 107.9	ONCH ₂ +48.4	O +0.769	O -0.294	MP2 ₂ -753.17619	MP2 ₂ -208.51984	
		NCH ₂ 111.3	ONCS -73.7	H ₁ -0.018	H ₁ +0.387	DFT -754.04777	DFT -250.05262	
		NCS 112.5						
	CN 1.399	CNO 110.6	ONCH ₁ +118.9	C +0.034	C +0.038	SCF -751.54151	SCF -261.44729	2.19
	NO 1.388	CNH ₁ 112.8	ONCH ₃ +0.9	N +0.045	N -0.411	MP2 -751.59407	MP2 ₁ 2879.91095*	
	OH ₂ 0.948	NCH ₃ 118.2	ONCS -177.2	O +0.043	O -0.597	MP2 ₂ -753.14303	MP2 ₂ -121.45826	
		NCS 121.0	CNOH ₁ -122.8	H ₁ 0.0	H ₁ +0.386	DFT -754.03515	DFT -216.91881	
		NOH ₂ 104.8		H ₂ 0.0	H ₂ +0.467			

Table A3c: Furoxan-4-yl nitron

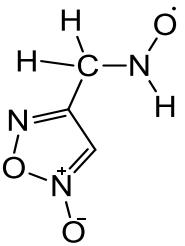
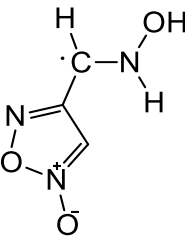
Optimized adducts ^a	Selected parameters			Spin populations	^b Charge populations	Energy ^c (a.u.)	ΔE^d (kJ/mol)	Dipole moments (D)
	Bond lengths (Å)	Bond angles (deg)	Dihedral angles (deg)					
	CN 1.450	CNO 117.7	ONCH ₁ +144.6	C -0.100	C -0.167	SCF -503.59900	SCF -330.78675	2.53
	NO 1.269	CNH ₁ 117.9	ONCH ₃ +85.1	N +0.276	N -0.301	MP2 ₁ -505.01714	MP2 ₁ -59.625105	
		NCH ₃ 112.2	ONCH ₂ -33.3	O +0.760	O -0.301	MP2 ₂ -505.50841	MP2 ₂ -105.12765	
		NCH ₂ 106.2	ONCS -153.3	H ₁ -0.015	H ₁ +0.383	DFT -506.13304	DFT -265.88439	
		NCS 110.6						
	CN 1.406	CNO 109.9	ONCH ₁ +116.9	C +1.015	C +0.007	SCF -503.58465	SCF -293.11082	5.14
	NO 1.391	CNH ₁ 112.0	ONCH ₃ +12.5	N -0.038	N -0.412	MP2 ₁ -504.99882	MP2 ₁ -11.525945	
	OH ₂ 0.948	NCH ₃ 118.8	ONCS -167.6	O -0.003	O -0.600	MP2 ₂ -505.49367	MP2 ₂ -66.42778	
		NCS 119.8	CNOH ₁ -120.9	H ₁ +0.027	H ₁ +0.382	DFT -506.11029	DFT -206.15426	
		NOH ₂ 104.9		H ₂ +0.001	H ₂ +0.466			

Table A3d: Furoxan-3-yl nitron

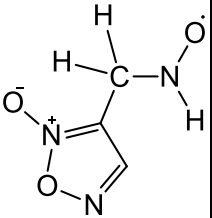
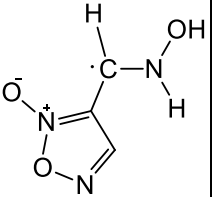
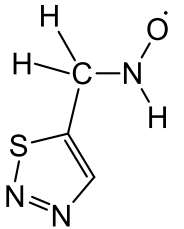
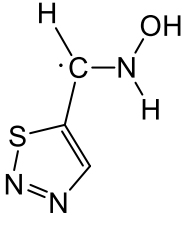
Optimized adducts ^a	Selected parameters			Spin populations	^b Charge populations	Energy ^c (a.u.)	ΔE^d (kJ/mol)	Dipole moments (D)
	Bond lengths (Å)	Bond angles (deg)	Dihedral angles (deg)					
	CN 1.446	CNO 117.9	ONCH ₁ +147.4	C +0.046	C -0.180	SCF -503.60065	SCF -335.40763	2.64
	NO 1.267	CNH ₁ 118.6	ONCH ₃ -50.3	N +0.277	N -0.275	MP2 ₁ -505.02015	MP2 ₁ -122.50583	
		NCH ₃ 107.1	ONCH ₂ -167.6	O +0.734	O -0.324	MP2 ₂ -505.5107	MP2 ₂ -112.32152	
		NCH ₂ 109.4	ONCS +71.5	H ₁ -0.021	H ₁ +0.385	DFT -506.13270	DFT -261.63108	
		NCS 112.9						
	CN 1.356	CNO 122.4	ONCH ₁ +180.0	C +0.739	C +0.021	SCF -503.56496	SCF -241.70353	4.85
	NO 1.380	CNH ₁ 126.9	ONCH ₃ 0.0	N +0.165	N -0.406	MP2 ₁ -504.99118	MP2 ₁ -46.445095	
	OH ₂ 0.949	NCH ₃ 117.2	ONCS +180.0	O -0.011	O -0.570	MP2 ₂ -505.48776	MP2 ₂ -52.09255	
		NCS 124.3	CNOH ₁ +180.0	H ₁ -0.022	H ₁ +0.411	DFT -506.09856	DFT -171.99651	
		NOH ₂ 107.1		H ₂ -0.0004	H ₂ +0.470			

Table A3e: 1,2,3-thiadiazol-5-yl nitrene

Optimized adducts ^a	Selected parameters			Spin populations	^b Charge populations	Energy ^c (a.u.)	ΔE^d (kJ/mol)	Dipole moments (D)
	Bond lengths (Å)	Bond angles (deg)	Dihedral angles (deg)					
	CN 1.448	CNO 117.5	ONCH ₁ -143.8	C +0.025	C -0.114	SCF -751.51203	SCF -303.06147	2.34
	NO 1.269	CNH ₁ 117.6	ONCH ₃ +38.1	N +0.258	N -0.301	MP2 ₁ -752.71618	MP2 ₁ -156.16474	
		NCH ₃ 106.5	ONCH ₂ -78.8	O +0.758	O -0.302	MP2 ₂ -753.11723	MP2 ₂ -147.55573	
		NCH ₂ 111.1	ONCS +158.2	H ₁ -0.017	H ₁ +0.378	DFT -754.01087	DFT -247.95222	
		NCS 110.7						
	CN 1.410	CNO 109.6	ONCH ₁ +116.5	C +0.937	C +0.029	SCF -751.50336	SCF -280.29838	4.06
	NO 1.392	CNH ₁ 111.7	ONCH ₃ +13.0	N -0.037	N -0.409	MP2 ₁ -752.69053	MP2 ₁ -88.82067	
	OH ₂ 0.948	NCH ₃ 117.0	ONCS -167.5	O -0.003	O -0.605	MP2 ₂ -753.09476	MP2 ₂ -88.56074	
		NCS 120.2	CNOH ₁ -120.4	H ₁ +0.024	H ₁ +0.380	DFT -753.99925	DFT -217.44391	
		NOH ₂ 104.8		H ₂ +0.001	H ₂ +0.465			

^aAll structures were optimized at the HF/6-31G* level and have no imaginary frequencies

^bMulliken population analysis

^c1 au = 2625.5 kJ/mol. The MP2₁ and MP2₂ energies are single point energies obtained with the cc-pVDZ and cc-pVTZ basis sets respectively at the 6-31G* optimized geometry, *i.e.* MP2/cc-pVDZ//HF/6-31G* and MP2/cc-pVTZ//HF/6-31G* respectively.

^d ΔE = energy change for gas phase species at equilibrium bond lengths at 0K

$$\Delta E = E_{\text{adduct}} - [E_{\text{new heteroaryl nitrene}} + E_{\text{hydrogen radical}}]$$

Table A4: The reaction of new heteroaryl nitrones with •CH₃ at C- site and O- site

Table A4a: 1,2,4-thiadiazol-3-yl nitron

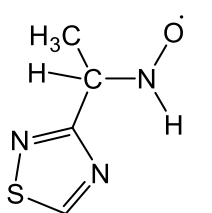
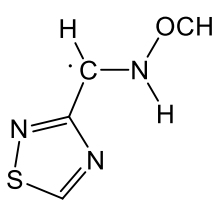
Optimized adducts ^a	Selected parameters			Spin populations	^b Charge populations	Energy ^c (a.u.)	ΔE ^d (kJ/mol)	Dipole moments (D)
	Bond lengths (Å)	Bond angles (deg)	Dihedral angles (deg)					
	C ₁ N 1.454	C ₁ NO 117.9	ONC ₁ C ₂ +70.7	C ₁ -0.038	C ₁ -0.016	SCF -790.59670	SCF -13.626345	4.24
	C ₁ C ₂ 1.532	C ₁ NH ₁ 118.0	ONC ₁ H ₁ +147.3	N +0.302	N -0.283	MP2 ₁ -791.96107	MP2 ₁ -191.11015	
	NO 1.266	NC ₁ C ₂ 112.2	NC ₁ C ₂ S +24.8	O +0.724	O -0.334	MP2 ₂ -792.40857	MP2 ₂ -182.36723	
			ONC ₁ H ₂ -49.6	H ₁ -0.020	H ₁ +0.390	DFT -793.33578	DFT -207.62454	
				C ₂ +0.027	C ₂ -0.495			
	C ₁ N 1.388	C ₁ NO 111.0	C ₁ NOC ₂ +127.3	C ₁ +0.937	C ₁ +0.036	SCF -790.57072	SCF 54.584145	1.81
	NO 1.390	NOC ₂ 110.2	ONC ₁ S +144.1	N -0.007	N -0.408	MP2 ₁ -791.90729	MP2 ₁ -49.910755	
	OC ₂ 1.402	CNH ₁ 112.4	ONC ₁ H ₂ -41.5	O +0.037	O -0.492	MP2 ₂ -792.35674	MP2 ₂ -46.287565	
			NOC ₂ H ₄ -179.4	C ₂ -0.004	C ₂ -0.142	DFT -793.30783	DFT -134.241815	
			ONC ₁ H ₁ +120.8					

Table A4b: 1,2,4-thiadiazol-5-yl nitron

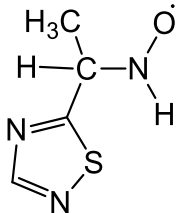
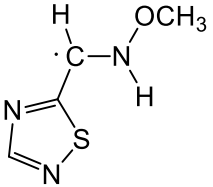
Optimized adducts ^a	Selected parameters			Spin populations	^b Charge populations	Energy ^c (a.u.)	ΔE^d (kJ/mol)	Dipole moments (D)
	Bond lengths (Å)	Bond angles (deg)	Dihedral angles (deg)					
	CN 1.458	CNO 119.0	ONC ₁ C ₂ +39.1	C ₁ -0.031	C ₁ -0.010	SCF -790.59483	SCF -32.81875	1.38
	CC 1.529	CNH ₁ 117.0	ONC ₁ H ₁ +143.7	N +0.257	N -0.309	MP2 ₁ -791.95849	MP2 ₁ -201.55964	
	NO 1.269	NCC 110.7	NC ₁ C ₂ S +1.7	O +0.761	O -0.302	MP2 ₂ -792.40549	MP2 ₂ -191.26768	
			ONC ₁ H ₂ -82.1	H ₁ -0.015	H ₁ +0.381	DFT -793.33476	DFT -222.45862	
				C ₂ +0.002	C ₂ -0.484			
	C ₁ N 1.398	C ₁ NO 110.7	C ₁ NOC ₂ +118.4	C ₁ +0.927	C ₁ +0.042	SCF -790.57052	SCF 31.007155	2.51
	NO 1.384	NOC ₂ 110.3	ONC ₁ S +177.7	N -0.009	N -0.400	MP2 ₁ -791.90136	MP2 ₁ -51.56482	
	OC ₂ 1.405	CNH ₁ 112.9	ONC ₁ H ₂ +0.4	O -0.004	O -0.492	MP2 ₂ -792.35077	MP2 ₂ -47.60032	
			NOC ₂ H ₄ -179.5	C ₂ +0.002	C ₂ -0.147	DFT -793.30661	DFT -148.55079	
			ONC ₁ H ₁ +119.1					

Table A4c: Furoxan-4-yl nitron

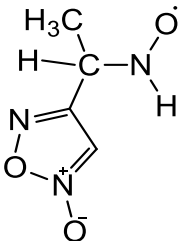
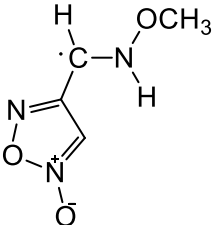
Optimized adducts ^a	Selected parameters			Spin populations	^b Charge populations	Energy ^c (a.u.)	ΔE^d (kJ/mol)	Dipole moments (D)
	Bond lengths (Å)	Bond angles (deg)	Dihedral angles (deg)					
	CN 1.454	CNO 118.7	ONC ₁ C ₂ +174.4	C ₁ +0.038	C ₁ +0.020	SCF -542.6365	SCF -60.622795	6.08
	CC 1.528	CNH ₁ 117.3	ONC ₁ H ₁ +145.4	N +0.270	N -0.319	MP2 ₁ -544.20237	MP2 ₁ -45.132345	
	NO 1.269	NCC 109.1	NC ₁ C ₂ S -11.8	O +0.751	O -0.308	MP2 ₂ -544.73582	MP2 ₂ -82.91329	
			ONC ₁ H ₂ +54.8	H ₁ -0.019	H ₁ +0.386	DFT -545.41698	DFT -230.28261	
				C ₂ -0.013	C ₂ -0.524			
	C ₁ N 1.406	C ₁ NO 109.9	C ₁ NOC ₂ +116.1	C ₁ +1.015	C ₁ +0.008	SCF -542.61373	SCF -0.84016	5.41
	NO 1.387	NOC ₂ 110.4	ONC ₁ S -167.1	N -0.039	N -0.401	MP2 ₁ -544.16534	MP2 ₁ 52.08992	
	OC ₂ 1.404	CNH ₁ 112.0	ONC ₁ H ₂ +13.1	O -0.003	O -0.495	MP2 ₂ -544.70116	MP2 ₂ 8.08654	
			NOC ₂ H ₄ -179.5	C ₂ +0.003	C ₂ -0.147	DFT -545.38402	DFT -143.74613	
			ONC ₁ H ₁ +116.9					

Table A4d: Furoxan-3-yl nitron

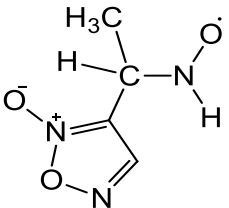
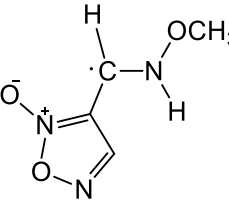
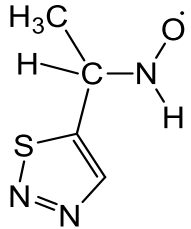
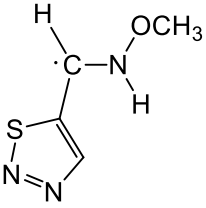
Optimized adducts ^a	Selected parameters			Spin populations	^b Charge populations	Energy ^c (a.u.)	ΔE^d (kJ/mol)	Dipole moments (D)
	Bond lengths (Å)	Bond angles (deg)	Dihedral angles (deg)					
	CN 1.446	CNO 120.2	ONC ₁ C ₂ +175.5	C ₁ -0.116	C ₁ +0.030	SCF -542.6376	SCF -63.79965	4.76
	CC 1.528	CNH ₁ 119.8	ONC ₁ H ₁ -159.0	N +0.320	N -0.302	MP2 ₁ -544.20364	MP2 ₁ -103.4447	
	NO 1.262	NCC 109.4	NC ₁ C ₂ S +10.1	O +0.720	O -0.322	MP2 ₂ -544.7369	MP2 ₂ -86.93031	
			ONC ₁ H ₂ +56.8	H ₁ -0.028	H ₁ +0.383	DFT -545.41841	DFT -230.67643	
				C ₂ +0.023	C ₂ -0.529			
	C ₁ N1.358	C ₁ NO 126.4	C ₁ NOC ₂ 0.0	C ₁ +0.727	C ₁ +0.018	SCF -542.59225	SCF 55.266775	5.51
	NO 1.379	NOC ₂ 116.0	ONC ₁ S +180.0	N +0.167	N -0.393	MP2 ₁ -544.15632	MP2 ₁ 20.79396	
	OC ₂ 1.400	CNH ₁ 124.7	ONC ₁ H ₂ 0.0	O -0.008	O -0.447	MP2 ₂ -544.69504	MP2 ₂ 22.973125	
			NOC ₂ H ₄ -61.9	C ₂ -0.0008	C ₂ -0.200	DFT -545.37287	DFT -111.11116	
			ONC ₁ H ₁ +180.0					

Table A4e: 1,2,3-thiadiazol-5-yl nitrene

Optimized adducts ^a	Selected parameters			Spin populations	^b Charge populations	Energy ^c (a.u.)	ΔE^d (kJ/mol)	Dipole moments (D)
	Bond lengths (Å)	Bond angles (deg)	Dihedral angles (deg)					
	CN 1.459	CNO 118.2	ONC ₁ C ₂ +50.5	C ₁ +0.029	C ₁ +0.023	SCF -790.54984	SCF -33.71142	2.03
	CC 1.529	CNH ₁ 117.0	ONC ₁ H ₁ +143.1	N +0.258	N -0.300	MP2 ₁ -791.90436	MP2 ₁ -149.41721	
	NO 1.268	NCC 110.2	NC ₁ C ₂ S +8.0	O +0.753	O -0.308	MP2 ₂ -792.34702	MP2 ₂ -131.59006	
			ONC ₁ H ₂ -69.0	H ₁ -0.016	H ₁ +0.378	DFT -793.33476	DFT-317.239165	
				C ₂ -0.010	C ₂ -0.475			
	C ₁ N1.410	C ₁ NO 110.0	C ₁ NOC ₂ +116.0	C ₁ +0.938	C ₁ +0.030	SCF -790.53233	SCF 12.261085	4.32
	NO 1.388	NOC ₂ 110.3	ONC ₁ S -166.7	N -0.038	N -0.398	MP2 ₁ -791.85703	MP2 ₁ -25.15229	
	OC ₂ 1.404	CNH ₁ 111.6	ONC ₁ H ₂ +14.0	O -0.002	O -0.499	MP2 ₂ -792.30216	MP2 ₂ -13.81013	
			NOC ₂ H ₄ -179.4	C ₂ +0.003	C ₂ -0.146	DFT -793.27273	DFT -154.3794	
			ONC ₁ H ₁ +116.4					

^aAll structures were optimized at the HF/6-31G* level and have no imaginary frequencies

^bMulliken population analysis

^c1 au = 2625.5 kJ/mol. The MP2₁ and MP2₂ energies are single point energies obtained with the cc-pVDZ and cc-pVTZ basis sets respectively at the 6-31G* optimized geometry, *i.e.* MP2/cc-pVDZ//HF/6-31G* and MP2/cc-pVTZ//HF/6-31G* respectively.

^d $\Delta E = E_{\text{adduct}} - [E_{\text{new heteroaryl nitrene}} + E_{\text{methyl radical}}]$

Table A5: The reaction of new heteroaryl nitrones with •OH at C- site and O- site

Table A5a: 1,2,4-thiadiazol-3-yl nitron

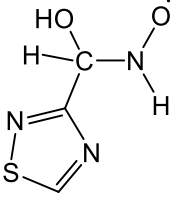
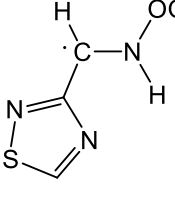
Optimized adducts ^a	Selected parameters			Spin populations	^b Charge populations	Energy ^c (a.u.)	ΔE^d (kJ/mol)	Dipole moments (D)
	Bond lengths (Å)	Bond angles (deg)	Dihedral angles (deg)					
	CN 1.429	CNO ₁ 117.2	O ₁ NCO ₂ +77.7	C -0.014	C +0.317	SCF -826.41068	SCF-615.33844	4.46
	NO ₁ 1.274	CNH ₁ 117.0	O ₁ NCH ₁ +143.4	N +0.224	N -0.305	MP2 ₁ -827.81433	MP2 ₁ -654.98349	
	CO ₂ 1.274	NCO ₂ 109.4	NCO ₂ H ₂ -166.2	O ₁ +0.791	O ₁ -0.291	MP2 ₂ -828.29661	MP2 ₂ -590.08113	
		CO ₂ H ₂ 109.7		O ₂ +0.009	O ₂ -0.731	DFT -829.23241	DFT -336.56285	
				H ₁ -0.014	H ₁ +0.396			
	CN 1.391	CNO ₁ 113.6	CNO ₁ O ₂ -67.4	C +0.956	C +0.023	SCF -826.30472	SCF -337.14046	3.48
	NO ₁ 1.359	NO ₁ O ₂ 109.6	NO ₁ O ₂ H ₄ -113.9	N -0.005	N -0.348	MP2 ₁ -827.69631	MP2 ₁ -345.12198	
	O ₁ O ₂ 1.403	O ₁ O ₂ H ₄ 102.0	O ₁ NCH ₁ +127.4	O ₁ -0.013	O ₁ -0.226	MP2 ₂ -828.17858	MP2 ₂ -280.19336	
		CNH ₁ 114.0	O ₁ NCH ₂ -38.0	O ₂ +0.038	O ₂ -0.453	DFT -829.16670	DFT -164.04124	
			O ₁ NCS +147.6	H ₁ +0.001	H ₁ +0.390			
			H ₄ -0.002	H ₄ +0.460				

Table A5b: 1,2,4-thiadiazol-5-yl nitron

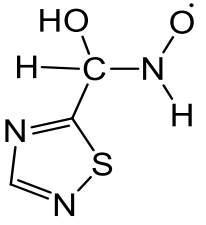
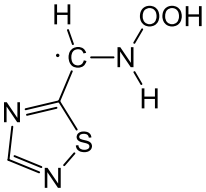
Optimized adducts ^a	Selected parameters			Spin populations	^b Charge populations	Energy ^c (a.u.)	ΔE^d (kJ/mol)	Dipole moments (D)
	Bond lengths (Å)	Bond angles (deg)	Dihedral angles (deg)					
	CN 1.436	CNO ₁ 116.6	O ₁ NCO ₂ +64.6	C -0.022	C +0.362	SCF -826.41356	SCF -647.00197	0.68
	NO ₁ 1.266	CNH ₁ 120.1	O ₁ NCH ₁ +151.0	N +0.287	N -0.290	MP2 ₁ -827.82036	MP2 ₁ -688.03853	
	CO ₂ 1.389	NCO ₂ 113.4	NCO ₂ H ₂ -63.9	O ₁ +0.738	O ₁ -0.324	MP2 ₂ -828.30285	MP2 ₂ -623.45123	
		CO ₂ H ₂ 109.4		O ₂ +0.015	O ₂ -0.743	DFT -829.24140	DFT -377.67818	
				H ₁ -0.021	H ₁ +0.394			
	CN 1.392	CNO ₁ 110.5	CNO ₁ O ₂ +137.0	C +0.893	C +0.048	SCF -826.30087	SCF -351.13437	1.52
	NO ₁ 1.375	NO ₁ O ₂ 108.1	NO ₁ O ₂ H ₄ -80.0	N +0.013	N -0.370	MP2 ₁ -827.68721	MP2 ₁ -338.45321	
	O ₁ O ₂ 1.381	O ₁ O ₂ H ₄ 103.5	O ₁ NCH ₁ +122.2	O ₁ +0.016	O ₁ -0.238	MP2 ₂ -828.16920	MP2 ₂ -272.55316	
		CNH ₁ 115.3	O ₁ NCH ₂ -24.1	O ₂ -0.009	O ₂ -0.406	DFT -829.13831	DFT -107.01538	
			O ₁ NCS +160.8	H ₁ +0.011	H ₁ +0.392			
				H ₄ -0.0001	H ₄ +0.458			

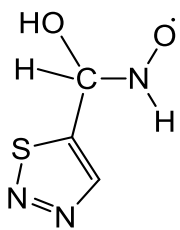
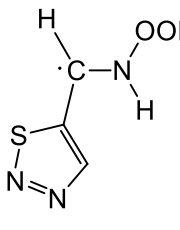
Table A5c: Furoxan-4-yl nitron

Optimized adducts ^a	Selected parameters			Spin populations	^b Charge populations	Energy ^c (a.u.)	ΔE^d (kJ/mol)	Dipole moments (D)
	Bond lengths (Å)	Bond angles (deg)	Dihedral angles (deg)					
	CN 1.454	CNO ₁ 115.9	O ₁ NCO ₂ +53.3	C +0.035	C +0.385	SCF -578.45364	SCF -670.63147	3.15
	NO ₁ 1.267	CNH ₁ 118.7	O ₁ NCH ₁ +145.4	N +0.275	N -0.299	MP2 ₁ -580.06375	MP2 ₁ -530.32475	
	CO ₂ 1.377	NCO ₂ 109.9	NCO ₂ H ₂ -46.6	O ₁ +0.735	O ₁ -0.326	MP2 ₂ -580.63187	MP2 ₂ -511.65744	
		CO ₂ H ₂ 108.6		O ₂ +0.0003	O ₂ -0.747	DFT -581.32130	DFT -379.411005	
				H ₁ -0.019	H ₁ +0.397			
	CN 1.393	CNO ₁ 113.7	CNO ₁ O ₂ +70.8	C +2.511	C 0.0101	SCF -578.34597	SCF -387.94388	3.55
	NO ₁ 1.360	NO ₁ O ₂ 109.4	NO ₁ O ₂ H ₄ -110.2	N +3.672	N -0.3394	MP2 ₁ -579.95622	MP2 ₁ -248.00473	
	O ₁ O ₂ 1.399	O ₁ O ₂ H ₄ 102.9	O ₁ NCH ₁ -126.2	O ₁ +4.112	O ₁ -0.2165	MP2 ₂ -580.52482	MP2 ₂ -230.59765	
		CNH ₁ 115.7	O ₁ NCH ₂ +39.9	O ₂ +4.209	O ₂ -0.4482	DFT -581.21448	DFT -98.955095	
			O ₁ NCS -149.0	H ₁ +0.309	H ₁ 0.3813			
			H ₄ +0.268	H ₄ 0.4653				

Table A5d: Furoxan-3-yl nitron

Optimized adducts ^a	Selected parameters			Spin populations	^b Charge populations	Energy ^c (a.u.)	ΔE^d (kJ/mol)	Dipole moments (D)
	Bond lengths (Å)	Bond angles (deg)	Dihedral angles (deg)					
	CN 1.458	CNO ₁ 115.7	O ₁ NCO ₂ +50.9	C +0.050	C +0.384	SCF -578.45405	SCF -671.99673	2.52
	NO ₁ 1.268	CNH ₁ 118.0	O ₁ NCH ₁ +142.3	N +0.263	N -0.297	MP2 ₁ -580.06424	MP2 ₁ -586.58921	
	CO ₂ 1.377	NCO ₂ 109.5	NCO ₂ H ₂ -45.3	O ₁ +0.740	O ₁ -0.324	MP2 ₂ -580.63178	MP2 ₂ -512.60262	
		CO ₂ H ₂ 108.5	O ₂ -0.002	O ₂ -0.743	DFT -581.32214	DFT -378.255785		
	CN 1.363	CNO ₁ 125.0	CNO ₁ O ₂ 0.0	C +0.762	C +0.042	SCF -578.31658	SCF -311.06924	6.68
	NO ₁ 1.384	NO ₁ O ₂ 107.7	NO ₁ O ₂ H ₄ +180.0	N +0.130	N -0.409	MP2 ₁ -579.93187	MP2 ₁ -239.05178	
	O ₁ O ₂ 1.391	O ₁ O ₂ H ₄ 99.9	O ₁ NCH ₁ +180.0	O ₁ -0.009	O ₁ -0.224	MP2 ₂ -580.50227	MP2 ₂ -172.57412	
		CNH ₁ 126.7	O ₁ NCH ₂ 0.0	O ₂ +0.0002	O ₂ -0.428	DFT -581.18728	DFT -24.180855	
	O ₁ NCS +180.0	H ₁ -0.019	H ₁ +0.411	H ₄ -0.0005	H ₄ +0.485			

Table A5e: 1,2,3-thiadiazol-5-yl nitron

Optimized adducts ^a	Selected parameters			Spin populations	^b Charge populations	Energy ^c (a.u.)	ΔE^d (kJ/mol)	Dipole moments (D)
	Bond lengths (Å)	Bond angles (deg)	Dihedral angles (deg)					
	CN 1.443	CNO ₁ +116.6	O ₁ NCO ₂ +75.2	C -0.068	C +0.362	SCF -826.37093	SCF -654.09082	3.02
	NO ₁ 1.273	CNH ₁ +117.7	O ₁ NCH ₁ +142.8	N +0.249	N -0.309	MP2 ₁ -827.76384	MP2 ₁ -629.62116	
	CO ₂ 1.388	NCO ₂ +112.9	NCO ₂ H ₂ -66.0	O ₁ +0.774	O ₁ -0.304	MP2 ₂ -828.24107	MP2 ₂ -555.08321	
		CO ₂ H ₂ +109.2		O ₂ +0.017	O ₂ -0.735	DFT -829.20130	DFT -367.17618	
			H ₁ -0.014	H ₁ +0.388				
	CN	CNO ₁	CNO ₁ O ₂	C	C	SCF -	SCF -	-
	NO ₁	NO ₁ O ₂	NO ₁ O ₂ H ₄	N	N	MP2 ₁ -	MP2 ₁ -	
	O ₁ O ₂	O ₁ O ₂ H ₄	O ₁ NCH ₁	O ₁	O ₁	MP2 ₂ -	MP2 ₂ -	
		CNH ₁	O ₁ NCH ₂	O ₂	O ₂	DFT -	DFT -107.96056	
		O ₁ NCS	H ₁	H ₁	829.10257			
			H ₄	H ₄				

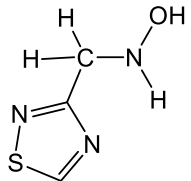
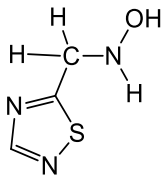
^aAll structures were optimized at the HF/6-31G* level and have no imaginary frequencies

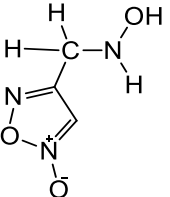
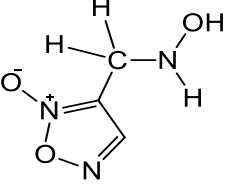
^bMulliken population analysis

^c1 au = 2625.5 kJ/mol. The MP2₁ and MP2₂ energies are single point energies obtained with the cc-pVDZ and cc-pVTZ basis sets respectively at the 6-31G* optimized geometry, *i.e.* MP2/cc-pVDZ//HF/6-31G* and MP2/cc-pVTZ//HF/6-31G* respectively.

^d $\Delta E = E_{\text{adduct}} - [E_{\text{new heteroaryl nitrene}} + E_{\text{hydroxyl radical}}]$

Table 6: The energetic studies of nitron double adducts**Table A6a:** Di •H spin adducts

Optimized adducts ^a	Selected parameters			Charge populations ^b	Energy (a.u.)	ΔE^d (kJ/mol)	Dipole moments (D)
	Bond lengths (Å)	Bond angles (deg)	Dihedral angles (deg)				
 1,2,4-thiadiazol-3-yl nitron	NO 1.401	CNO 107.2	CNOH ₂ +122.2	C -0.138	SCF -752.14573	SCF -515.70071	2.06
	CN 1.452	CNH ₁ 108.8	ONCH ₁ +112.7	N -0.397	MP2 ₁ -753.39683	MP2 ₁ -525.17877	
	OH ₂ 0.947	NOH ₂ 104.5	ONCS +171.3	O -0.620	MP2 ₂ -753.8124	MP2 ₂ -549.65368	
				H ₁ +0.376	DFT -754.67003	DFT -558.9952	
				H ₂ +0.457			
 1,2,4-thiadiazol-5-yl nitron	NO 1.397	CNO 107.9	CNOH ₂ +123.7	C -0.135	SCF -752.14639	SCF -541.53563	1.91
	CN 1.450	CNH ₁ 109.7	ONCH ₁ +113.4	N -0.411	MP2 ₁ -753.39737	MP2 ₁ -543.81982	
	OH ₂ 0.948	NOH ₂ 104.7	ONCS -174.0	O -0.609	MP2 ₂ -753.81613	MP2 ₂ -576.43378	
				H ₁ +0.368	DFT -754.67160	DFT -580.62932	

				H ₂ +0.462			
 <p>Furoxan-4-yl nitronium</p>	NO 1.398 CN 1.453 OH ₂ 0.948	CNO 107.0 CNH ₁ 110.1 NOH ₂ 104.6	CNOH ₂ +122.4 ONCH ₁ +112.7 ONCS +175.5	C -0.147 N -0.382 O -0.616 H ₁ +0.358 H ₂ +0.465	SCF -504.17685 MP2 ₁ -505.67923 MP2 ₂ -506.18402 DFT -506.75566	SCF -539.90782 MP2 ₁ -487.10902 MP2 ₂ -566.69317 DFT -593.28423	4.60
 <p>Furoxan-3-yl nitronium</p>	NO 1.398 CN 1.454 OH ₂ 0.948	CNO 107.2 CNH ₁ 109.7 NOH ₂ 104.5	CNOH ₂ -121.2 ONCH ₁ -112.9 ONCS -177.6	C -0.116 N -0.372 O -0.620 H ₁ +0.357 H ₂ +0.465	SCF -504.17701 MP2 ₁ -505.6818 MP2 ₂ -506.18613 DFT -506.75056	SCF -540.616705 MP2 ₁ -548.83452 MP2 ₂ -573.41445 DFT -576.53354	4.37

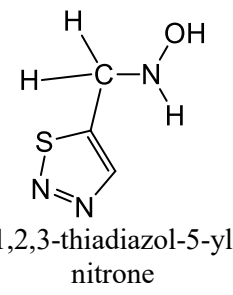
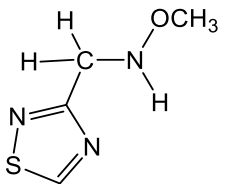
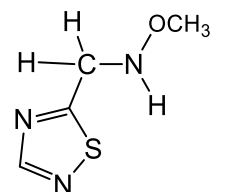
 <p>1,2,3-thiadiazol-5-yl nitronium</p>	NO	1.398	CNO	107.5	CNOH ₂	+124.1	C	-0.117	SCF	-752.10158	SCF	-542.90089	3.69
	CN	1.452	CNH ₁	109.4	ONCH ₁	+113.2	N	-0.395	MP2 ₁	-753.36426	MP2 ₁	-546.86540	
	OH ₂	0.947	NOH ₂	104.7	ONCS	+178.0	O	-0.615	MP2 ₂	-752.27449*	MP2 ₂	3377.30667*	
							H ₁	+0.366	DFT	-754.63406	DFT	-576.84860	
							H ₂	+0.462					

Table A6b: $\bullet\text{H} + \bullet\text{CH}_3$ spin adducts

Optimized adducts ^a	Selected parameters			Charge populations ^b	Energy ^c (a.u.)	ΔE^d (kJ/mol)	Dipole moments (D)
	Bond lengths (Å)	Bond angles (deg)	Dihedral angles (deg)				
 <p>1,2,4-thiadiazol-3-yl nitronium</p>	C ₁ N 1.452 NO 1.396 OC ₂ 1.399	C ₁ NO 107.1 NOC ₂ 110.1 C ₁ NH ₁ 108.8 NC ₁ S 109.6	C ₁ NOC ₂ +125.6 ONC ₁ H ₁ +112.7 ONC ₁ S +171.7 NOCH ₃ -178.7	C ₁ -0.137 N -0.383 O -0.513 C ₂ -0.134 H ₁ +0.375	SCF -791.17431 MP2 ₁ -792.56327 MP2 ₂ -793.01945 DFT -793.94355	SCF -222.1173 MP2 ₁ -461.35286 MP2 ₂ -473.98414 DFT -558.99521	1.96
 <p>1,2,4-thiadiazol-5-yl nitronium</p>	C ₁ N 1.450 NO 1.392 OC ₂ 1.402	C ₁ NO 107.8 NOC ₂ 110.2 C ₁ NH ₁ 109.7 NC ₁ S 109.8	C ₁ NOC ₂ -125.9 ONC ₁ H ₁ -113.5 ONC ₁ S +173.6 NOCH ₃ +179.0	C ₁ -0.135 N -0.398 O -0.502 C ₂ -0.141 H ₁ +0.366	SCF -791.17523 MP2 ₁ -792.56395 MP2 ₂ -793.01999 DFT -793.94512	SCF -248.63485 MP2 ₁ -480.36148 MP2 ₂ -492.38890 DFT -580.62933	2.19

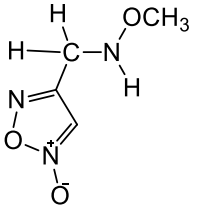
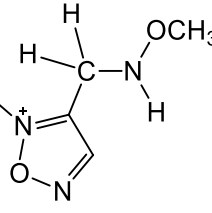
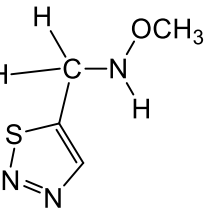
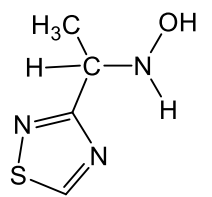
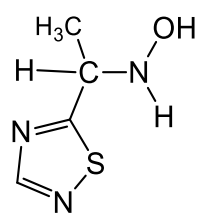
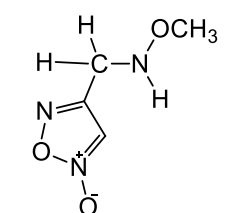
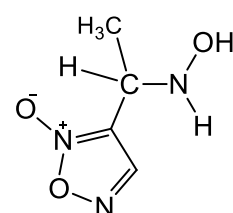
 <p>Furoxan-4-yl nitronium</p>	<p>C₁N 1.453</p> <p>NO 1.393</p> <p>OC₂ 1.403</p>	<p>C₁NO 106.8</p> <p>NOC₂ 110.1</p> <p>C₁NH₁ 110.0</p> <p>NC₁S 110.1</p>	<p>C₁NOC₂ +125.1</p> <p>ONC₁H₁ +112.6</p> <p>ONC₁S +176.5</p> <p>NOCH₃ -178.6</p>	<p>C₁ -0.147</p> <p>N -0.370</p> <p>O -0.510</p> <p>C₂ -0.142</p> <p>H₁ +0.356</p>	<p>SCF -543.20561</p> <p>MP2₁ -544.84553</p> <p>MP2₂ -545.39112</p> <p>DFT -546.02289</p>	<p>SCF -246.79700</p> <p>MP2₁ -422.91554</p> <p>MP2₂ -491.15491</p> <p>DFT -593.28424</p>	4.91
 <p>Furoxan-3-yl nitronium</p>	<p>C₁N 1.454</p> <p>NO 1.393</p> <p>OC₂ 1.403</p>	<p>C₁NO 107.0</p> <p>NOC₂ 110.0</p> <p>C₁NH₁ 109.7</p> <p>NC₁S 110.4</p>	<p>C₁NOC₂ -123.1</p> <p>ONC₁H₁ -112.8</p> <p>ONC₁S -177.0</p> <p>NOCH₃ +178.2</p>	<p>C₁ -0.117</p> <p>N -0.360</p> <p>O -0.513</p> <p>C₂ -0.142</p> <p>H₁ +0.353</p>	<p>SCF -543.20566</p> <p>MP2₁ -544.84817</p> <p>MP2₂ -545.39334</p> <p>DFT -546.02435</p>	<p>SCF -247.21708</p> <p>MP2₁ -484.82483</p> <p>MP2₂ -498.16500</p> <p>DFT -576.53355</p>	4.56
 <p>1,2,3-thiadiazol-5-yl nitronium</p>	<p>C₁N</p> <p>NO</p> <p>OC₂</p>	<p>C₁NO</p> <p>NOC₂</p> <p>C₁NH₁</p> <p>NC₁S</p>	<p>C₁NOC₂</p> <p>ONC₁H₁</p> <p>ONC₁S</p> <p>NOCH₃</p>	<p>C₁</p> <p>N</p> <p>O</p> <p>C₂</p> <p>H₁</p>	<p>SCF -</p> <p>MP2₁ -</p> <p>MP2₂ -</p> <p>DFT -793.81042</p>	<p>SCF -</p> <p>MP2₁ -</p> <p>MP2₂ -</p> <p>DFT -576.84861</p>	-

Table A6c: •CH₃ + •H spin adducts

Optimized adducts ^a	Selected parameters			Charge populations ^b	Energy ^c (a.u.)	ΔE ^d (kJ/mol)	Dipole moments (D)
	Bond lengths (Å)	Bond angles (deg)	Dihedral angles (deg)				
 1,2,4-thiadiazol-3-yl nitrene	C ₁ N 1.458	C ₁ NO 108.4	ONC ₁ C ₂ +58.1	C ₁ -0.014	SCF -791.18274	SCF -244.25027	1.91
	NO 1.401	NC ₁ C ₂ 114.3	C ₁ NOH ₂ +121.4	C ₂ -0.506	MP2 ₁ -792.58298	MP2 ₁ -513.10147	
	C ₁ C ₂ 1.532	C ₁ C ₂ H ₃ 109.9	ONC ₁ H ₁ +113.7	N -0.385	MP2 ₂ -793.03994	MP2 ₂ -527.78064	
		NOH ₂ 104.2	NC ₁ C ₂ H ₃ -57.7	O -0.624	DFT -793.95547	DFT -527.33168	
		C ₁ NH ₁ 109.6		H ₁ +0.370			
				H ₂ +0.458			
 1,2,4-thiadiazol-5-yl nitrene	C ₁ N 1.457	C ₁ NO 108.6	ONC ₁ C ₂ +66.6	C ₁ +0.004	SCF -791.18435	SCF -272.57941	2.04
	NO 1.397	NC ₁ C ₂ 114.7	C ₁ NOH ₂ +123.0	C ₂ -0.490	MP2 ₁ -792.58498	MP2 ₁ -535.57575	
	C ₁ C ₂ 1.527	C ₁ C ₂ H ₃ 109.4	ONC ₁ H ₁ +113.8	N -0.410	MP2 ₂ -793.0413	MP2 ₂ -548.33830	
		NOH ₂ 104.5	NC ₁ C ₂ H ₃ -57.2	O -0.610	DFT -793.95871	DFT -553.35038	
		C ₁ NH ₁ 109.7		H ₁ +0.364			

				H ₂ +0.463			
 <p>Furoxan-4-yl nitronium</p>	C ₁ N 1.459 NO 1.398 C ₁ C ₂ 1.527	C ₁ NO 108.2 NC ₁ C ₂ 114.8 C ₁ C ₂ H ₃ 109.3 NOH ₂ 104.6 C ₁ NH ₁ 109.4	ONC ₁ C ₂ +62.9 C ₁ NOH ₂ +124.4 ONC ₁ H ₁ +113.4 NC ₁ C ₂ H ₃ -56.7	C ₁ -0.004 C ₂ -0.500 N -0.399 O -0.611 H ₁ +0.364 H ₂ +0.462	SCF -543.21796 MP2 ₁ -544.86879 MP2 ₂ -545.41433 DFT -546.03944	SCF -279.221925 MP2 ₁ -483.98467 MP2 ₂ -552.09277 DFT -557.262375	5.03
 <p>Furoxan-3-yl nitronium</p>	C ₁ N 1.457 NO 1.387 C ₁ C ₂ 1.533	C ₁ NO 111.4 NC ₁ C ₂ 114.3 C ₁ C ₂ H ₃ 114.3 NOH ₂ 109.2 C ₁ NH ₁ 110.8	ONC ₁ C ₂ +76.9 C ₁ NOH ₂ -62.9 ONC ₁ H ₁ +119.5 NC ₁ C ₂ H ₃ -60.8	C ₁ +0.012 C ₂ -0.523 N -0.378 O -0.590 H ₁ +0.348 H ₂ +0.442	SCF -543.20754 MP2 ₁ -544.86162 MP2 ₂ -545.40685 DFT -546.03069	SCF -252.15302 MP2 ₁ -520.13780 MP2 ₂ -533.63550 DFT -530.92861	4.85

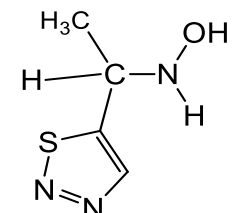
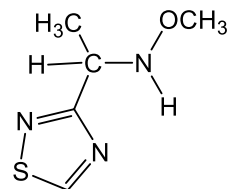
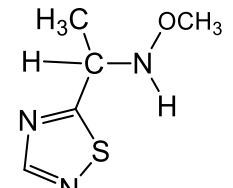
 <p>1,2,3-thiadiazol-5-yl nitronium</p>	C ₁ N 1.458	C ₁ NO 108.0	ONC ₁ C ₂ -69.0	C ₁ +0.04	SCF -791.13786	SCF -269.53383	0.46
	NO 1.399	NC ₁ C ₂ 110.4	C ₁ NOH ₂ +124.5	C ₂ -0.478	MP2 ₁ -792.551	MP2 ₁ -536.33714	
	C ₁ C ₂ 1.529	C ₁ C ₂ H ₃ 110.0	ONC ₁ H ₁ +112.7	N -0.391	MP2 ₂ -793.00617	MP2 ₂ -549.93986	
		NOH ₂ 104.8	NC ₁ C ₂ H ₃ +62.0	O -0.617	DFT -793.41860	DFT +769.92788*	
		C ₁ NH ₁ 108.8		H ₁ +0.366			
				H ₂ +0.461			

Table A6d: di •CH₃ spin adducts

Optimized adducts ^a	Selected parameters			Charge populations ^b	Energy ^c (a.u.)	ΔE ^d (kJ/mol)	Dipole moments (D)
	Bond lengths (Å)	Bond angles (deg)	Dihedral angles (deg)				
 <p>1,2,4-thiadiazol-3-yl nitron</p>	C ₁ N 1.459 NO 1.396 OC ₃ 1.399 C ₁ C ₂ 1.532	C ₁ NO 108.2 NOC ₃ 109.9 NC ₁ C ₂ 114.3 C ₁ C ₂ H ₂ 109.9 OC ₃ H ₃ 106.3	C ₁ NOC ₃ +124.3 ONC ₁ C ₂ +58.9 NOC ₃ H ₃ -178.7 NC ₁ C ₂ H ₂ -57.8 ONC ₁ H ₁ +113.8	C ₁ -0.013 C ₂ -0.504 N -0.371 O -0.514 C ₃ -0.133 H ₁ +0.368	SCF -830.21125 MP2 ₁ -831.74958 MP2 ₂ -832.24718 DFT -833.22912	SCF +49.51693 MP2 ₁ -449.69564 MP2 ₂ -452.60995 DFT -464.7135	1.80
 <p>1,2,4-thiadiazol-5-yl nitron</p>	C ₁ N 1.457 NO 1.392 OC ₃ 1.402 C ₁ C ₂ 1.527	C ₁ NO 108.6 NOC ₃ 110.1 NC ₁ C ₂ 114.8 C ₁ C ₂ H ₂ 109.4	C ₁ NOC ₃ +125.0 ONC ₁ C ₂ +67.3 NOC ₃ H ₃ -179.2 NC ₁ C ₂ H ₂ -57.2	C ₁ +0.005 C ₂ -0.488 N -0.397 O -0.502	SCF -830.21313 MP2 ₁ -831.75174 MP2 ₂ -832.24888 DFT -833.23218	SCF +20.47890 MP2 ₁ -472.59000 MP2 ₂ -474.06028 DFT -490.25962	2.32

		OC ₃ H ₃ 106.2	ONC ₁ H ₁ +113.9	C ₃ -0.140 H ₁ +0.362			
<p>Furoxan-4-yl nitronium</p>	C ₁ N 1.459 NO 1.394 OC ₃ 1.403 C ₁ C ₂ 1.531	C ₁ NO 107.9 NOC ₃ 110.0 NC ₁ C ₂ 114.4 C ₁ C ₂ H ₂ 109.6 OC ₃ H ₃ 106.2	C ₁ NOC ₃ +123.7 ONC ₁ C ₂ +63.7 NOC ₃ H ₃ -178.9 NC ₁ C ₂ H ₂ +113.0 ONC ₁ H ₁ -57.4	C ₁ -0.032 C ₂ -0.500 N -0.363 O -0.510 C ₃ -0.141 H ₁ -0.141	SCF -582.24307 MP2 ₁ -584.03147 MP2 ₂ -584.6185 DFT -585.30874	SCF +23.47197 MP2 ₁ -410.28689 MP2 ₂ -468.86179 DFT -483.22328	5.19
<p>Furoxan-3-yl nitronium</p>	C ₁ N 1.449 NO 1.393 OC ₃ 1.404 C ₁ C ₂ 1.52	C ₁ NO 109.7 NOC ₃ 110.3 NC ₁ C ₂ 108.5 C ₁ C ₂ H ₂ 110.9 OC ₃ H ₃ 109.6	C ₁ NOC ₃ -122.2 ONC ₁ C ₂ -175.1 NOC ₃ H ₃ +59.3 NC ₁ C ₂ H ₂ -58.2 ONC ₁ H ₁ -115.6	C ₁ +0.017 C ₂ -0.510 N -0.367 O -0.522 C ₃ -0.139 H ₁ +0.353	SCF -582.24686 MP2 ₁ -584.03664 MP2 ₂ -584.62351 DFT -585.31344	SCF +13.23252 MP2 ₁ -478.83869 MP2 ₂ -483.19702 DFT -492.20249	5.51

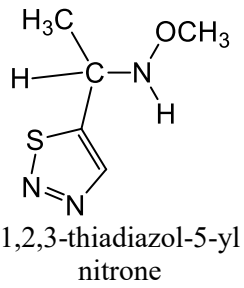
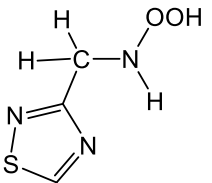
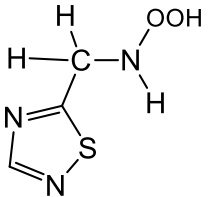
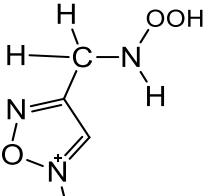
 <p>1,2,3-thiadiazol-5-yl nitron</p>	C ₁ N 1.459	C ₁ NO 108.5	C ₁ NOC ₃ +125.6	C ₁ +0.04	SCF -830.16683	SCF 23.025635	4.29
	NO 1.392	NOC ₃ 110.1	ONC ₁ C ₂ +61.6	C ₂ -0.506	MP2 ₁ -831.7171	MP2 ₁ -471.61857	
	OC ₃ 1.402	NC ₁ C ₂ 114.2	NOC ₃ H ₃ -178.8	N -0.385	MP2 ₂ -832.21347	MP2 ₂ -474.92670	
	C ₁ C ₂ 1.529	C ₁ C ₂ H ₂ 109.4	NC ₁ C ₂ H ₂ -54.8	O -0.507	DFT -833.19462	DFT -486.42639	
		OC ₃ H ₃ 106.2	ONC ₁ H ₁ +114.1	C ₃ -0.140			
				H ₁ +0.361			

Table A6e: •H + HO• spin adducts

Optimized adducts ^a	Selected parameters			Charge populations ^b	Energy ^c (a.u.)	ΔE^d (kJ/mol)	Dipole moments (D)
	Bond lengths (Å)	Bond angles (deg)	Dihedral angles (deg)				
 1,2,4-thiadiazol-3-yl nitronium	CN 1.454	CNO ₁ 106.1	CNO ₁ O ₂ +148.8	O ₁ -0.260	SCF -826.90589	SCF -607.48819	3.27
	NO ₁ 1.390	NO ₁ O ₂ 107.8	O ₁ NCH ₁ +113.8	C -0.154	MP2 ₁ -828.34859	MP2 ₁ -746.84973	
	O ₁ O ₂ 1.381	O ₁ O ₂ H ₂ 103.2	NO ₁ O ₂ H ₂ -70.7	N -0.361	MP2 ₂ -828.8375	MP2 ₂ -697.93929	
	O ₂ H ₂ 0.952		O ₁ NCS +172.1	O ₂ -0.414	DFT -829.77255	DFT -447.41146	
				H ₁ +0.382			
				H ₂ +0.453			

 <p>1,2,4-thiadiazol-5-yl nitron</p>	CN 1.453 NO ₁ 1.361 O ₁ O ₂ 1.403 O ₂ H ₂ 0.950	CNO ₁ 111.5 NO ₁ O ₂ 109.2 O ₁ O ₂ H ₂ 101.7	CNO ₁ O ₂ +67.3 O ₁ NCH ₁ -120.5 NO ₁ O ₂ H ₂ +121.7 O ₁ NCS +161.8	O ₁ -0.224 C -0.158 N -0.346 O ₂ -0.465 H ₁ +0.360 H ₂ +0.465	SCF -826.90914 MP2 ₁ -828.35397 MP2 ₂ -828.84264 DFT -829.77668	SCF -640.123155 MP2 ₁ -778.1982 MP2 ₂ -728.42135 DFT -475.76686	3.16
 <p>Furoxan-4-yl nitron</p>	CN 1.452 NO ₁ 1.361 O ₁ O ₂ 1.404 O ₂ H ₂ 0.951	CNO ₁ 112.0 NO ₁ O ₂ 109.2 O ₁ O ₂ H ₂ 102.3	CNO ₁ O ₂ +66.5 O ₁ NCH ₁ -120.2 NO ₁ O ₂ H ₂ -127.0 O ₁ NCS +167.0	O ₁ -0.225 C -0.174 N -0.333 O ₂ -0.462 H ₁ +0.374 H ₂ +0.465	SCF -578.94298 MP2 ₁ -580.63937 MP2 ₂ -581.21676 DFT -581.85837	SCF -647.369535 MP2 ₁ -730.78167 MP2 ₂ -735.03761 DFT -482.19933	4.95

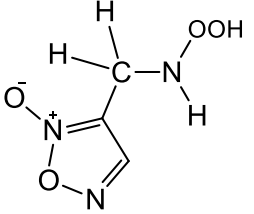
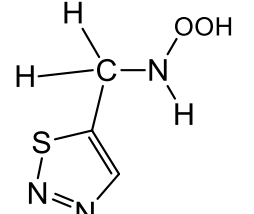
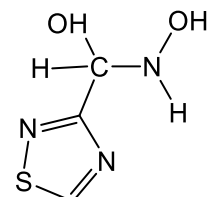
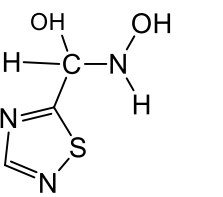
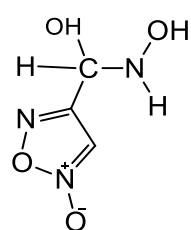
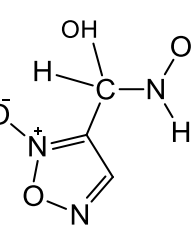
 <p>Furoxan-3-yl nitronium</p>	CN 1.454 NO ₁ 1.362 O ₁ O ₂ 1.403 O ₂ H ₂ 0.951	CNO ₁ 111.9 NO ₁ O ₂ 109.3 O ₁ O ₂ H ₂ 102.5	CNO ₁ O ₂ -66.8 O ₁ NCH ₁ +119.8 NO ₁ O ₂ H ₂ +122.6 O ₁ NCS -166.7	O ₁ -0.226 C -0.158 N -0.334 O ₂ -0.460 H ₁ +0.372 H ₂ +0.464	SCF -578.94282 MP2 ₁ -580.63984 MP2 ₂ -581.21677 DFT -581.85827	SCF -647.23826 MP2 ₁ -786.99363 MP2 ₂ -736.24534 DFT -478.57614	3.63
 <p>1,2,3-thiadiazol-5-yl nitronium</p>	CN NO ₁ O ₁ O ₂ O ₂ H ₂	CNO ₁ NO ₁ O ₂ O ₁ O ₂ H ₂	CNO ₁ O ₂ O ₁ NCH ₁ NO ₁ O ₂ H ₂ O ₁ NCS	O ₁ C N O ₂ H ₁ H ₂	SCF - MP2 ₁ - MP2 ₂ - DFT -	SCF - MP2 ₁ - MP2 ₂ - DFT -	-

Table A6f: •OH + •H spin traps

Optimized adducts ^a	Selected parameters			Charge populations ^b	Energy ^c (a.u.)	ΔE^d (kJ/mol)	Dipole moments (D)
	Bond lengths (Å)	Bond angles (deg)	Dihedral angles (deg)				
 1,2,4-thiadiazol-3-yl nitronium	CN 1.441 NO ₁ 1.404 CO ₂ 1.391 O ₂ H ₂ 0.950 O ₁ H ₃ 0.947	C ₁ NO ₁ 106.8 NCO ₂ 113.1 CO ₂ H ₂ 108.0 CNH ₁ 108.6 NO ₁ H ₃ 104.7	CNO ₁ H ₃ +122.2 O ₁ NCO ₂ +56.8 NCO ₂ H ₂ -56.0 O ₁ NCH ₁ +112.5	O ₁ -0.641 C +0.300 N -0.390 O ₂ -0.744 H ₁ +0.381 H ₂ +0.467 H ₃ +0.465	SCF -827.00376 MP2 ₁ -828.44645 MP2 ₂ -828.93855 DFT -829.86184	SCF -864.445875 MP2 ₁ -1003.78116 MP2 ₂ -963.24607 DFT -681.84235	1.77
 1,2,4-thiadiazol-5-yl nitronium	CN 1.444 NO ₁ 1.383 CO ₂ 1.371 O ₂ H ₂ 0.951	C ₁ NO ₁ 111.6 NCO ₂ 111.1 CO ₂ H ₂ 108.4 CNH ₁ 112.2	CNO ₁ H ₃ +57.6 O ₁ NCO ₂ +67.7 NCO ₂ H ₂ +56.5 O ₁ NCH ₁ -121.8	O ₁ -0.587 C +0.324 N -0.357 O ₂ -0.706	SCF -826.98912 MP2 ₁ -828.43533 MP2 ₂ -828.92734 DFT -829.84962	SCF -850.110645 MP2 ₁ -991.80888 MP2 ₂ -950.79070 DFT -667.270825	2.30

	O ₁ H ₃ 0.953	NO ₁ H ₃ 109.2		H ₁ +0.356 H ₂ +0.470 H ₃ +0.434			
 <p>Furoxan-4-yl nitronium</p>	CN 1.442 NO ₁ 1.401 CO ₂ 1.390 O ₂ H ₂ 0.950 O ₁ H ₃ 0.948	C ₁ NO ₁ 106.5 NCO ₂ 113.3 CO ₂ H ₂ 108.5 CNH ₁ 109.4 NO ₁ H ₃ 104.8	CNO ₁ H ₃ +123.1 O ₁ NCO ₂ +57.8 NCO ₂ H ₂ -57.1 O ₁ NCH ₁ +112.5	O ₁ -0.637 C +0.317 N -0.368 O ₂ -0.752 H ₁ +0.365 H ₂ +0.477 H ₃ +0.472	SCF -579.03794 MP2 ₁ -580.73184 MP2 ₂ -581.31275 DFT -582.24759	SCF -896.687015 MP2 ₁ -973.56166 MP2 ₂ -987.05935 DFT -1504.09644	5.79
 <p>Furoxan-3-yl nitronium</p>	CN 1.428 NO ₁ 1.386 CO ₂ 1.393 O ₂ H ₂ 0.953 O ₁ H ₃ 0.953	C ₁ NO ₁ 109.8 NCO ₂ 109.6 CO ₂ H ₂ 110.3 CNH ₁ 109.3 NO ₁ H ₃ 107.6	CNO ₁ H ₃ -55.4 O ₁ NCO ₂ +66.7 NCO ₂ H ₂ +173.3 O ₁ NCH ₁ +117.5	O ₁ -0.600 C +0.354 N -0.365 O ₂ -0.777 H ₁ +0.358 H ₂ +0.460	SCF -579.03666 MP2 ₁ -580.73192 MP2 ₂ -581.31199 DFT -581.94381	SCF -893.61518 MP2 ₁ -1028.7497 MP2 ₂ -986.24545 DFT -703.16141	2.09

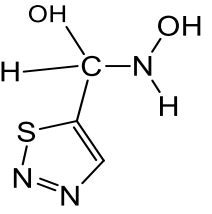
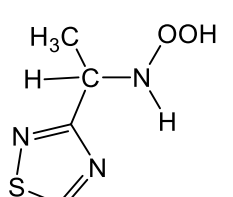
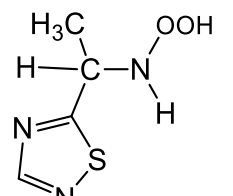
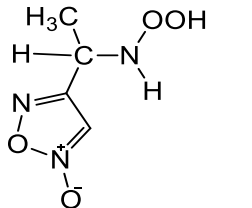
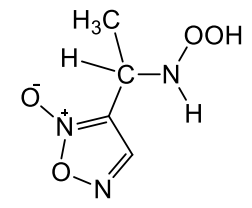
				H ₃ +0.494			
 1,2,3-thiadiazol-5-yl nitronium	CN 1.440	C ₁ NO ₁ 106.8	CNO ₁ H ₃ +124.2	O ₁ -0.634	SCF -826.96191	SCF -897.68471	5.17
	NO ₁ 1.401	NCO ₂ 113.5	O ₁ NCO ₂ +58.5	C +0.369	MP2 ₁ -828.41642	MP2 ₁ -1032.13656	
	CO ₂ 1.391	CO ₂ H ₂ 108.7	NCO ₂ H ₂ -60.8	N -0.385	MP2 ₂ -828.90696	MP2 ₂ -991.12888	
	O ₂ H ₂ 0.949	CNH ₁ 108.8	O ₁ NCH ₁ +112.7	O ₂ -0.754	DFT -829.82980	DFT -710.01397	
	O ₁ H ₃ 0.947	NO ₁ H ₃ 104.9		H ₁ +0.370			
				H ₂ +0.473			
				H ₃ +0.467			

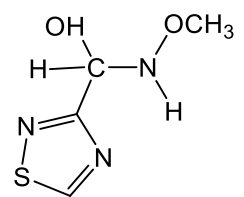
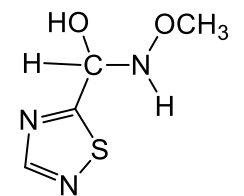
Table A6g: •CH₃ + •OH spin adducts

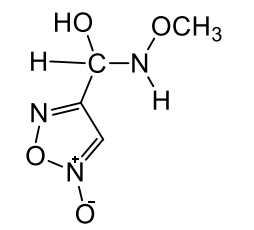
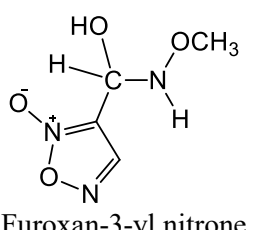
Optimized adducts ^a	Selected parameters			Charge populations ^b	Energy ^c (a.u.)	ΔE ^d (kJ/mol)	Dipole moments (D)
	Bond lengths (Å)	Bond angles (deg)	Dihedral angles (deg)				
 1,2,4-thiadiazol-3-yl nitronium	C ₁ N 1.462 NO ₁ 1.365 O ₁ O ₂ 1.404 C ₁ C ₂ 1.525	C ₁ NO 112.8 NC ₁ C ₂ 110.4 NO ₁ O ₂ 109.8 O ₁ O ₂ H ₂ 102.6	C ₁ NO ₁ O ₂ +67.0 O ₁ NC ₁ H ₁ -119.2 NO ₁ O ₂ H ₂ -118.6 O ₁ NC ₁ C ₂ +60.8	O ₁ -0.233 C ₁ -0.025 N -0.314 O ₂ -0.466 H ₁ +0.369 H ₂ +0.459 C ₂ -0.483	SCF -865.94315 MP2 ₁ -867.53918 MP2 ₂ -868.06903 DFT -869.06181	SCF -336.69412 MP2 ₁ -746.42965 MP2 ₂ -686.54200 DFT -425.77734	2.78
 1,2,4-thiadiazol-5-yl nitronium	C ₁ N 1.461 NO ₁ 1.362 O ₁ O ₂ 1.403 C ₁ C ₂ 1.529	C ₁ NO 112.6 NC ₁ C ₂ 110.7 NO ₁ O ₂ 109.4 O ₁ O ₂ H ₂ 101.8	C ₁ NO ₁ O ₂ +65.2 O ₁ NC ₁ H ₁ -120.1 NO ₁ O ₂ H ₂ +119.8 O ₁ NC ₁ C ₂ +52.5	O ₁ -0.228 C ₁ -0.019 N -0.337 O ₂ -0.466	SCF -865.94652 MP2 ₁ -867.54168 MP2 ₂ -868.07195 DFT -869.05792	SCF -369.644145 MP2 ₁ -770.21668 MP2 ₂ -711.19544 DFT -433.07623	2.84

				H ₁ +0.359 H ₂ +0.465 C ₂ -0.4844			
 <p>Furoxan-4-yl nitronium</p>	C ₁ N 1.459 NO ₁ 1.361 O ₁ O ₂ 1.405 C ₁ C ₂ 1.529	C ₁ NO 113.0 NC ₁ C ₂ 110.5 NO ₁ O ₂ 109.0 O ₁ O ₂ H ₂ 102.2	C ₁ NO ₁ O ₂ +66.8 O ₁ NC ₁ H ₁ -119.8 NO ₁ O ₂ H ₂ -130.2 O ₁ NC ₁ C ₂ +58.5	O ₁ -0.229 C ₁ -0.0363 N -0.325 O ₂ -0.463 H ₁ +0.373 H ₂ +0.465 C ₂ -0.483	SCF -617.97987 MP2 ₁ -619.8256 MP2 ₂ -620.44471 DFT -546.03944*	SCF -375.60403 MP2 ₁ -718.91441 MP2 ₂ -714.24102 DFT -	5.14
 <p>Furoxan-3-yl nitronium</p>	C ₁ N 1.456 NO ₁ 1.366 O ₁ O ₂ 1.402 C ₁ C ₂ 1.529	C ₁ NO 112.1 NC ₁ C ₂ 108.6 NO ₁ O ₂ 109.6 O ₁ O ₂ H ₂ 101.7	C ₁ NO ₁ O ₂ -66.6 O ₁ NC ₁ H ₁ +119.9 NO ₁ O ₂ H ₂ -121.8 O ₁ NC ₁ C ₂ +170.3	O ₁ -0.239 C ₁ -0.003 N -0.347 O ₂ -0.457 H ₁ +0.365 H ₂ +0.467 C ₂ -0.517	SCF -617.98311 MP2 ₁ -619.82824 MP2 ₂ -620.44766 DFT -621.46768	SCF -384.399455 MP2 ₁ -780.8237 MP2 ₂ -723.16772 DFT -1297.49585*	6.53

<p>1,2,3-thiadiazol-5-yl nitronium</p>	C ₁ N 1.462	C ₁ NO 109.8	C ₁ NO ₁ O ₂ +96.3	O ₁ -0.249	SCF -865.89919	SCF -364.393145	3.34
	NO ₁ 1.384	NC ₁ C ₂ 114.0	O ₁ NC ₁ H ₁ +114.3	C ₁ +0.028	MP2 ₁ -867.5037	MP2 ₁ -760.47608	
	O ₁ O ₂ 1.382	NO ₁ O ₂ 107.7	NO ₁ O ₂ H ₂ +75.6	N -0.371	MP2 ₂ -868.03245	MP2 ₂ -701.32356	
	C ₁ C ₂ 1.528	O ₁ O ₂ H ₂ 103.2	O ₁ NC ₁ C ₂ +62.5	O ₂ -0.417	DFT -869.01864	DFT -424.727135	
				H ₁ +0.371			
				H ₂ +0.457			
				C ₂ -0.511			

Table A6h: •OH + •CH₃ spin adducts

Optimized adducts ^a	Selected parameters			Charge populations ^b	Energy ^c (a.u.)	ΔE ^d (kJ/mol)	Dipole moments (D)
	Bond lengths (Å)	Bond angles (deg)	Dihedral angles (deg)				
 1,2,4-thiadiazol-3-yl nitronium	C ₁ N 1.441	C ₁ NO ₁ 106.7	C ₁ NO ₁ C ₂ +125.1	O ₁ -0.535	SCF -866.03236	SCF -570.914975	1.75
	NO ₁ 1.399	NO ₁ C ₂ 110.3	O ₁ NC ₁ H ₁ +112.6	C ₁ +0.303	MP2 ₁ -867.61288	MP2 ₁ -939.92900	
	C ₁ O ₂ 1.392	NC ₁ O ₂ 113.2	O ₁ NC ₁ O ₂ +57.7	N -0.376	MP2 ₂ -868.14558	MP2 ₂ -887.52402	
	O ₁ C ₂ 1.402		NC ₁ O ₂ H ₂ -55.2	O ₂ -0.746	DFT -869.13521	DFT -618.48904	
				H ₁ +0.379			
				H ₂ +0.466			
				C ₂ -0.138			
 1,2,4-thiadiazol-5-yl nitronium	C ₁ N 1.442	C ₁ NO ₁ 107.1	C ₁ NO ₁ C ₂ +128.1	O ₁ -0.521	SCF -866.02962	SCF -587.823195	3.60
	NO ₁ 1.395	NO ₁ C ₂ 110.4	O ₁ NC ₁ H ₁ +112.8	C ₁ +0.337	MP2 ₁ -867.61098	MP2 ₁ -952.16383	
	C ₁ O ₂ 1.383	NC ₁ O ₂ 113.7	O ₁ NC ₁ O ₂ +64.6	N -0.395	MP2 ₂ -868.14369	MP2 ₂ -899.54881	
	O ₁ C ₂ 1.404		NC ₁ O ₂ H ₂ -63.819	O ₂ -0.720	DFT -869.13454	DFT -634.242035	

				H ₁ +0.370 H ₂ +0.464 C ₂ -0.145			
 <p>Furoxan-4-yl nitrone</p>	C ₁ N 1.441 NO ₁ 1.396 C ₁ O ₂ 1.391 O ₁ C ₂ 1.405	C ₁ NO ₁ 106.3 NO ₁ C ₂ 110.3 NC ₁ O ₂ 113.3	C ₁ NO ₁ C ₂ +126.7 O ₁ NC ₁ H ₁ +112.6 O ₁ NC ₁ O ₂ +58.6 NC ₁ O ₂ H ₂ -56.3	O ₁ -0.534 C ₁ +0.319 N -0.356 O ₂ -0.754 H ₁ +0.362 H ₂ +0.475 C ₂ -0.145	SCF -618.06674 MP2 ₁ -619.89814 MP2 ₂ -620.51987 DFT -621.21798	SCF -603.681215 MP2 ₁ -909.36818 MP2 ₂ -911.57360 DFT -645.26914	6.13
 <p>Furoxan-3-yl nitrone</p>	C ₁ N 1.451 NO ₁ 1.388 C ₁ O ₂ 1.388 O ₁ C ₂ 1.403	C ₁ NO ₁ 108.8 NO ₁ C ₂ 110.8 NC ₁ O ₂ 107.5	C ₁ NO ₁ C ₂ -115.1 O ₁ NC ₁ H ₁ -114.4 O ₁ NC ₁ O ₂ -172.6 NC ₁ O ₂ H ₂ -59.3	O ₁ -0.509 C ₁ +0.322 N -0.379 O ₂ -0.747 H ₁ +0.359	SCF -618.06293 MP2 ₁ -619.89488 MP2 ₂ -620.51702 DFT -621.21299	SCF -593.966865 MP2 ₁ -955.78702 MP2 ₂ -905.2724 DFT -628.80725	5.38

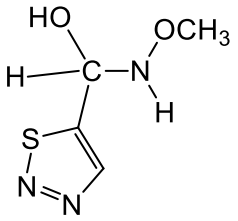
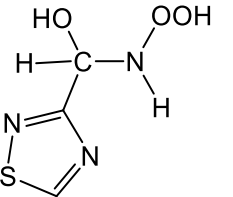
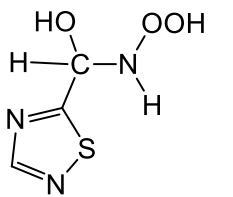
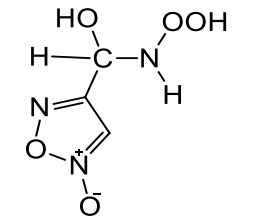
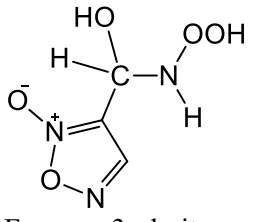
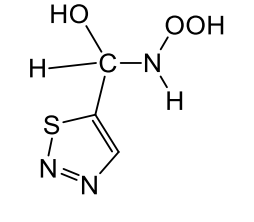
				H ₂ +0.4643			
				C ₂ -0.1402			
 <p>1,2,3-thiadiazol-5-yl nitron</p>	C ₁ N 1.441 NO ₁ 1.396 C ₁ O ₂ 1.389 O ₁ C ₂ 1.404	C ₁ NO ₁ 106.8 NO ₁ C ₂ 110.4 NC ₁ O ₂ 113.6	C ₁ NO ₁ C ₂ 128.1 O ₁ NC ₁ H ₁ 112.9 O ₁ NC ₁ O ₂ +59.4 NC ₁ O ₂ H ₂ -58.9	O ₁ -0.529 C ₁ +0.368 N -0.378 O ₂ -0.749 H ₁ +0.369 H ₂ +0.470 C ₂ -0.144	SCF -865.99065 MP2 ₁ -867.58307 MP2 ₂ -868.11419 DFT -869.10347	SCF -604.521375 MP2 ₁ -968.86201 MP2 ₂ -915.93193 DFT -647.44830	5.29

Table A6i: Di •OH spin adducts

Optimized adducts ^a	Selected parameters			Charge populations ^b	Energy ^c (a.u.)	ΔE^d (kJ/mol)	Dipole moments (D)
	Bond lengths (Å)	Bond angles (deg)	Dihedral angles (deg)				
 <p>1,2,4-thiadiazol-3-yl nitron</p>	CN 1.449 NO ₁ 1.362 CO ₂ 1.385 O ₁ O ₃ 1.400	CNO ₁ 113.3 NO ₁ O ₃ 110.4 O ₁ O ₃ H ₂ 103.0 NCO ₂ 107.9 CO ₂ H ₃ 108.3	CNO ₁ O ₃ +71.7 NO ₁ O ₃ H ₂ -107.7 O ₁ NCO ₂ +161.4 NCO ₂ H ₃ -49.3 O ₁ NCH ₁ -123.4	O ₁ -0.231 C +0.310 N -0.360 O ₂ -0.731 O ₃ -0.461	SCF -901.76282 MP2 ₁ -903.40002 MP2 ₂ -903.96529 DFT -904.96554	SCF -953.345305 MP2 ₁ -1230.20428 MP2 ₂ -1115.8375 DFT -573.35407	2.06
 <p>1,2,4-thiadiazol-5-yl nitron</p>	CN 1.448 NO ₁ 1.369 CO ₂ 1.383 O ₁ O ₃ 1.402	CNO ₁ 110.0 NO ₁ O ₃ 110.0 O ₁ O ₃ H ₂ 101.9 NCO ₂ 111.0 CO ₂ H ₃ 109.5	CNO ₁ O ₃ +68.9 NO ₁ O ₃ H ₂ +114.1 O ₁ NCO ₂ +69.6 NCO ₂ H ₃ -56.3 O ₁ NCH ₁ -120.3	O ₁ -0.251 C +0.357 N -0.332 O ₂ -0.751 O ₃ -0.462	SCF -901.76535 MP2 ₁ -903.40222 MP2 ₂ -903.96805 DFT -904.96419	SCF -984.08991 MP2 ₁ -1253.20366 MP2 ₂ -1140.07086 DFT -587.32435	3.60

 <p>Furoxan-4-yl nitronium</p>	CN 1.455	CNO ₁ 110.0	CNO ₁ O ₃ +68.1	O ₁ -0.251	SCF -653.79778	SCF -987.634335	5.83
	NO ₁ 1.368	NO ₁ O ₃ 109.8	NO ₁ O ₃ H ₂ +116.6	C +0.339	MP2 ₁ -655.68546	MP2 ₁ -1200.11605	
	CO ₂ 1.381	O ₁ O ₃ H ₂ 101.9	O ₁ NCO ₂ +63.3	N -0.326	MP2 ₂ -656.34039	MP2 ₂ -1142.01374	
	O ₁ O ₃ 1.403	NCO ₂ 110.1	NCO ₂ H ₃ -55.0	O ₂ -0.745	DFT -657.04745	DFT -597.87886	
		CO ₂ H ₃ 109.2	O ₁ NCH ₁ -119.5	O ₃ -0.461			
 <p>Furoxan-3-yl nitronium</p>	CN 1.449	CNO ₁ 112.0	CNO ₁ O ₃ -63.3	O ₁ -0.218	SCF -653.79602	SCF -983.30226	6.71
	NO ₁ 1.362	NO ₁ O ₃ 109.8	NO ₁ O ₃ H ₂ -118.6	C +0.323	MP2 ₁ -655.6862	MP2 ₁ -1257.03689	
	CO ₂ 1.387	O ₁ O ₃ H ₂ 102.4	O ₁ NCO ₂ +90.3	N -0.348	MP2 ₂ -656.33952	MP2 ₂ -1140.91103	
	O ₁ O ₃ 1.405	NCO ₂ 113.4	NCO ₂ H ₃ -73.7	O ₂ -0.731	DFT -657.04763	DFT -594.99081	
		CO ₂ H ₃ 109.0	O ₁ NCH ₁ +120.1	O ₃ -0.480			
 <p>1,2,3-thiadiazol-5-yl nitronium</p>	CN 1.445	CNO ₁ 108.3	CNO ₁ O ₃ +98.2	O ₁ -0.266	SCF -901.72202	SCF -989.34091	4.07
	NO ₁ 1.387	NO ₁ O ₃ 107.9	NO ₁ O ₃ H ₂ +77.6	C +0.354	MP2 ₁ -903.36877	MP2 ₁ -1255.35657	
	CO ₂ 1.388	O ₁ O ₃ H ₂ 103.2	O ₁ NCO ₂ +60.6	N -0.364	MP2 ₂ -903.93222	MP2 ₂ -1139.83457	
	O ₁ O ₃ 1.382	NCO ₂ 113.6	NCO ₂ H ₃ -67.0	O ₂ -0.744	DFT -904.92959	DFT -591.26260	
		CO ₂ H ₃ 108.9	O ₁ NCH ₁ +113.0	O ₃ -0.415			

^aAll structures were optimized at the HF/6-31G* level and have no imaginary frequencies

^bMulliken population analysis

^c1 au = 2625.5 kJ/mol. The MP2₁ and MP2₂ energies are single point energies obtained with the cc-pVDZ and cc-pVTZ basis sets respectively using the 6-31G* optimized geometry, *i.e.* MP2/cc-pVDZ//HF/6-31G* and MP2/cc-pVTZ//HF/6-31G* respectively.

$$\text{^d\Delta E} = E_{\text{adduct}} - [E_{\text{new heteroaryl nitrene}} + E_{\text{radical 1}} + E_{\text{radical 2}}]$$

Table A7: Energetics of the addition reactions of DMPO, PBN and FxBN with •OH

^a Nitron	ΔE (kJ/mol)				^d $t_{1/2}$ (s)	^d $k_{ST} \cdot 10^9$ ($\text{dm}^3 \text{mol}^{-1} \text{s}^{-1}$)
	DFT		HF			
	Monoadduct ^b	Diadduct ^c	Monoadduct ^b	Diadduct ^c		
DMPO	-1123.81	-571.73	-628.14	-935.92	3300.0	3.6
PBN	+5940.85	+5739.95	+5471.65	+5195.04	36.0	2.6
FxBN	-1548.71	-1847.18	-698.44	-979.83	7560.0	12.2

^aAll structures were optimized and their energies were obtained at the DFT/m06/6-31G* and HF/6-31G* levels and have no imaginary frequencies

$$^b \Delta E = E_{\text{adduct}} - [E_{\text{nitron}} + E_{\text{OH radical}}]$$

$$^c \Delta E = E_{\text{adduct}} - [E_{\text{nitron}} + E_{\text{OH radical}} + E_{\text{OH radical}}]$$

^dExperimental data obtained from Barriga *et al.*⁶⁴

Table A8: Molecular energies of DMPO, PBN and FxBN spin traps and adducts at DFT/m06/6-31* and HF/6-31G* levels

Molecule	Molecular energy, E_h (hartree)	
	DFT	HF
•OH	-75.642945	-75.22340
DMPO	-364.922063	-362.841659
PBN	-560.110596	-556.831192
FxBN	-662.659219	-659.102469
DMPO-OH	-440.993092	-438.304334
PBN-OH	-633.490532	-629.970314
FxBN-OH	-738.892104	-734.591920
DMPO-diOH	-516.425738	-513.644974
PBN-diOH	-709.210005	-705.299281
FxBN-diOH	-814.648744	-809.922508

VITA

EYRAM AKOSUA ASEMPA

- EDUCATION MSc. Chemistry, East Tennessee State University (ETSU), Johnson City, Tennessee (2014-2016)
- B.Sc. Chemistry, (First Class Honor) Kwame Nkrumah University of Science and Technology, Ghana, West Africa (2009-2013)
- EXPERIENCE Graduate Teaching Assistant, Chemistry Department, College of Arts and Sciences, East Tennessee State University, Johnson City Tennessee (2014-2016)
- Teaching Assistant, Chemistry Department, College of Science, Kwame Nkrumah University of Science and technology, Kumasi, Ghana (2013-2014)
- PUBLICATIONS R. Tia, E. Asempa, E. Adei, "Computational Studies of the Reactivity, Regio-Selectivity and Stereo-Selectivity of Pericyclic Diels-Alder Reactions of Substituted Cyclobutenones", *J. Theor. Comput. Sci.* (2014) 1:114.
- E. Asempa, Scott J. Kirkby, "Computational Studies of Spin Trapping of Biologically Relevant Radicals by New Heteroaryl Nitrones", Abstracts,

71st Southwest/67th Southeast Joint Regional Meeting of the American Chemical Society, Memphis, Tennessee, United States, 4-7 November 2015 (2015) COMP-15, American Chemical Society, Washington, D.C.

E. Asempa, Scott J. Kirkby, “Computational Studies of Spin Trapping of Biologically Relevant Radicals by New Heteroaryl Nitrones”, Abstracts of Papers, 251st ACS National Meeting, San Diego, CA, United States, 13-17 March 2016 (2016), COMP-514, American Chemical Society, Washington D.C.

E. Asempa, Scott J. Kirkby, “Computational Studies of Spin Trapping of Biologically Relevant Radicals by New Heteroaryl Nitrones,” Abstract 81, 2016 Appalachian Student Research Forum, ETSU, Johnson City, Tennessee, 6-7 April 2016.

GRANT

Applied for and awarded

Eyram Asempa and Scott Kirkby, ETSU School of Graduate Studies and ETSU Graduate Council Research Grant (2015-2016) “Computational Studies of the Spin Trapping of Biologically Relevant Radicals by New Heteroaryl Nitrones”: \$800